U.S. DEPARTMENT OF COMMERCE
National Technical Information Service

PB-264 632

Characterization and Research Investigation of Methanol & Methyl Fuels in Automobile Engines. First Year Report

Santa Clara Univ, Calif Dept of Mechanical Engineering

Prepared for

Environmental Protection Agency, Ann Arbor, Mich Emission Control Technology Div

Aug 76

EPA-460/3-76-016
August 1976

PB 264 632

CHARACTERIZATION AND RESEARCH INVESTIGATION OF METHANOL AND METHYL FUELS IN AUTOMOBILE ENGINES FIRST YEAR REPORT

U.S. ENVIRONMENTAL PROTECTION AGENCY
Office of Air and Waste Management
Office of Mobile Source Air Pollution Control
Emission Control Technology Division
Ann Arbor, Michigan 48105

REPRODUCED BY
NATIONAL TECHNICAL
INFORMATION SERVICE
U. S. DEPARTMENT OF COMMERCE
SPRINGFIELD, VA. 22161

TECHNICAL REPORT DATA
(Please read Instructions on the reverse before completing)

1. REPORT NO.	2.	3. RECIPIENT'S ACCESSION NO.
EPA 460/3-76-016		

4. TITLE AND SUBTITLE
Characterization and Research Investigation of Methanol and Methyl Fuel in Automobile Engines: 1st Year Report

5. REPORT DATE
August 1976

6. PERFORMING ORGANIZATION CODE

7. AUTHOR(S)
R.K. Pefley, A.E. Bayce, L.H. Browning, M.C. McCormack
M.A. Sweeney

8. PERFORMING ORGANIZATION REPORT NO.

9. PERFORMING ORGANIZATION NAME AND ADDRESS
University of Santa Clara
Department of Mechanical Engineering
Santa Clara, California 95053

10. PROGRAM ELEMENT NO.

11. CONTRACT/GRANT NO.
R803548-01

12. SPONSORING AGENCY NAME AND ADDRESS
Environmental Protection Agency
Motor Vehicle Emission Laboratory
2565 Plymouth Rd.
Ann Arbor, Michigan 48105

13. TYPE OF REPORT AND PERIOD COVERED
1 Year Feb. 75 - Feb. 76

14. SPONSORING AGENCY CODE

15. SUPPLEMENTARY NOTES

16. ABSTRACT

Methanol is compared with gasoline in steady state dynamometer test evaluations of power, thermal efficiency, and emissions. The reported comparisons are from OEM equipment with gasoline and low cost modifications of the fuel preparation system to accommodate methanol. Maldistribution of fuel-air mixture among the cylinders is severe for gasoline and somewhat worse for methanol. Even so, methanol is found superior in thermal efficiency. NOx emissions, and equivalence ratio range, and is comparable with gasoline in power, hydrocarbons and CO. Methanol produces somewhat more aldehydes, particularly from lean equivalence ratios, but the absolute levels for both fuels are low.

Also presented is some engine friction-wear data based on analysis of engine oil for various metals. Preliminary computer modeling of engine thermochemical processes predicts both emissions and performance in good agreement wich experimental data.

17. KEY WORDS AND DOCUMENT ANALYSIS

a. DESCRIPTORS	b. IDENTIFIERS/OPEN ENDED TERMS	c. COSATI Field/Group
Methanols Methyl Alchol Exhaust Emissions		

18. DISTRIBUTION STATEMENT	19. SECURITY CLASS *(This Report)*	21. NO. OF PAGES
Not Restricted	Unclassified	91
	20. SECURITY CLASS *(This page)* Unclassified	22. PRICE PC A05 / MF A01

EPA Form 2220-1 (9-73)

EPA-460/3-76-016

CHARACTERIZATION AND RESEARCH INVESTIGATION OF METHANOL AND METHYL FUELS IN AUTOMOBILE ENGINES FIRST YEAR REPORT

by

R.K. Pefley, A.E. Royce, L.H. Browning,
M.C. McCormick, and M.A. Sweeney

University of Santa Clara
Department of Mechanical Engineering
Santa Clara, California 95053

Grant No. R8035480-01

EPA Project Officer: Robert J. Garbe

Prepared for

ENVIRONMENTAL PROTECTION AGENCY
Office of Air and Waste Management
Office of Mobile Source Air Pollution Control
Emission Control Technology Division
Ann Arbor, Michigan 48105

August 1976

This report is issued by the Environmental Protection Agency to report technical data of interest to a limited number of readers. Copies are available free of charge to Federal employees, current contractors and grantees, and nonprofit organizations - in limited quantities - from the Library Services Office (MD-35), Research Triangle Park, North Carolina 27711; or, for a fee, from the National Technical Information Service, 5285 Port Royal Road, Springfield, Virginia 22161.

This report was furnished to the Environmental Protection Agency by the University of Santa Clara, Department of Mechanical Engineering, Santa Clara, California 95053, in fulfillment of Grant No. R803540-01. The contents of this report are reproduced herein as received from the University of Santa Clara. The opinions, findings, and conclusions expressed are those of the author and not necessarily those of the Environmental Protection Agency. Mention of company or product names is not to be considered as an endorsement by the Environmental Protection Agency.

Publication No. EPA-460/3-76-016

INDEX

		Page
LIST OF FIGURES		ii
I.	INTRODUCTION	1
II.	PROGRAM OBJECTIVES	1
III.	SUMMARY OF ACTIVITIES RELATING TO THE FIRST YEAR OF THE GRANT...	1
IV.1	ENGINE PERFORMANCE AND EMISSIONS CHARACTERIZATION - METHANOL VERSUS INDOLENE	4
IV.1.1	Introduction and Summary	4
IV.1.1.1	Indolene Base Line	5
IV.1.1.2	Methanol Base Line	6
IV.1.2	Comparative Experimental Results	7
IV.1.2.1	Experimental System Description and Engine Modifications	9
IV.1.2.2	Carburetor Modification for Methanol Operation	11
IV.1.2.3	Experimental Procedure	11
IV.1.3	Engine Performance - Indolene Versus Methanol	12
IV.1.3.1	Lean Misfire Limit and MBT Spark Advance for a Multicylinder Engine	13
IV.1.3.2	Comparative Power at 2000 RPM	17
IV.1.3.3	Comparative Thermal Efficiency at 2000 RPM	19
IV.1.4	Engine Exhaust Emissions	21
IV.1.4.1	Cylinder-to-Cylinder Equivalence Ratio Variations	23
IV.1.4.2	CO_2, CO and O_2	27
IV.1.4.3	CO_2, CO, O_2 Comparative Results	27
IV.1.4.4	UHC, Aldehydes, and NO_x-Indolene	27
IV.1.4.5	Comparative NO_x, UBF, and Aldehydes	42
IV.1.5	Conclusions and Projected Activities	46
IV.2	ALTERNATIVE FUEL INDUCTION SYSTEMS	48
IV.2.1	The WHB Shock Wave Induction System	48
IV.2.2	Electronically Controlled Fuel Injection System	49
IV.3	COLD STARTING	52
IV.4	INFLUENCES RESULTING FROM VARIATIONS IN COMPOSITION OF METHANOL BASED FUELS	53
IV.4.1	Volatility of Fuels	53
IV.4.2	Types of Fuels Tested	53
IV.5	ENGINE WEAR	59
IV.5.1	Pinto Engine Wear Results	59
IV.6	THERMOCHEMICAL ENGINE PROCESS MODELING	67
V.	REFERENCES	72
APPENDIX		74

LIST OF FIGURES

Figure		Page
1	Test Engine - Dynamometer Configuration	10
2	MBT Spark Timing Effective Lean Limit for Two Load Conditions - Methanol Vs. Indolene	14
3	MBT Spark Timing Showing True Lean Limit and Cylinder ϕ Variation, Wide Open Throttle - Methanol Vs. Indolene	15
4	MBT Spark Timing Showing True Lean Limit and Cylinder ϕ Variation for Part Load Condition - Methanol Vs. Indolene	16
5	Brake Horsepower Vs. Equivalence Ratio - Methanol Vs. Indolene	18
6	Comparative Brake Thermal Efficiency - Methanol Vs. Indolene	20
7	Exhaust Emissions Sampling System	22
8	Cylinder-to-Cylinder Equivalence Ratio Variations - Indolene	24
9	Cylinder-to-Cylinder Equivalence Ratio Variations - Methanol	25
10	Methanol Vs. Indolene - Cylinder-to-Cylinder Equivalence Ratio Variation	26
11	CO_2 Vs. Equivalence Ratio - Indolene Data	28
12	CO Vs. Equivalence Ratio - Indolene Data	29
13	O_2 Vs. Equivalence Ratio - Indolene Data	30
14	CO_2 Vs. Equivalence Ratio - Individual Cylinder Data - Methanol Vs. Indolene	31
15	CO Vs. Equivalence Ratio - Individual Cylinder Data - Methanol Vs. Indolene	32
16	O_2 Vs. Equivalence Ratio - Individual Cylinder Data - Methanol Vs. Indolene	33
17	Unburned Fuel Vs. Equivalence Ratio - Composite Cylinder Data	35
18	Aldehydes Vs. Equivalence Ratio - Composite Cylinder Data	36
19	Oxides of Nitrogen Vs. Equivalence Ratio - Composite Cylinder Data	37
20	Oxides of Nitrogen Vs. Equivalence Ratio - Individual Cylinder Data	38
21	Oxides of Nitrogen Vs. Equivalence Ratio - Speed Dependency - Individual Cylinder Data	39
22	Oxides of Nitrogen Vs. Equivalence Ratio - Load Dependency - Individual Cylinder Data	40
23	Effects of Spark Timing on NO_X and IHP	41
24	Effects of Spark Advance on the Oxides of Nitrogen - Individual Cylinder Data	43
25	Oxides of Nitrogen Vs. Equivalence Ratio - Individual Cylinder Data	44

Figure		Page
26	Unburned Fuel Vs. Equivalence Ratio - Methanol Vs. Indolene - Composite Cylinder Data	45
27	Aldehydes as a Function of Equivalence Ratio - Methanol Vs. Indolene	47
28	Electronic Fuel Injection System	51
29	ASTM Distillation	56
30	Wear of Pinto Engine No. 1 During Break-in	64
31	Wear of Pinto Engine No. 1	65
32	Wear of Pinto Engine No. 2	66
33	Factors Being Considered in Combustion Modeling	68
A1	Maldistribution & Performance Trends for Indolene - Repetitive Test Points	77
A2	Trends in Brake Thermal Efficiency - Part and Full Load Comparisons at Various Speeds	78
A3	Brake Horsepower and Maldistribution - Indolene	79
A4	Brake Horsepower and Maldistribution - Methanol	80
A5	Cylinder-to-Cylinder Equivalence Ratio Variations - Indolene	81
A6	CO_2 Vs. Equivalence Ratio - Composite Cylinder Data	82
A7	CO Vs. Equivalence Ratio - Composite Cylinder Data	83
A8	O_2 Vs. Equivalence Ratio - Composite Cylinder Data	84

I. INTRODUCTION

Although this is the first year of grant activities, this report marks the eighth year of research at the University of Santa Clara relating to methanol based fuel* as a reducer of pollution and as an extender and supplement of energy supplies. Over that time period the authors have experienced a cautious growth in optimism that methanol based fuels are the most attractive alternate fuels from a user viewpoint which can be produced from coal, remote natural gas, agricultural and municipal wastes. This attractiveness is not to be found in any one major advantage. Rather, it is a composite of the advantages to be found in combustion behavior, emissions, handling safety, ecology factors, and ease of power plant conversion as weighed against the cost of fuel production. The past year's progress reported herein adds to this favorable evidence. While this work relates primarily to the automotive possibilities, the broader potential advantages of the fuel should be kept in mind.

II. PROGRAM OBJECTIVES

The program objectives as proposed for the two year grant period are:

(1) To characterize multicylinder, automotive engine performance and emissions when operating on methanol and methyl fuel by comparison with gasoline.

(2) To identify and assess alternatives for improvement of engine performance and reduction of emissions.

(3) To select the best alternates and modify the engine fuel induction system accordingly.

(4) To evaluate the modifications in terms of performance and emissions and interpret the results.

III. SUMMARY OF ACTIVITIES RELATING TO THE FIRST YEAR OF THE GRANT

During the past year, literature searches, experimental investigations, analytical modeling studies and publications have all been parts of the work program. These efforts have provided some answers to the grant's investigative objectives and have added focus to the ensuing work. The highlights of the activities and evidence that have been obtained are:

*Methanol based fuel includes methanol, dissociated methanol (a gaseous fuel--$CO + 2H_2$) and methyl fuel which contains higher alcohols resulting from high volume, low cost production and other additives for cold start up of automotive engines or gas turbines.

(1) By the end of the grant year, two identical (2.3 litre, 4-cylinder, 1975 model year Ford) engines have been completely instrumented and have become fully operational. One engine is designated as the test engine. The second engine is a back-up to the test engine and is used for adaptation and check-out of modified fuel preparation systems.

(2) Using equivalence ratio* as the primary basis for comparison, our engine test program is indicating that methanol is superior to gasoline in thermal efficiency, operational range of equivalence ratio, and emissions levels with the exception of aldehydes. This evidence corroborates our published findings[1] which resulted from our earlier experimental work and literature search.

(3) The OEM carburetor, intake manifold, fuel pump combination for the test engine show such wide cylinder-to-cylinder and time variant equivalence ratios as to emphasize the need for the development of alternate mixture preparation hardware. This evidence accentuates the importance of the portion of our work relating to the investigation of alternate fuel preparation systems.

(4) Several fuel preparation systems have been identified as offering advantages over the OEM venturi carburetor and intake manifold. Two of these systems have been built under purchase agreements and will be delivered in the next sixty days. One is a pressure wave carburetion system which uses the strength of the rarefaction pressure wave generated by the intake valve opening to meter and nebulize the fuel for each intake charge. This system has fewer moving parts and fewer total parts for a four-cylinder engine when compared with the OEM system. The other is a fuel injection system with electronic control to allow management of equivalence ratio for each cylinder as well as injection timing. Prototypes of both of these systems have been operated in our experimental program during this past year.

(5) With the use of ASTM distillation and Reid vapor pressure procedures, several interesting possibilities have been observed relative to a methanol based fuel that has cold starting enhancement. The two most interesting mixtures to date are pure methanol with a small percentage of butane addition and the methanol-gasoline blend consisting of 16% methanol and 4% isobutanol.

---

*Equivalence ratio is stoichiometric air-fuel divided by actual air-fuel.

(6) Lubricity of engines using methanol fuel and petroleum based lubricating oil is important from a wear viewpoint. To track the contrast between methanol and gasoline in this regard, atomic absorbtion spectrophotometry has been employed to examine the metal accumulation in the oil with respect to time. Engine test time using methanol as a fuel is too limited as yet to draw any comparative conclusions. However, the method being used appears to provide a suitable basis from which to draw comparative evidence.

(7) Computer modeling of the JT8D gas turbine using chemical kinetic reaction rate schemes for jet fuel and methanol shows, that without reduction in thrust level, NO_x emissions can be reduced by as much as 80% if methanol is substituted for jet fuel.[2] Experimental investigations by others in adiabatic burners and automotive gas turbines appear to confirm this prediction.[3,4] This computer model is now being adapted to model the 2.3 litre test engine. Should the model predict satisfactory contrasts in emissions between gasoline and methanol, it will be extremely useful in making parametric projections toward improved methanol fueled engine performance.

(8) Two vehicles, a 1972 Plymouth Valiant and a 1970 American Motors Gremlin, have successfully completed their fourth and fifth year, respectively, of continuous operation on pure methanol with no major component failures. The Plymouth, which is in service in the City of Santa Clara, ranks competively in fuel economy (miles/mm Btu) over its operational lifetime with vehicles in like service operating on gasoline. Cold starting is the most serious driver reported difficulty.[5] An additional 1972 Plymouth Valiant belonging to the City of Santa Clara has been operating on a 10% methanol-90% gasoline blend for over a year with no modifications and no operational problems.

IV.1 ENGINE PERFORMANCE AND EMISSIONS CHARACTERIZATION - METHANOL VERSUS INDOLENE

Results of an experimental parametric investigation of a four-cylinder spark ignition engine operating on methanol and on indolene are presented in this section. This phase of the investigation represents the major proportion of work performed under the first year effort. In order to keep the presentation and discussion of the results brief, experimental procedure and technique, along with data acquisition and analysis methods, will be covered in more detail in the final report. The following sections cover the topical matter in five steps. Section IV.1.1 is an introduction and a summary of the conclusions based on the experimental evidence. Section IV.1.2 describes the test procedure and engine modifications. Section IV.1.3 compares in detail engine performance while operating on the two fuels. Section IV.1.4 compares and discusses at length the exhaust emissions resulting from the use of the two fuels. Interpretations and projected activities are covered in Section IV.1.5.

IV.1.1 Introduction and Summary: There is considerable literature evidence comparing engine performance and exhaust emissions of methanol versus gasoline fueled engines.[1] The majority of these studies, however, has concentrated on steady state, single cylinder engine comparisons. To fill the need for comparative evidence in multicylinder engines, the first year effort in this investigation has been directed towards the acquisition of complete exhaust emissions and performance data for a conventional four-cylinder engine operating on methanol and a reference gasoline (indolene). The engine exhaust was analyzed for principal combustion species, as well as for the pollutant species of CO, NO, NO_x, unburned fuel (UBF) and aldehydes. Engine performance was described by indicated and brake thermal efficiency (a measure of fuel economy on an energy basis) and power. Results are presented primarily as functions of fuel-air equivalence ratio (ϕ) since this is, in general, the most influential operating variable affecting specific exhaust emissions (grams pollutant per indicated horsepower hour - [gms/ihp-hr]) and engine fuel economy (on an energy basis).

Multicylinder engine operation introduces an important parameter which is not seen in single cylinder operation. This is the cylinder-to-cylinder variation in equivalence ratio which is a result of the less than perfect mixing and distribution of the fuel and air in the intake manifold. The exhaust emissions are a strong function of equivalence ratio and thus composite

exhaust emissions (exhaust contributions from each of the cylinders combined) often show what appears to be confused emissions data because of this "maldistribution" effect. Through treatment of multicylinder engines as a combination of single cylinder engines, the confused emissions data becomes explicable. In addition, this approach leads to the understanding of the apparent inconsistencies in the setting of MBT (minimum spark advance for best torque) spark timing. Finally, it leads to an understanding of why conventional multicylinder engines operate over narrower ranges of equivalence ratio and spark timing when compared to single cylinder engine operation.

Our principal objective in this first year of the experimental program has been to provide a comparative study: (1) using a stock four-cylinder engine (with the exception that the stock exhaust gas recirculation [EGR] was not used) operating at steady state on indolene for a base line, (2) then minimally modifying the fuel induction system for methanol operation at equivalent engine conditions. This is a first step in progressive studies aimed at achieving optimal engine performance and minimum pollutant emissions with methanol as a fuel in automotive spark ignition multicylinder engines.

IV.1.1.1 Indolene Base Line: The characterization of engine performance and emissions with indolene consisted of 140 steady state engine conditions, the data from which provides a basis for the following observations:

(1) Multicylinder engine operation at steady state yielded a range of equivalence ratio variations (maldistribution) among the cylinders for the speed and load range observed. The effect was most pronounced at wide open throttle conditions.

(2) Exhaust emissions were dramatically affected by this maldistribution. The oxides of nitrogen, owing to their characteristic strong dependency on equivalence ratio and spark advance, displayed the most complex behavior. Resolution of the data in terms of the chosen parameters of this investigation led to an understanding of why NO_x emissions are difficult to control in multicylinder engines.

Composite carbon monoxide and unburned hydrocarbons showed characteristic lean side minimums up to the lean misfire limit; however, at times the maldistribution phenomena led to significant quantities of CO near the composite stoichiometric air to fuel ratio. Aldehydes, a toxic and therefore important exhaust species to be measured, showed composite exhaust sample values characteristically increasing with the leaning of the air-fuel mixture.

(3) Engine power, fuel economy, and thermal efficiency were somewhat degraded by the maldistribution, but general trends closely follow results obtained for laboratory single cylinder engines.[6] The only exception to this general rule is that acceptable engine operation was obtained over a narrower range of spark settings and equivalence ratios.

In summary, while acceptable steady state engine performance was attainable for this conventional venturi carbureted four-cylinder engine, fundamental design defects in the intake manifold-carburetor system led to equivalence ratio variation among the cylinders. This variation in equivalence ratio caused composite pollutant emissions to be at times higher and at times lower than those if all four cylinders were operating at the composite equivalence ratio. Consequently, it is concluded that control over exhaust emissions (especially NO_X) is precluded by the lack of control over the individual cylinder equivalence ratios for this and the majority of conventional venturi carbureted multicylinder engines. However, it is anticipated that if control over equivalence ratio is attained and spark timing is programmed for speed and load conditions, then the 0.4 gms/mi NO_X standard might be met without the use of extensive add-on controls even for gasoline. Steady state data supports this contention; however, transient engine characterization is needed before it can be truly verified.

IV.1.1.2 Methanol Base Line: At the conclusion of the indolene fueled engine characterization, the stock carburetor was rejetted for methanol. The resulting characterization for similar testing conditions (i.e., same inlet air conditions, manifold vacuum settings, equivalence ratio range, and MBT spark timing) was termed as the "base line" for methanol. Results have been compiled for 2000 and 2500 RPM. Based on the comparative evidence at 2000 RPM, the following observations are presented:

(1) Cylinder-to-cylinder variations in equivalence ratio for steady state operation were consistently worse than those found in the indolene characterization. Again, the effects were most pronounced at wide open throttle settings and to a lesser degree at part throttle settings.

(2) Even with this aggravated operating condition, engine power levels were similar to those produced by indolene. The thermal efficiency improved from 4% to 10% for the load conditions and, as expected, the "true" lean misfire limit was extended. However, the maldistribution phenomena did lead to an instance where the "effective" lean misfire limit was not as lean as that attained with the indolene.

(3) Composite exhaust emissions showed trends similar to those for indolene; however, the absolute values of the constituent species showed some differences. NO_x emissions were reduced by a factor of two. Unburned hydrocarbons and CO were comparable in value. The only species showing an increase were the aldehydes, which ranged from two to eight times higher.

In summary, even though the methanol base line is incomplete, the data indicates that methanol yields improved engine thermal efficiency although the maldistribution phenomenon was more severe. Emissions of NO_x, the most difficult of the pollutant species to control in present day automotive engines, were reduced by a factor of two. In replacing the jets of the stock two-barrel carburetor, it was found that internal flow passage dimensions limited the methanol delivery rate. This indicates, at least for the carburetor used, that jet replacement would not be an adequate technique for conversion to methanol even for steady state engine operation. It is anticipated that the modified carburetor will lead to driveability problems during transient engine operation, in addition to the lack of control over cylinder-to-cylinder equivalence ratio already indicated by the steady state testing.

The results of the collective emissions so far obtained indicated that precise control over cylinder-to-cylinder variations in equivalence ratio would make possible a significant improvement in operation of spark ignition automotive engines. And, when operated on methanol, the resulting expanded lean burning capability could produce higher thermal efficiency and a reduction in oxides of nitrogen approaching one order of magnitude in comparison to current emissions levels in gasoline fueled engines.

IV.1.2 Comparative Experimental Results: The experimental program in the first year was devoted primarily to a parametric investigation of steady state engine performance and emissions of two laboratory dynamometer mounted 2.3 litre four-cylinder engines (Ford Pinto).

The parameters chosen for the characterization appear in Table 1 and are collectively termed the "base line test matrix". These five variables (speed, equivalence ratio (ϕ), load, spark timing, and inlet air temperature) are most commonly employed in the mapping of engine performance and exhaust emissions in single cylinder engines. Multicylinder engine operation, although, adds a new variable which we have already termed "maldistribution". This new variable results from the inadequate mixing and distribution of the fuel-air mixture in the carburetor.

TABLE 1

BASE LINE TEST MATRIX

Engine Speed (RPM)	ϕ (1)	Load (Fraction) (2)	Spark Setting (°BTDC)	Temperature (°F)
Idle	0.6 (5)	1/3	MBT (3)	70
1500	0.7 (5)	2/3	Other (4)	Other (4)
2000	0.8	Full		
2500	0.9			
3000	1.0			
3500	1.1			
4000	1.2			

Notes:
(1) Equivalence ratio, i.e., stoichiometric ÷ actual A/F.
(2) Fraction load is designated by intake manifold vacuum: Full = 0" hg vac; 2/3 = 7"; 1/4 = 14".
(3) Minimum spark advance for best torque.
(4) Implies less than a full complement of speed, equivalence ratio, and load settings will be used for these conditions.
(5) Methanol only

and intake manifold. It is present in all conventional venturi type carbureted multicylinder engines and differs only in degree from one carburetor-manifold system to the next. Maldistribution implies variations in ϕ among the cylinders. The data indicates that engine power and thermal efficiency were not strongly affected by the range of maldistribution encountered. In other words, when the data was compared with single cylinder engine data[6] the trends were similar. Certain of the exhaust emissions (notably NO_x) and the determination of spark timing were greatly affected by these ϕ variations. To adequately explain the experimental exhaust emissions data, it was necessary to make individual cylinder exhaust emissions analyses. Presentation of this data appears on an individual cylinder basis. Mathematically speaking, this implies that we have constrained engine performance to one equation form and composite engine emissions to another form. These are:

$$\text{performance output (ihp, Bhp, } \eta_{ti}, \eta_{tb}) = f \text{ (speed, load, composite } \phi, \text{ spark timing, and air temperature)}$$

where η_{ti} and η_{tb} are brake and indicated thermal efficiency, respectively, and composite ϕ is the average of ϕ of the four cylinders, and

$$\text{composite emissions species (gms/ihp-hr)} = f \text{ (speed, load, } \phi_1, \phi_2, \phi_3, \phi_4, \text{ spark timing, and inlet air temperature)}$$

where ϕ_i is the individual cylinder equivalence ratio.

Note that ϕ is defined on a fuel-air basis; that is, values less than unity are fuel lean and values greater than unity are fuel rich. However, due to the considerable lack of clarity in the literature of defining and presenting this variable in a consistent manner, "lean" or "rich" conditions are indicated on each graph where ϕ appears as the independent variable.

IV.1.2.1 Experimental System Description and Engine Modifications: Figure 1 is a schematic of the engine-electric dynamometer test configuration and associated equipment. The engine depicted was designated as the principal test engine from which all data appearing in this report was taken. A second engine-dynamometer system provided a back-up in the event that the principal engine failed. No engine failures occurred in the first year and the second system served primarily as a "check-out" system for the modified stock carburetor. In the second year this system will be used in the transient engine characterization and for initial testing of the alternative fuel-air induction systems.

The principal test engine was instrumented with conventional equipment; however, a few additional pieces of specialized instrumentation are worth noting. A fast time response hot wire anemometer flow transducer was used to measure instantaneous fuel flow rate into the carburetor. In addition, a fast time response pressure transducer was connected upstream of the float bowl fuel shutoff valve for observation of instantaneous pressure. Together, they provided a means for observing the dynamic fuel flow characteristics. Stainless steel exhaust sampling probes and thermocouples were placed in each runner of the exhaust manifold. Their location is indicated in the detail of Figure 1. Likewise, thermocouples were placed in the intake manifold runners as pictured. The thermocouples provided temperature measurement one-quarter inch above the runner floor. A high sensitivity load cell was connected in the linkage hardware of the dynamometer scale for more precise measurement of torque during the setting of MBT spark advance. Manual control over the spark timing was provided by a bracket and lever device which rotated the

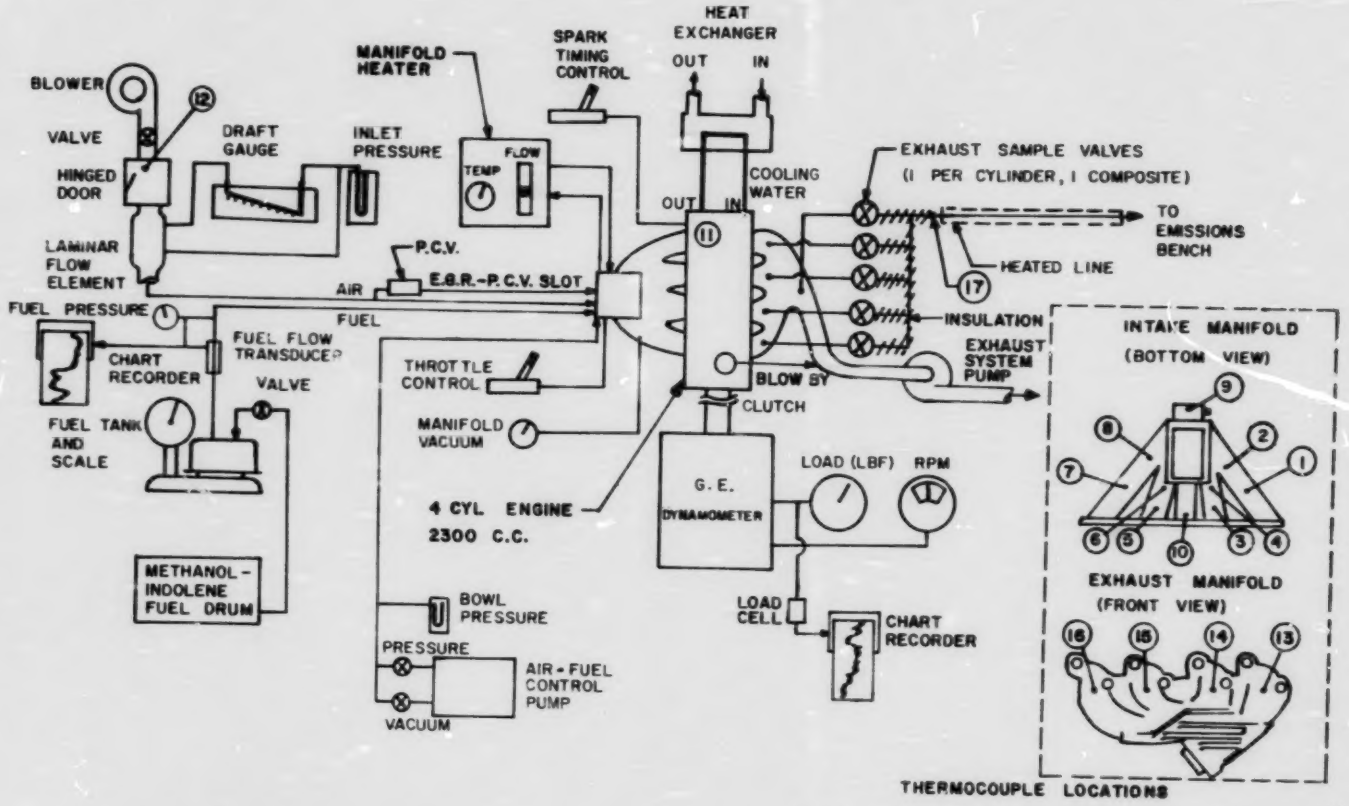

FIG. 1 TEST ENGINE-DYNAMOMETER CONFIGURATION

1. CYL 1 - HEAD
2. CYL 1 - PLENUM
3. CYL 2 - HEAD
4. CYL 2 - PLENUM
5. CYL 3 - HEAD
6. CYL 3 - PLENUM
7. CYL 4 - HEAD
8. CYL 4 - PLENUM
9. WATER TEMP - PLENUM
10. WATER TEMP - HEAD
11. OIL TEMP
12. L.F.E. AIR TEMP
13. CYL 1 EXHAUST
14. CYL 2 EXHAUST
15. CYL 3 EXHAUST
16. CYL 4 EXHAUST
17. EXHAUST EMISSIONS SAMPLE

distributor. An external heating source and fluid was substituted for heating of the intake manifold plenum. (Normally, the stock engine provides engine coolant for this heating.) The external source permits exploration of plenum temperature effects on engine operation; however, comparative test data to date has been taken for a fixed plenum heating temperature of 180 $\pm$ 5°F (consistent with engine coolant temperature).

Air to fuel ratio (or ϕ) control was obtained primarily through pressurization or evacuation of the air space in the float bowl chamber of the carburetor. A small vacuum-pressure pump provided the necessary range of pressures. In addition, an intake air blower provided small positive intake air pressure and thus permitted additional control over the air to fuel ratio. Combined with appropriate main jet changes for methanol, this control technique provided the desired ϕ range for both fuels.

For all testing the EGR system was disconnected; however, the positive crankcase ventilation (PCV) valve was connected in such a way that precarburetor air was passed into the EGR-PCV slot of the carburetor. Blow-by gases were vented into the laboratory exhaust removal system as were the engine exhaust gases. Engine coolant temperature was maintained by the stock thermostat, and a shell and tube heat exchanger provided cooling capability for all engine load conditions.

IV.1.2.2 Carburetor Modification for Methanol Operation: The stoichiometry of methanol-air mixtures dictates a fuel flow rate approximately double that required for gasoline-air mixtures. This is understood a little more clearly in terms of the lower heating values of the two fuels. Methanol's heating value (Btu/lbm basis) is roughly half that of gasoline; thus, to produce comparable power levels roughly twice as much methanol must be burned (assuming comparable thermal efficiencies). After 130 steady state runs on indolene, the stock two barrel venturi carburetor was minimally modified to permit this increased fuel flow. The main and idle jets were replaced but it was found that internal flow passages would not permit adequate fuel flow rates. After sealing off the primary emulsion tube, acceptable fuel flow rates were attainable. This constituted a first-cut conversion, and all the methanol data presented in the report was taken with this configuration.

IV.1.2.3 Experimental Procedure: The procedure for setting a test condition consisted of the following:

(1) Setting a speed and load condition.

(2) Fixing ϕ.

(3) Finally checking the spark timing for MBT conditions.

In the early stages of the testing, MBT was found by noting changes in torque reading on the dynamometer scale. Repeatability in making this setting was not particularly good (primarily in the lean region) and it was found that the condition could be established more accurately using a high sensitivity load cell and strip chart recorder. Even with this improvement, the MBT spark timing curve still showed some erratic behavior. As discussed in the following sections this behavior was attributed to engine operating characteristics rather than errors in experimental technique.

To establish changes in engine performance resulting from the number of test hours or "aging" of the engine, a specified test condition was repeated at regular intervals throughout the steady state testing. This data was used to establish a correction factor which when applied to the performance data eliminated the time dependency or engine "aging" effect. In this way, a fair comparison of indolene and methanol has been made. An illustration of these time dependent effects appears in the Appendix.

The sequence of testing to date has been:

(1) 130 steady state test conditions on indolene, followed by

(2) 47 steady state test conditions on methanol, followed by

(3) 10 steady state runs on a commercial unleaded gasoline.

The latter 10 runs were repeat points of various indolene test conditions. Equivalency of power, thermal efficiency, and emissions for indolene and the commercial unleaded gasoline was established at the end of the indolene base line thus permitting subsequent comparisons of engine results for the repeat test condition.

In the discussion sections that follow, the results are interpreted in light of the maldistribution phenomena. Engine performance appeared to be less sensitive than engine emissions to this phenomena and therefore we have chosen to present performance results initially. More detail of the ϕ variations among the cylinders (maldistribution) will be presented in the emissions section.

IV.1.3 Engine Performance - Indolene versus Methanol: The 140 steady state test points obtained on indolene provided a comprehensive map of engine

performance. Plots of brake power and thermal efficiency across the speed and load range showed behavior typical of multicylinder spark ignition engines. (Some of these plots appear in the Appendix.) The general performance trends also closely follow typical single cylinder engine results such as those presented by Ebersole and Manning.[6] It should be noted that all the power results presented are both temperature and manifold vacuum corrected ($T_{reference}$ = 70°F, and $P_{manifold}$ = 14.0, 7.0, or 0.0 in. Hg vacuum, and $P_{atmosphere}$ = 29.92 in Hg). Some of the performance data will be taken at 4000 RPM; however, the low speed, part load conditions are considered to be of more importance since it is at these conditions that typical automotive engines spend the majority of their operating lifetimes.

IV.1.3.1. Lean Misfire Limit and MBT Spark Advance for a Multicylinder Engine: The lean burning capability of methanol in engines is well documented in the literature; however, most of the data is for single cylinder engine operation. In multicylinder engines, nevertheless, this lean operating capability can be effectively masked if significant ϕ variations exist among the cylinders. Figure 2, a comparative plot of MBT spark advance as a function of the composite (average) ϕ for two load conditions, demonstrates this fact. Note that at the wide open throttle condition (0 in. Hg manifold vacuum), the indolene shows an "effective" lean limit which is leaner than the methanol results. The lean limit is termed "effective" because one cylinder is operating much leaner than the composite ϕ indicates. Figures 3 and 4 indicate the "true" lean limit for the two fuels in this four-cylinder engine. In these plots, four individual cylinder ϕ's appear for each composite ϕ that appears in Figure 2. Figure 3 (wide open throttle conditions) shows that methanol's true lean limit is beyond that of indolene. This is not obvious in Figure 2. These ϕ variations among cylinders are responsible for indicating an apparent (or effective) lean limit at ϕ = 0.82 when, in fact, it is due to the leanest cylinder operating at ϕ = 0.64. Figure 4, the part load comparison corroborates the effective lean limit results of Figure 2. This results from the fairly good agreement in ϕ among the cylinders for both fuels.

The results indicate that as the cylinder-to-cylinder variation in ϕ is decreased, the effective lean limit approaches the true lean limit. Practically speaking, this means that in the absence of maldistribution, engines can operate at leaner ϕ's without engine misfire for any fuel. This condition was approached at the higher manifold vacuum setting, as indicated in Figure 4.

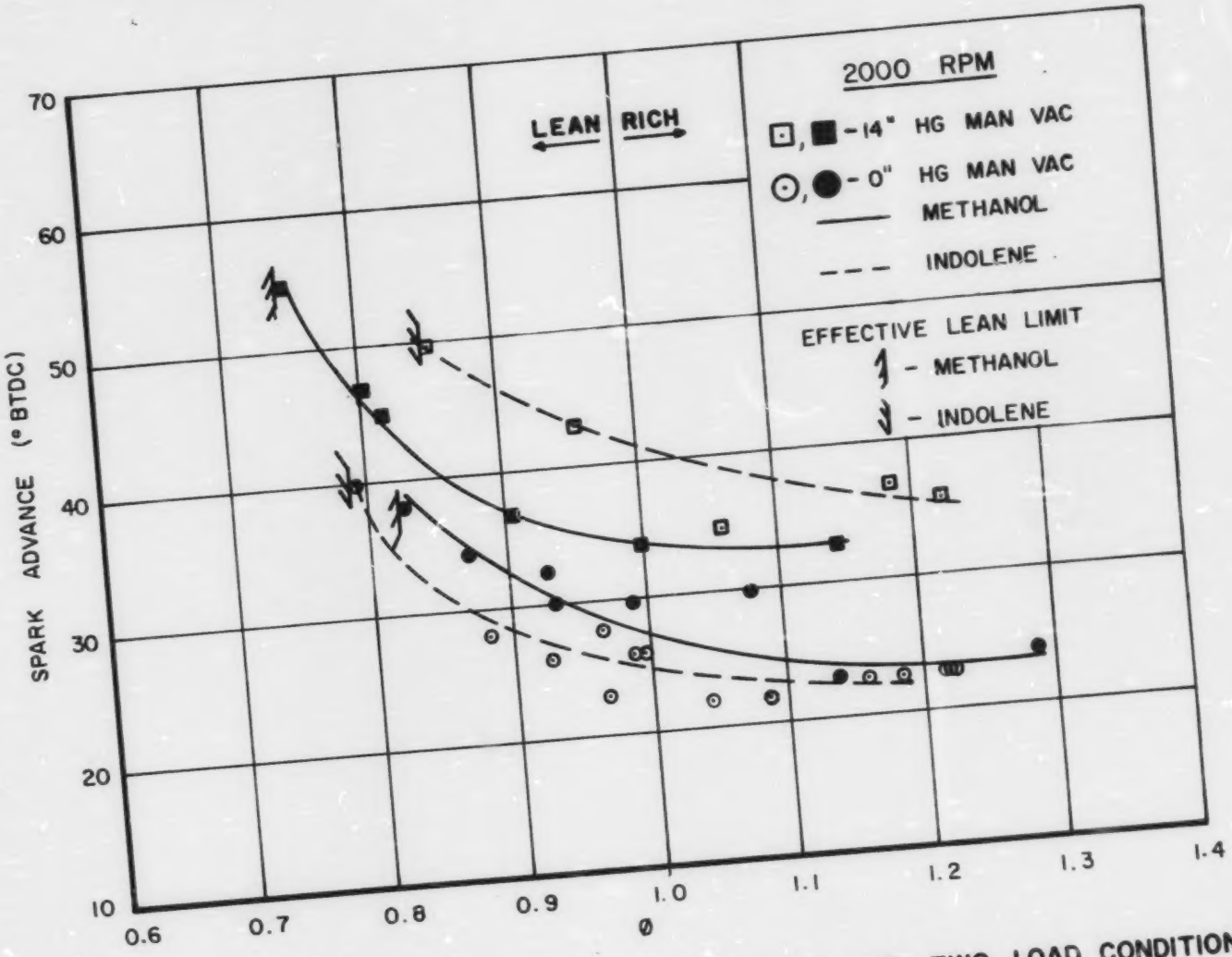

FIG. 2 MBT SPARK TIMING EFFECTIVE LEAN LIMIT FOR TWO LOAD CONDITIONS METHANOL vs INDOLENE

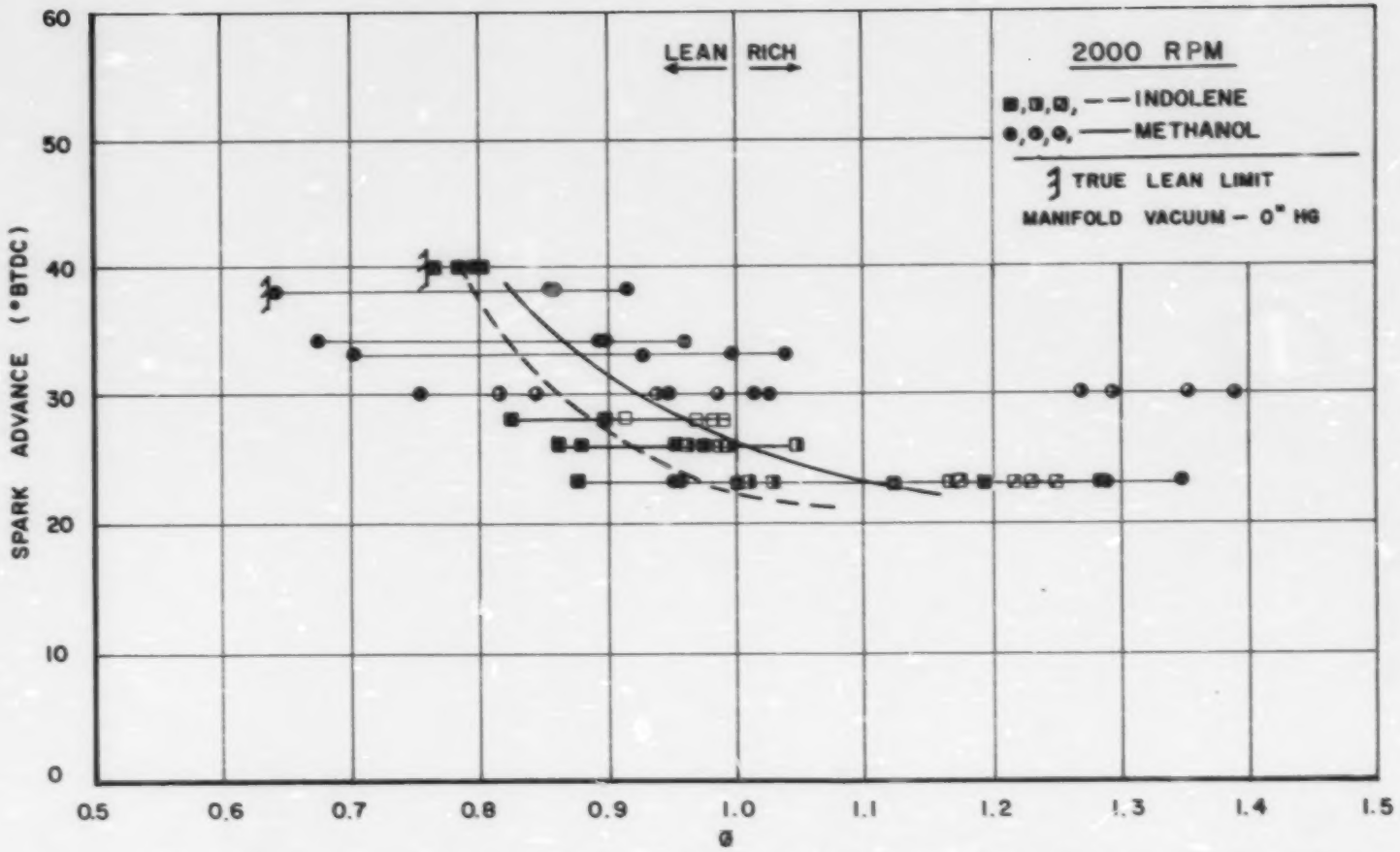

FIG. 3 MBT SPARK TIMING SHOWING TRUE LEAN LIMIT AND CYLINDER Ø VARIATIONS, WIDE OPEN THROTTLE — METHANOL vs INDOLENE

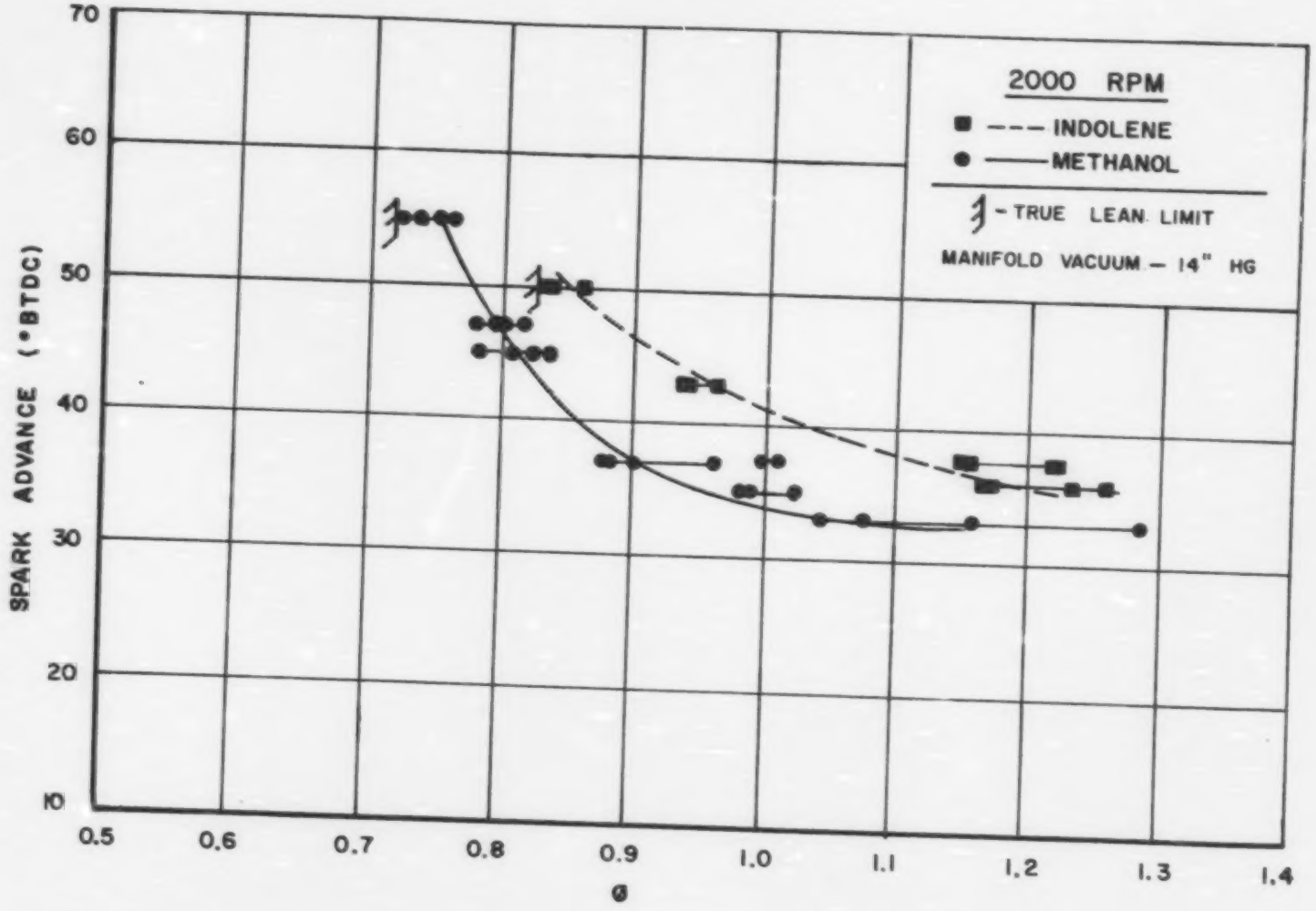

FIG. 4 MBT SPARK TIMING SHOWING TRUE LEAN LIMIT AND CYLINDER Ø VARIATIONS FOR PART LOAD CONDITION — METHANOL vs INDOLENE

Both Figures 3 and 4 clearly show methanol's leaner operating ability in comparison with indolene.

These MBT curves supply one additional piece of information. With significant maldistribution, none of the four cylinders are operating at their individual MBT spark settings, and this is especially true in the lean region where spark sensitivity to equivalence ratio is the greatest. The engine's MBT spark setting is actually a compromise. Maldistribution, where one cylinder is excessively lean,as seen in Figure 3,causes spark timing to be advanced to keep that cylinder from misfiring. But, this in turn reduces power and efficiency in the richer cylinders because the spark is over-advanced for those cylinders. This results in lower overall power and efficiency for the four cylinder engine. The over-advanced and retarded spark condition also limits the range of acceptable spark timing at which the engine will operate. During the indolene runs, there was one condition in which this spark tolerance band was only 5 degrees in width (27° to 33° BTDC). This condition was at 2000 RPM-wide open throttle with a composite ϕ of 0.80. This lean setting was an unstable condition for which load had to be adjusted constantly to maintain engine speed. Data was taken at both spark settings; however, at greater spark advances severe knocking occurred, and at lower spark advances misfire occurred.

These non-optimized spark settings also affect hydrocarbon, aldehydes, and oxides of nitrogen emissions. Special attention is paid to the NO_x in the section on emissions results.

IV.1.3.2 Comparative Power at 2000 RPM: As indicated in Figure 5, even with the severe maldistribution of the methanol runs, comparable power was delivered by the engine for like load and equivalence ratio settings. The leanest operating engine condition occurred with methanol at a manifold vacuum of 7 in. Hg. The distribution of ϕ values among the cylinders is indicated for this point. The maldistribution was relatively small in this instance, thus allowing stable engine operation at a composite ϕ of 0.65.

Characteristic of all spark ignition engine operation is the more abrupt fall-off of power in the lean region. This is seen a little more clearly in an expanded ordinate plot of BHP versus ϕ (see Appendix). Given maldistribution, the individual cylinder power can be estimated from Figure 5, which is really a plot of "composite" engine power. For the worst instance of maldistribution at wide open throttle on methanol, ϕ varied by 0.72 between the

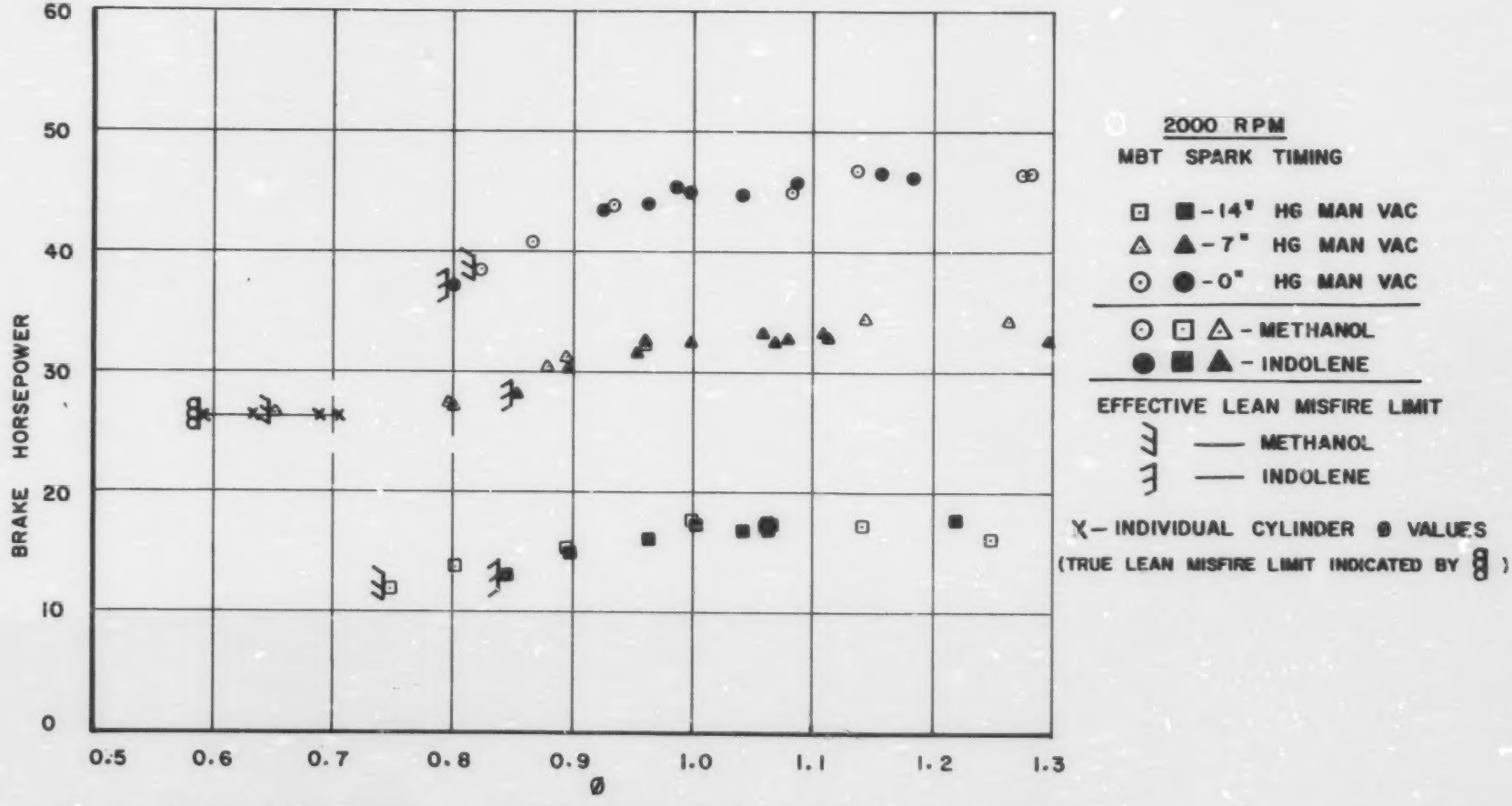

FIG 5: BRAKE HORSEPOWER VS EQUIVALENCE RATIO - METHANOL VS INDOLENE

worst two cylinders (cylinder 4, ϕ = 0.93 and cylinder 3, ϕ = 1.65). The corresponding BHP for these two cylinders was approximately 43.7 and 46.6, or a variation of about 6%. In the lean region, though, variation of ϕ in one instance was only 0.27 ϕ, but this resulted in cylinder BHP values of 34.0 and 45.7, or a 34% variation in power. This indicates that lean burning engines must have good control over individual cylinder ϕ in order to maintain maximum engine power.

IV.1.3.3 Comparative Thermal Efficiency at 2000 RPM: From an energy standpoint the engine brake thermal efficiency indicates the true merit of one fuel over another, since it is a measure of the useful work supplied for the fuel energy input. In Figure 6, the brake thermal efficiency is plotted for the three engine load conditions; again as a function of the equivalence ratio. For each load condition, methanol shows an improvement over indolene. The increase in thermal efficiency at ϕ = 1.0 for each case translates in a fuel savings on an energy basis of 9% for full load, 4% for the two-third load condition, and 10% for the one-third load condition. At the 7 in. Hg manifold vacuum setting, note that indolene's effective lean limit is located at ϕ = 0.82. In comparison, at this ϕ, methanol is showing an 18% savings in fuel.

Thermal efficiency decreases eventually for both fuels as the lean region is penetrated because of the approach to the flammability limit. However, if maldistribution could be eliminated,the thermal efficiency curves for both fuels would maintain higher values in the lean region than is indicated by these engine results. In addition, the results for methanol indicate superior performance when compared to indolene, even with the increased maldistribution.

In summary, the steady state experimental performance results at 2000 RPM indicate that even with a non-optimized fuel-air induction system (which results in a characteristic maldistribution of the fuel-air mixture among the cylinders),methanol shows comparable power and improved thermal efficiency over indolene. Methanol also shows a leaner operating capability than indolene at the two lower load settings. Maldistribution phenomena can be so severe (as is indicated by the wide open throttle results) that the true lean limit for both fuels is effectively masked, and an effective lean limit at higher ϕ determines the lean operating limit of a multicylinder engine.

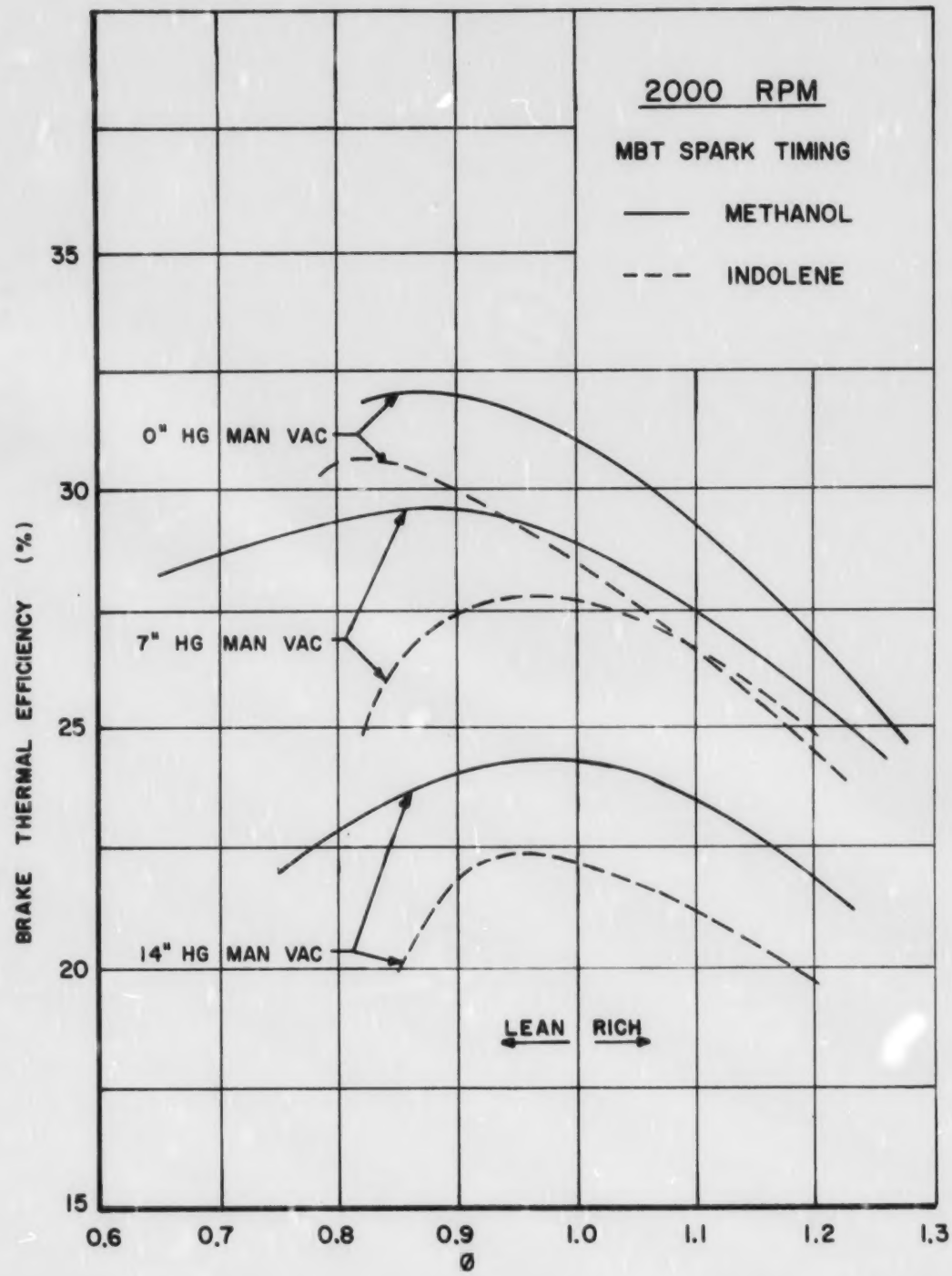

FIG. 6 COMPARATIVE BRAKE THERMAL EFFICIENCY – METHANOL vs INDOLENE

IV.1.4 Engine Exhaust Emissions: Constituent exhaust species measured during the steady state testing of methanol and indolene have included CO_2, CO, O_2, unburned hydrocarbons (UBF), NO, NO_x, and total aldehydes. A schematic of the exhaust sampling system appears in Figure 7. The system includes conventional continuous on-line analyzers for detection of individual chemical species. Non-dispersive infrared (NDIR) was used for CO_2 and CO analysis, a polarographic sensor was used for O_2 analysis, a heated flame ionization detection (HFID) was used for UBF analysis, and a heated chemiluminescent analyzer was used for NO and NO_x analysis. Aldehydes were the only chemical species not continuously monitored. They were determined through the use of a wet chemical technique, known as 3-methyl-2-benzothiazolone hydrazone (MBTH), which measures the total aldehydes. Two instruments needed special calibration for methanol exhaust emissions analysis. The HFID was found to have a relative linear response factor of 0.85 to methanol vapor in comparison to propane. In addition, the NO/NO_x analyzer showed a slight response to methanol vapor. This was a nonlinear effect when plotted as a function of ppm methanol. The response asymptotically approached 80 ppm NO_x (indicated) for increasing ppm methanol.

All emissions results are presented on a dry basis. Traditionally, NO_x has been reported as NO_2, even though NO_2 may not have been the primary constituent. For the sake of comparison with literature and previous progress reports, it will be reported in this manner. It should be noted, however, that no NO_2 was detected in the indolene exhaust, and little has been detected during methanol testing to date.

For steady state testing, emissions results are presented primarily on a grams per indicated horsepower hour basis. This normalizes emissions with respect to the useful energy developed by the engine. On this basis, emissions are strongly influenced by equivalence ratio (ϕ) and usually to a lesser degree by engine speed, load, spark timing, and inlet air temperature (with the exception of NO/NO_x). For this reason ϕ is chosen as the independent variable for presentation of the exhaust emissions results. Emissions, with the possible exception of unburned hydrocarbons, did not appear to be highly influenced by the range of inlet temperatures encountered during testing. For this reason temperature reference does not appear on the graphs. It should be noted that intake air temperatures ranged between 70°F and 95°F for the indolene runs and between 62°F and 84°F for the methanol runs.

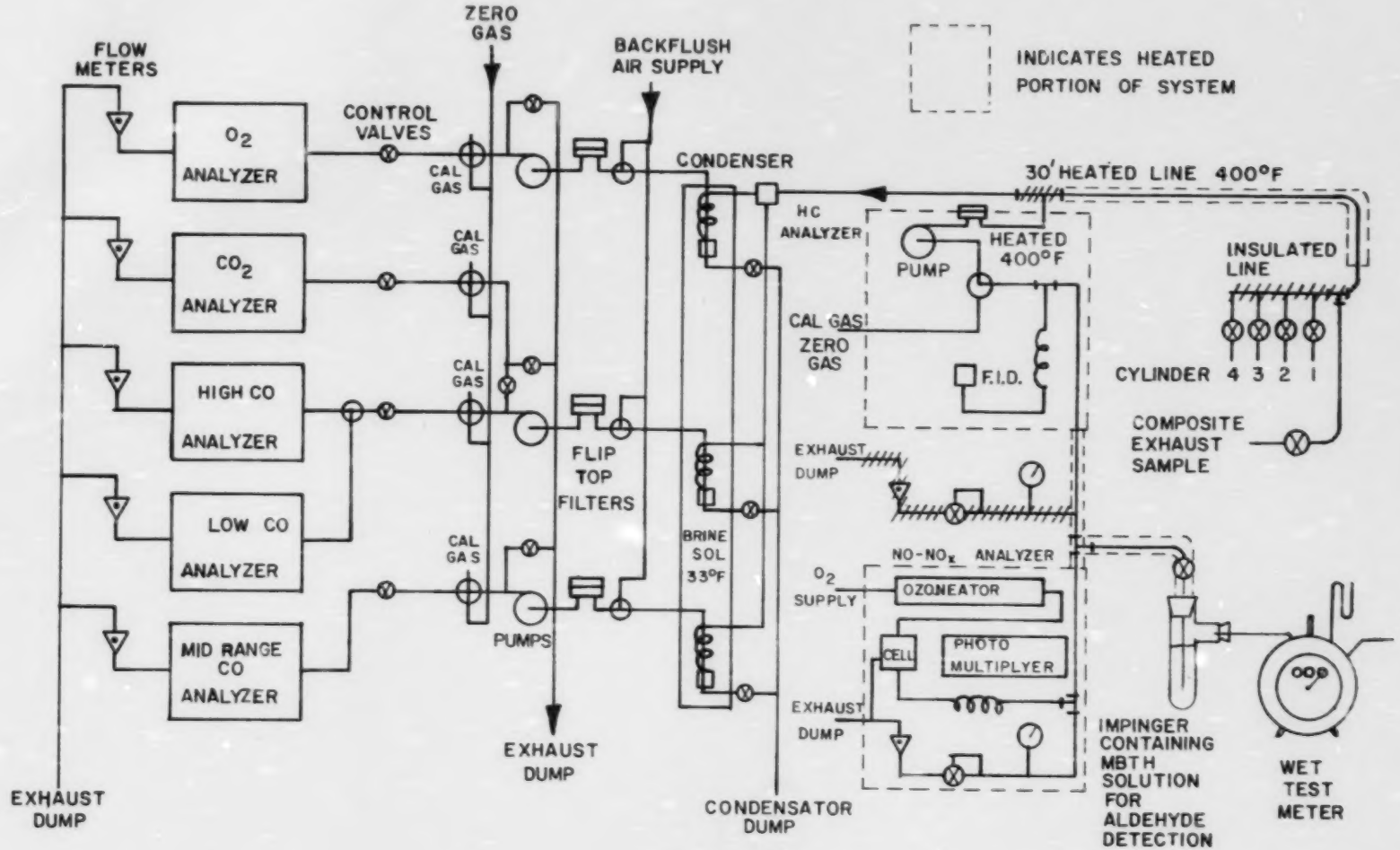

FIGURE 7: EXHAUST EMISSIONS SAMPLING SYSTEM

IV.1.4.1 Cylinder-to-Cylinder Equivalence Ratio Variations: In the engine performance results, certain behavior was attributed to the cylinder-to-cylinder equivalence ratio variations. Figure 8 shows this maldistribution for the individual cylinders at 2000 and 3000 RPM while operating on indolene. Note that cylinder equivalence ratio (ϕ_{cyl}) has been normalized with respect to the composite equivalence ratio (ϕ_{comp}); also, this composite equivalence ratio is the average of the four ϕ_{cyl}. The variations appear to be systematic at high manifold vacuum with little dependence on ϕ_{comp}. At wide open throttle the behavior becomes erratic. At times, cyclinder 2 and 3 are lean relative to cylinders 1 and 4, and at times just the opposite effect occurs: 1 and 4 are lean relative to 2 and 3. This behavior is illustrated in Figure A3 (Appendix) where the maldistribution and BHP appear as functions of ϕ_{comp} at 2000 RPM. This anomalous behavior is believed in part due to the operation of the secondary power jet in the carburetor and its interaction with the test procedure utilized for controlling ϕ_{comp}. The worst distribution for indolene (3000 RPM, ϕ_{comp} = 0.9, 0 in. Hg manifold vacuum) shows a 26% variation in ϕ_{cyl}. This represents a variation of 3.8 in air to fuel ratio for indolene. The complete range of maldistribution for indolene at all speeds, excluding 4000 RPM, can be seen in Figure A5 (Appendix).

Figure 9 displays the maldistribution for methanol at 2000 RPM for the same carburetor rejetted for methanol. Figure 10 compares the two fuels at similar equivalence ratios. Note that in comparison to the 2000 RPM indolene data, the maldistribution is greatly exaggerated with methanol. The worst distribution (ϕ = 1.3, 0 in. Hg manifold vacuum) shows a 0.72 variation in ϕ_{cyl}, which represents a 3.2 variation in air to fuel ratio (stoichiometric air-fuel = 6.4). Maldistribution results for the two fuels at wide open throttle (see Figures A3 and A4, Appendix) show that methanol yields more consistent trends but greater cylinder to cylinder variations than indolene. Cylinder 4 is always the leanest and cylinders 2 and 3 are almost always the richest. This comparative evidence indicates that the carburetor modifications for methanol use have not improved the serious maldistribution of the OEM system. An iteration on carburetor modification before the bulk of the methanol baseline data is acquired is expected to reduce the severity of this maldistribution.

In summary, the methanol data represents results for a first attempt at modifying the carburetor through simple jet replacement to allow for the increased fuel flow. Yet, even though this modification resulted in increased

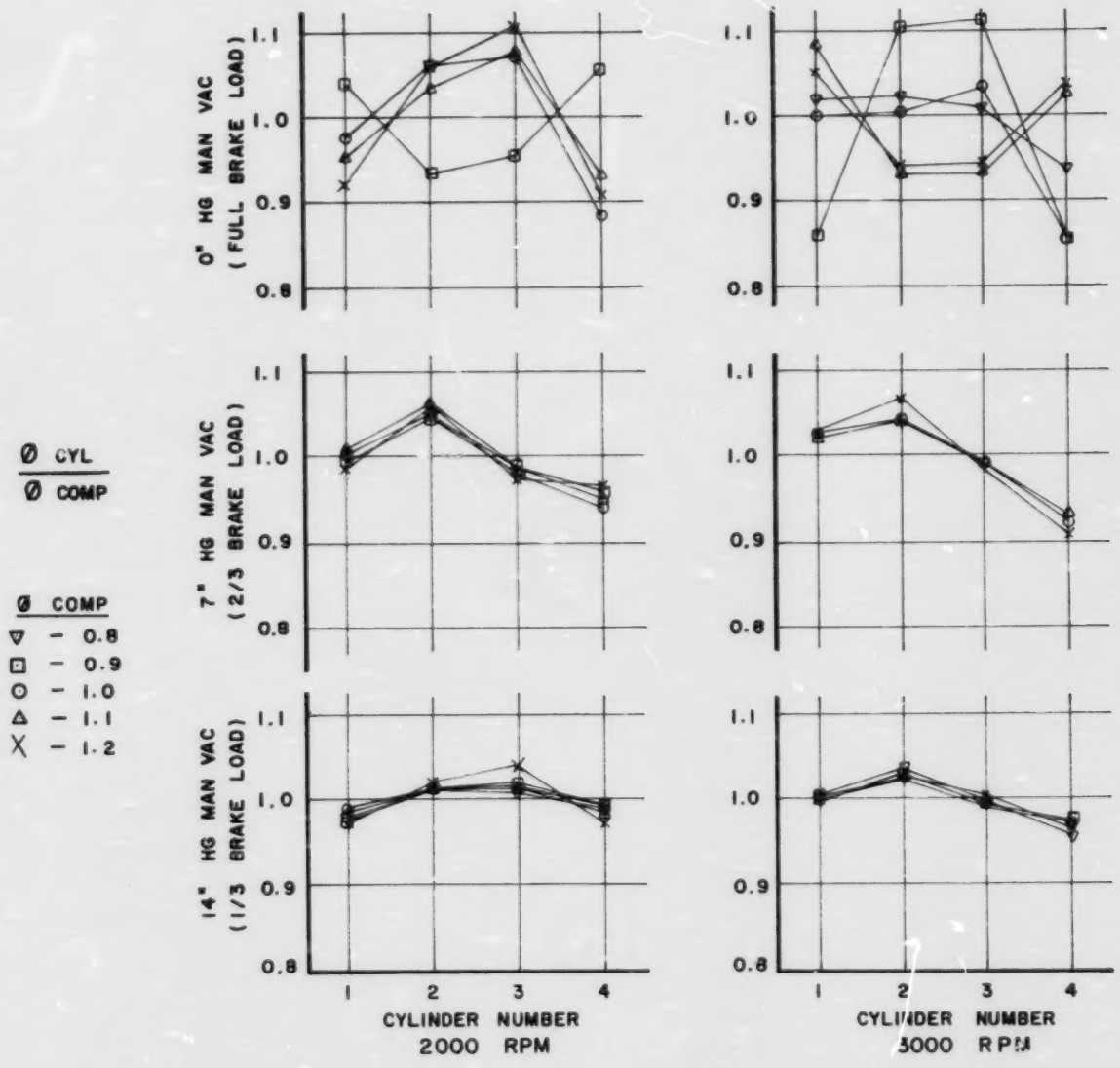

FIG. 8: CYLINDER TO CYLINDER EQUIVALENCE RATIO VARIATIONS – INDOLENE

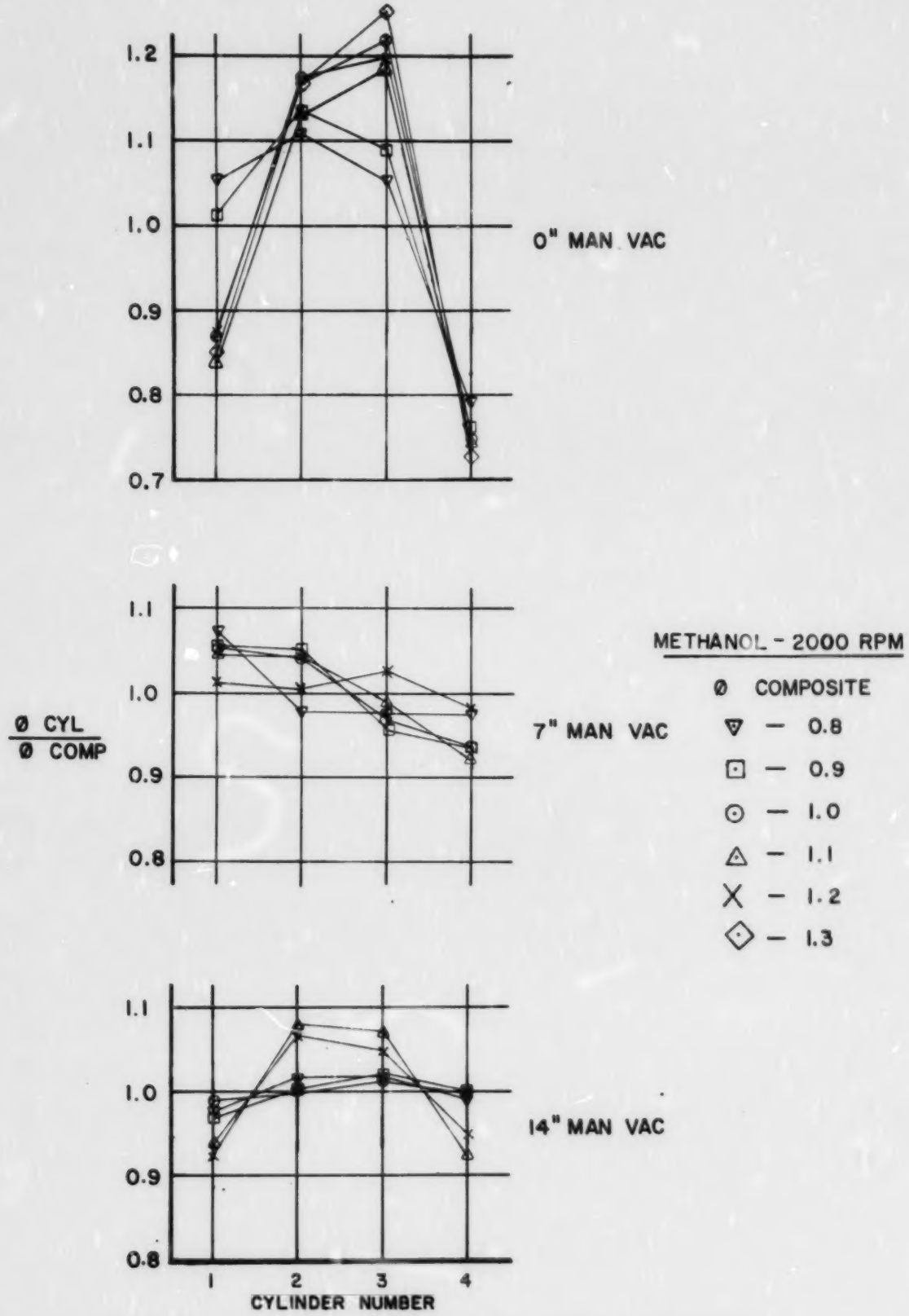

FIG. 9: CYLINDER TO CYLINDER EQUIVALENCE RATIO VARIATIONS METHANOL

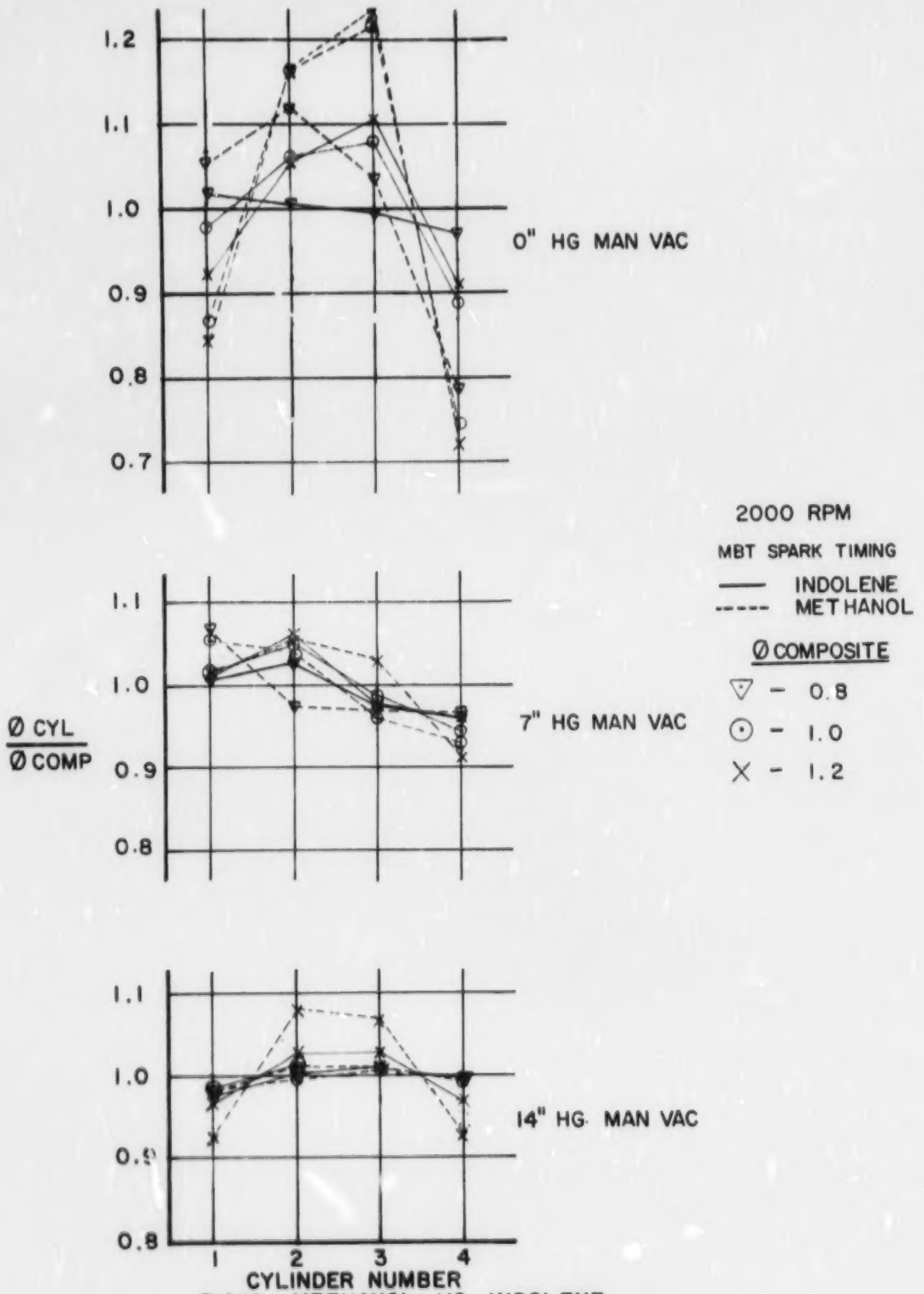

FIG.10 METHANOL VS INDOLENE
CYLINDER TO CYLINDER EQUIVALENCE RATIO VARIATION

maldistribution for methanol, the engine performance data indicated improved engine thermal efficiency, comparable power, and an extended lean operating range.

IV 1.4.2 CO_2, CO and O_2: Exhaust emissions are much more sensitive to variations in ϕ resulting from the maldistribution phenomena than are engine performance characteristics. Figures 11, 12 and 13 show individual cylinder measurements of CO_2, CO, and O_2 for all the indolene test conditions. These plots, presented on a per cent (dry exhaust) versus ϕ_{cyl} basis, serve to illustrate this point. On each graph three runs are indicated (four similar symbols representing the four cylinder ϕ values for a test condition). These indicate the typical spread caused by maldistribution. As is well documented in the literature,[7] values of these three constituents are virtually independent of engine speed, load, spark timing, and inlet air temperature. Our results confirm this.

With these three constituents and knowledge of the fuel composition, ϕ can be readily calculated after balancing the chemical equation which represents the combustion process. The equation form and solution technique, which provides an internal check on the experimental determination of the three species, is detailed in the Appendix. The water-gas reaction with a constant of 3.5 was used to determine hydrogen in the exhaust. Since these constituent gases are dependent on the stoichiometry only, they serve as an excellent check on data being generated in new test conditions.

The ϕ_{comp} values for the engine show data deviating from the individual cylinder plots. These composite results for indolene can be found in the Appendix.

IV.1.4.3 CO_2, CO, O_2 Comparative Results: Figures 14, 15 and 16 show comparative individual cylinder results for indolene and methanol. The curves represent best fit of all the indolene data and the symbols represent results for methanol at 2000 RPM. Methanol data points nearly match the indolene curves except in the rich region where CO_2 and CO start to diverge. The most obvious difference, however, is the extension of the equivalence ratio range when operating on methanol. The lean limit for indolene is close to $\phi = 0.7$, while for methanol it is closer to $\phi = 0.6$.

IV.1.4.4 UHC, Aldehydes, and NO_x-Indolene: Unburned hydrocarbons (or fuel), oxides of nitrogen, and aldehydes for indolene show marked dependence on the

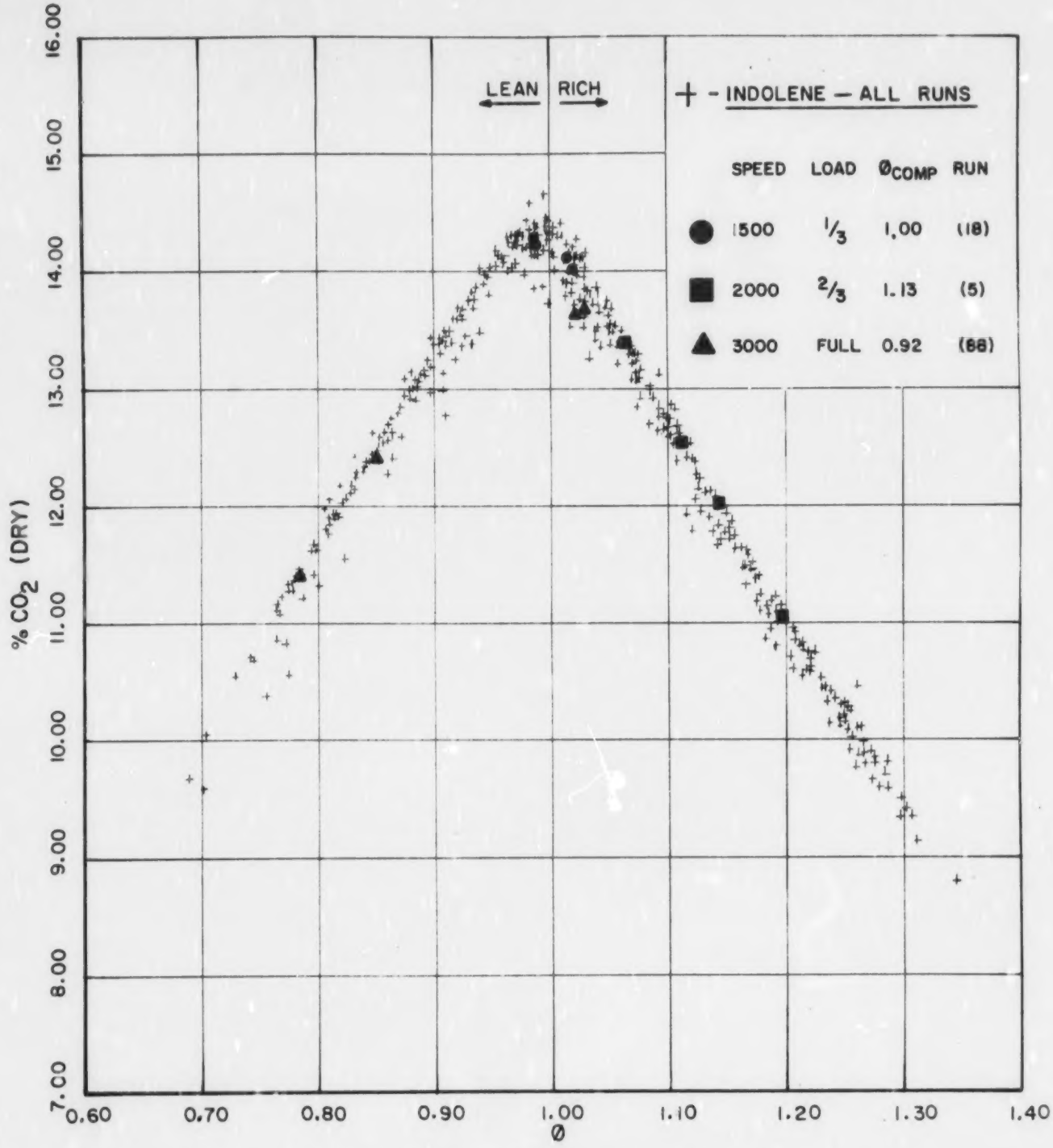

FIG. 11: CO_2 VS EQUIVALENCE RATIO — INDOLENE DATA

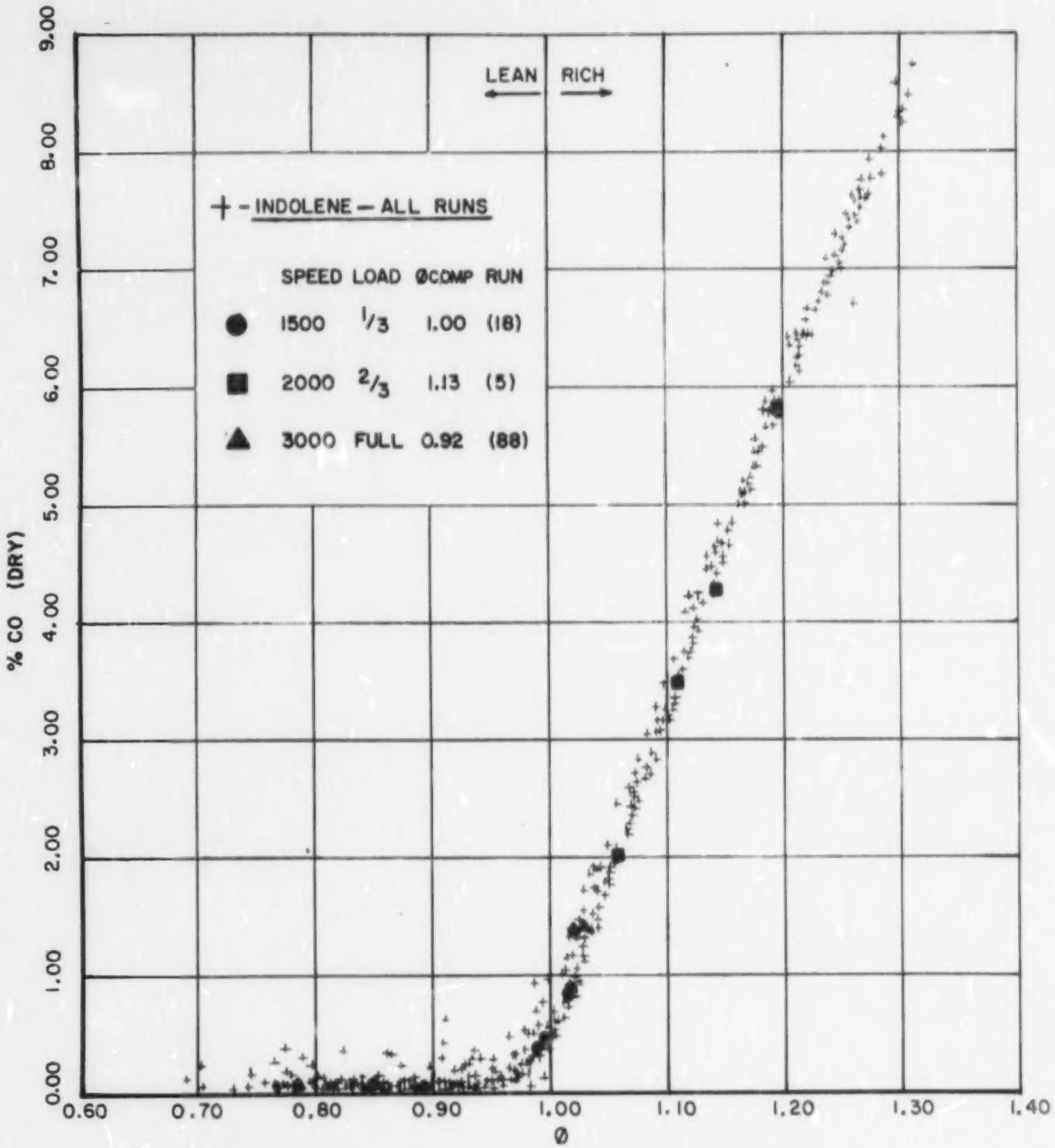

FIG. 12 CO vs EQUIVALENCE RATIO — INDOLENE DATA

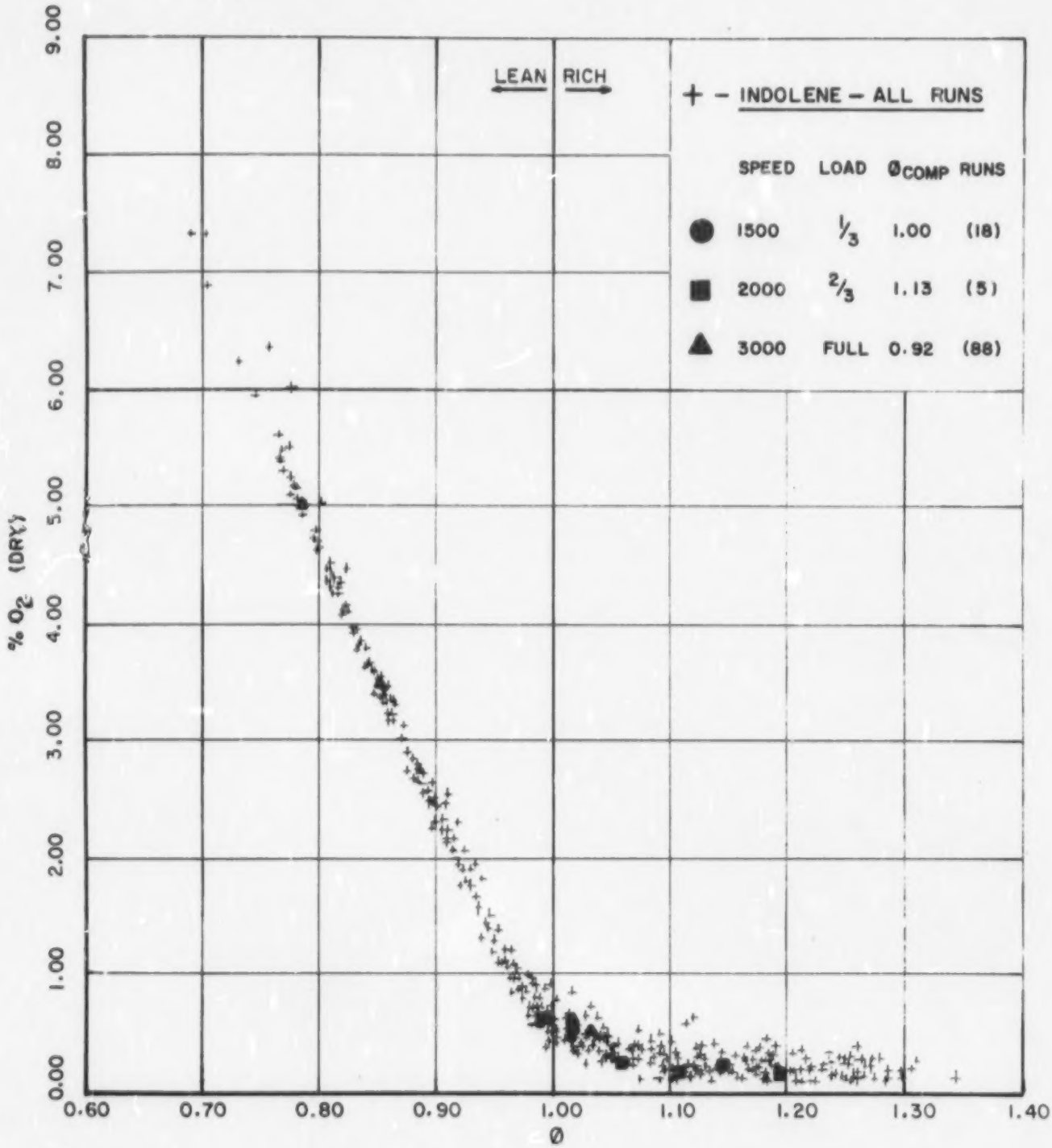

FIG.13 O_2 vs EQUIVALENCE RATIO – INDOLENE DATA

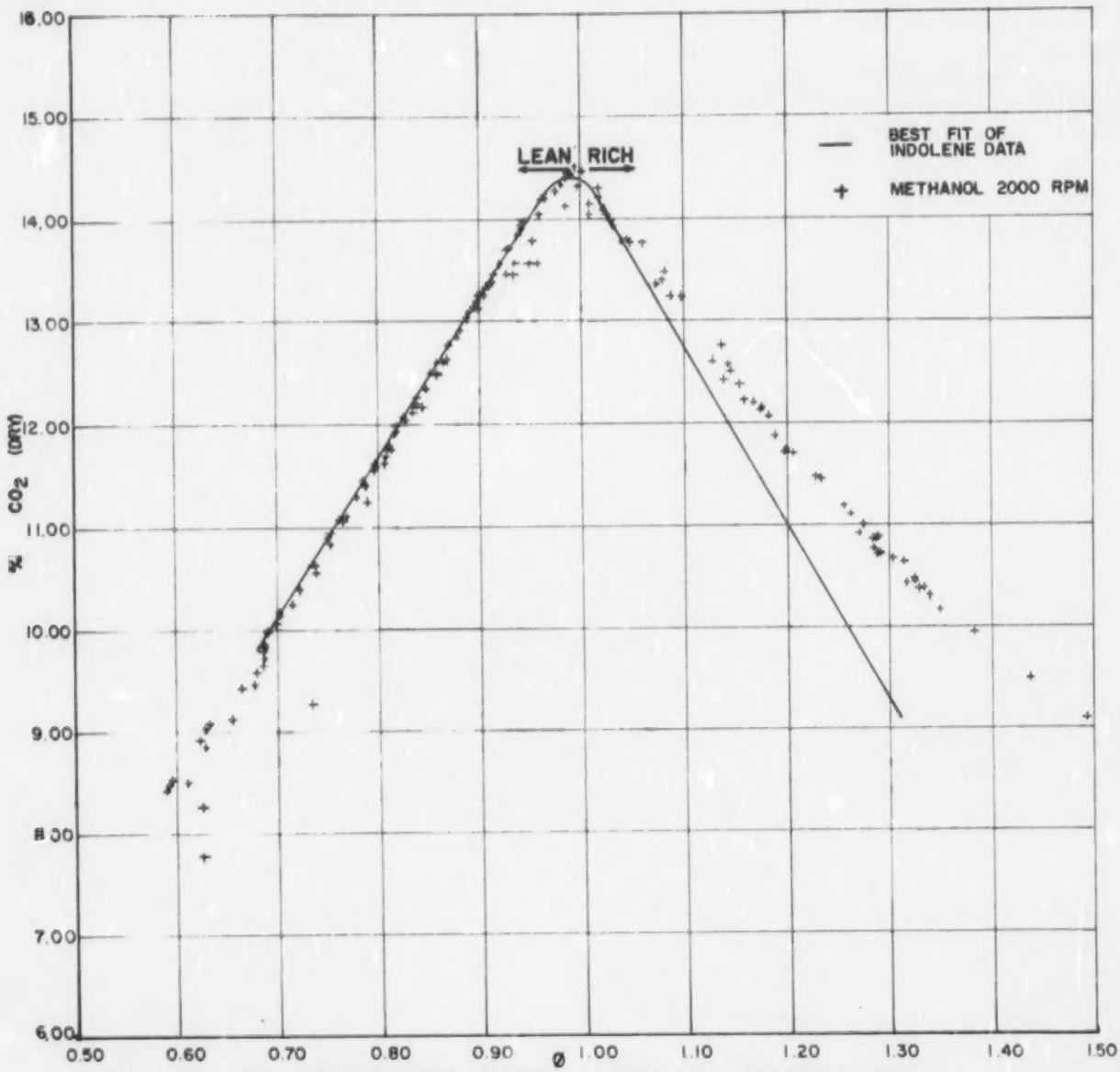

FIG. 14 CO_2 VS EQUIVALENCE RATIO — INDIVIDUAL CYLINDER DATA

METHANOL VS INDOLENE

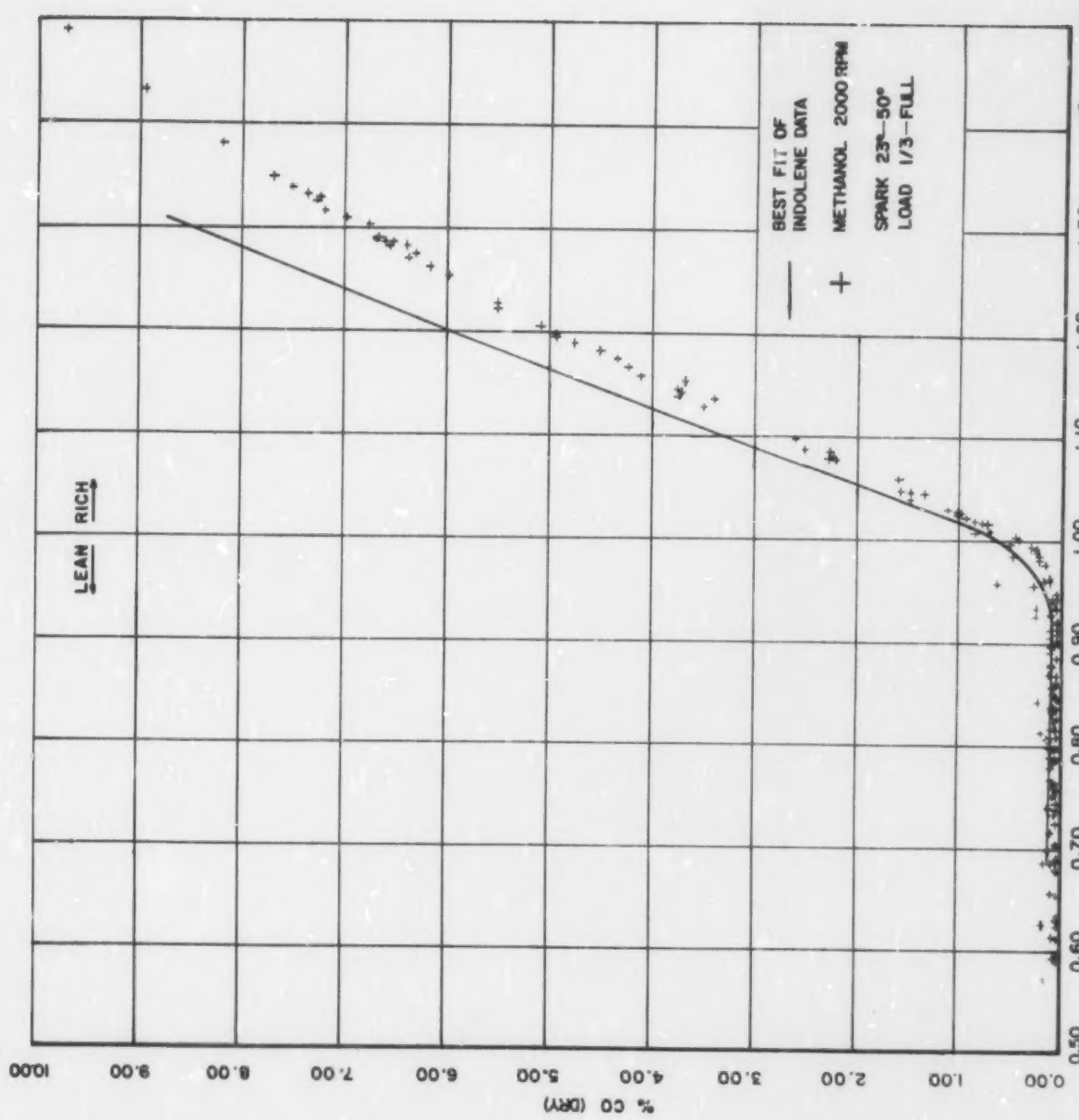

FIG.15 CO VS EQUIVALENCE RATIO - INDIVIDUAL CYLINDER DATA - METHANOL VS INDOLENE

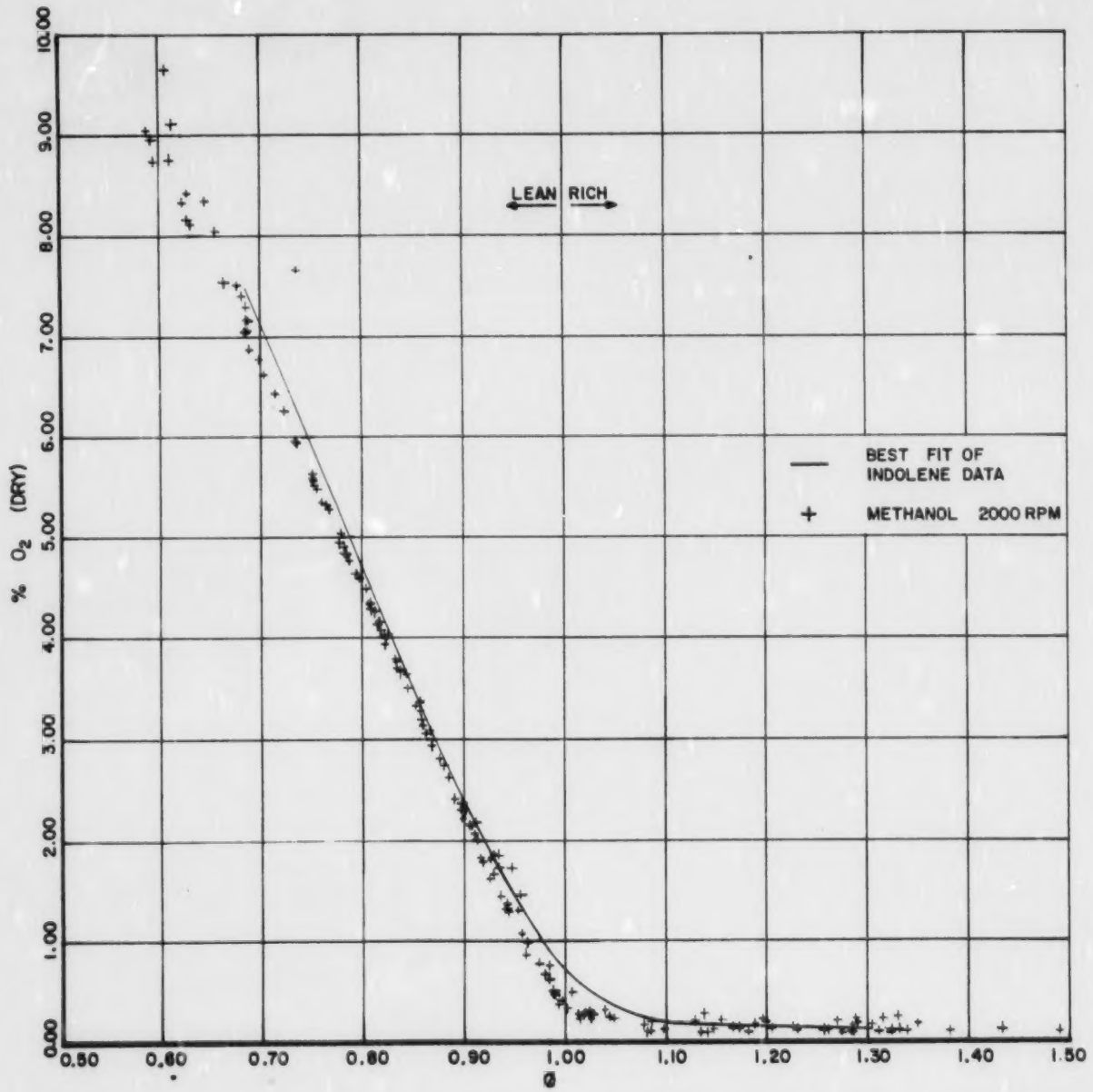

FIG. 16 O_2 VS EQUIVALENCE RATIO - INDIVIDUAL CYLINDER DATA – METHANOL VS INDOLENE

other engine variables. Figures 17, 18 and 19 display composite exhaust results for these respective pollutants. The data represents all the indolene runs. Aldehydes are calculated as formaldehyde, since the total aldehyde technique by MBTH method of analysis was used. This method cannot distinguish among the various aldehydes present in the exhaust sample but it is generally accepted that formaldehyde makes up 70% to 90% of the total.

General trends show unburned hydrocarbons increasing in the rich region, aldehydes increasing in the lean region, and oxides of nitrogen peaking on the lean side of stoichiometric air-fuel ratio. The oxides of nitrogen show the most sensitive dependency on ϕ (and therefore on the degree of maldistribution) of any of the measured emissions species. The scatter of the data in Figure 19 is due to the combined effects of maldistribution and the influences of other engine variables (notably the spark timing). By separating all the influencing parameters, the NO_X data becomes amenable to analysis.

Beginning with Figure 19, one important feature of the composite NO_X results is seen clearly. High levels occur nearly to the effective lean misfire limit ($\phi = 0.8$). This indicates that control over NO_X by lean engine operation was not possible. If the maldistribution phenomena is eliminated, control may be possible, as is indicated in Figure 20, where the individual cylinder results appear. Low levels of NO_X occur at $\phi = 0.8$ and leaner, and the peak is defined more clearly. This latter effect is just the result of eliminating the non-linear averaging of the four cylinder values of NO_X.

Figures 21 and 22 are speed and load dependency plots of NO_X at MBT spark timing. The coherency of the data for rich ϕ indicates that neither parameter significantly alters the production of NO_X. However, in the lean region significant scatter occurs near the peak NO_X equivalence ratios. The scatter principally results from the effect that maldistribution has on the setting of MBT spark timing. As previously discussed in Section IV.1.2.1, two cylinders usually operate at retarded spark, while the other two operate at over-advanced spark setting. In other words, MBT conditions for the engine are not MBT conditions for the individual cylinders. The effect that retard or over-advance has on engine power and NO_X emissions is indicated in Figure 23. (The NO_X shown is that being produced by one cylinder operating near peak NO_X equivalence ratio.) Here, MBT spark timing is 31.5 degrees before top dead center (BTDC). By over-advancing the spark by another 12 degrees to 43.5°BTDC, the NO_X has doubled. At the same time, indicated power has decreased by 4%. Retarding from 31.5° further reduces NO_X emissions, but power and fuel economy (not shown)

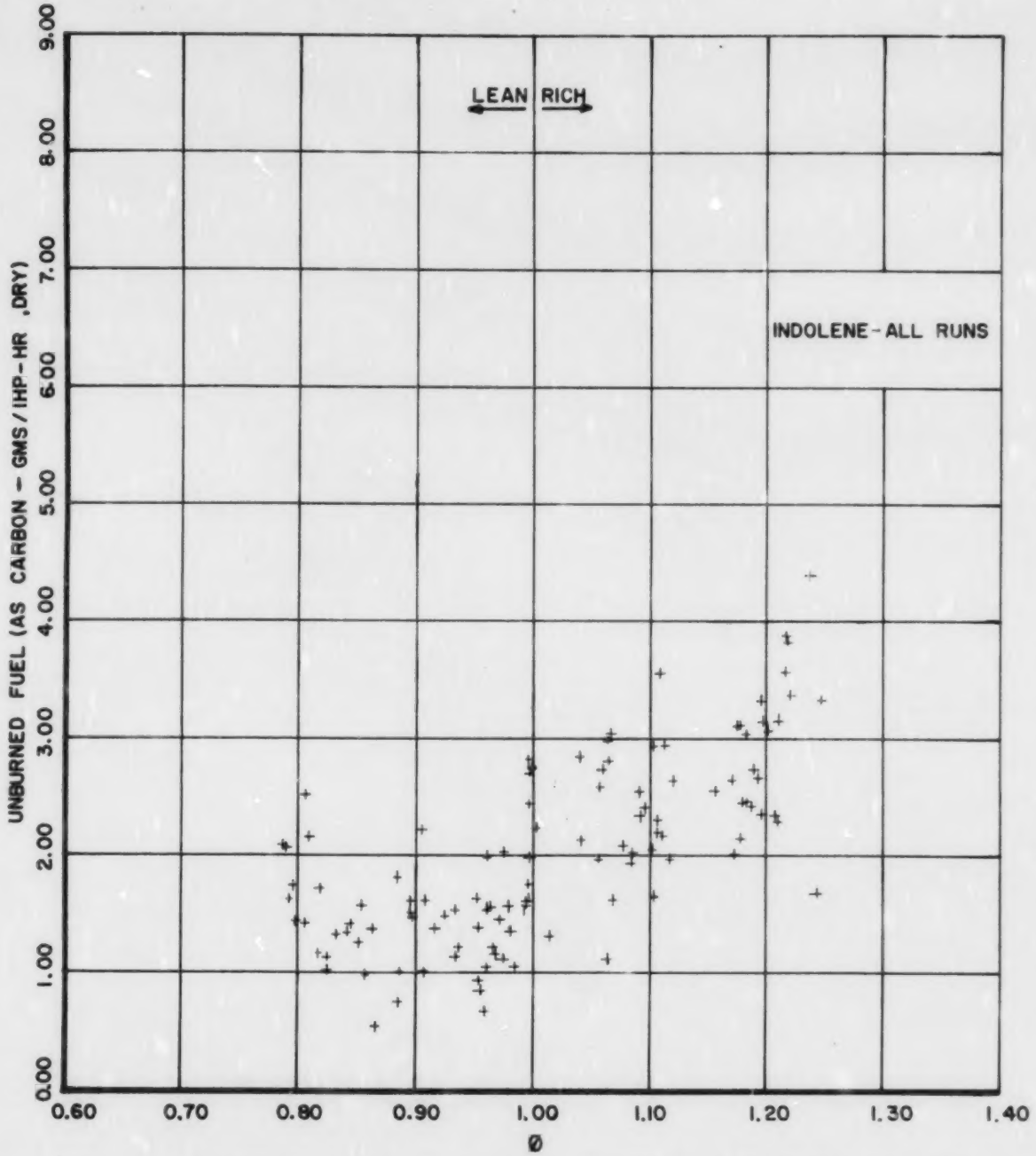

FIG. 17: UNBURNED FUEL VS EQUIVALENCE RATIO—COMPOSITE CYLINDER DATA

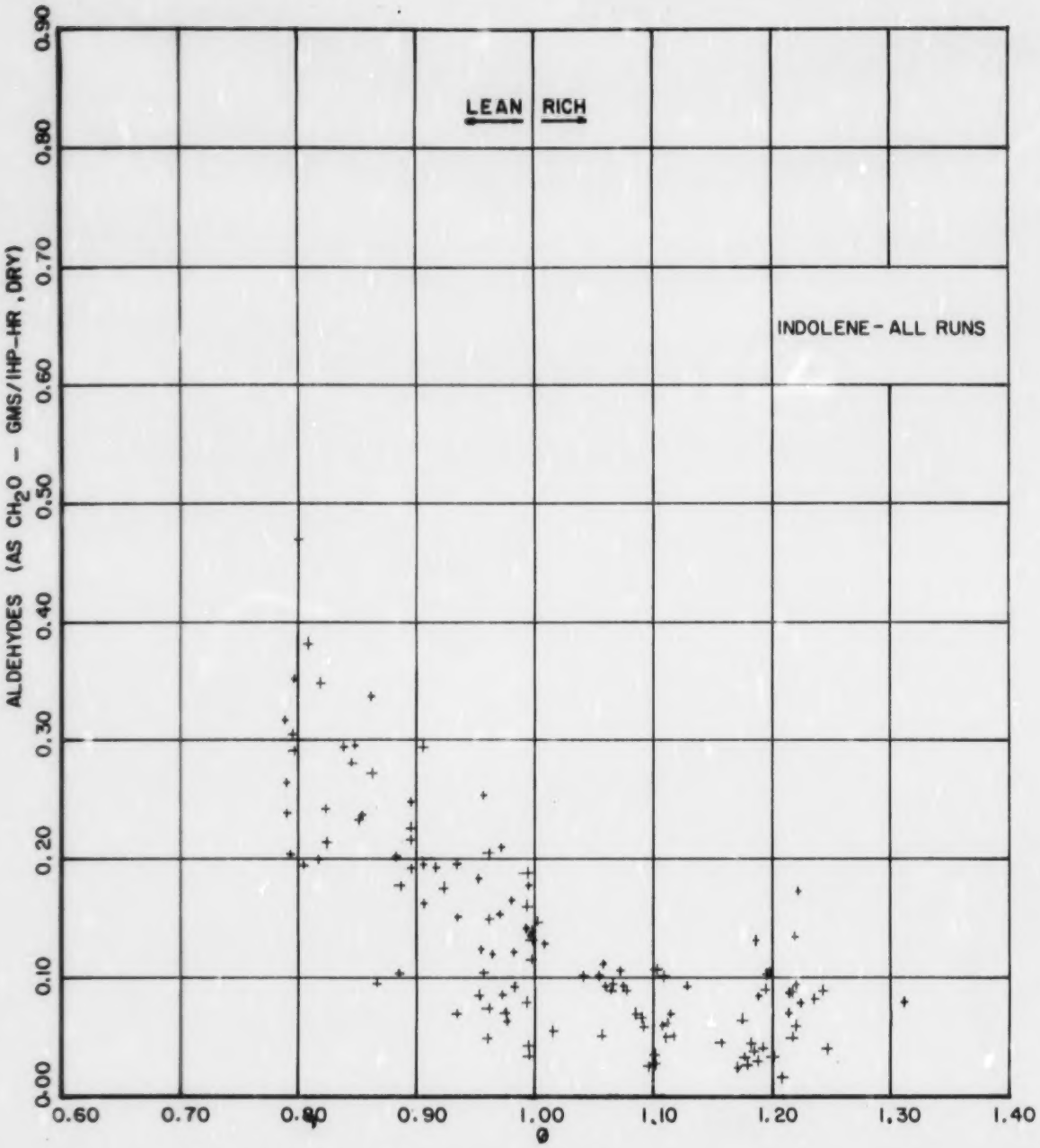

FIG. 18: ALDEHYDES vs EQUIVALENCE RATIO - COMPOSITE CYLINDER DATA

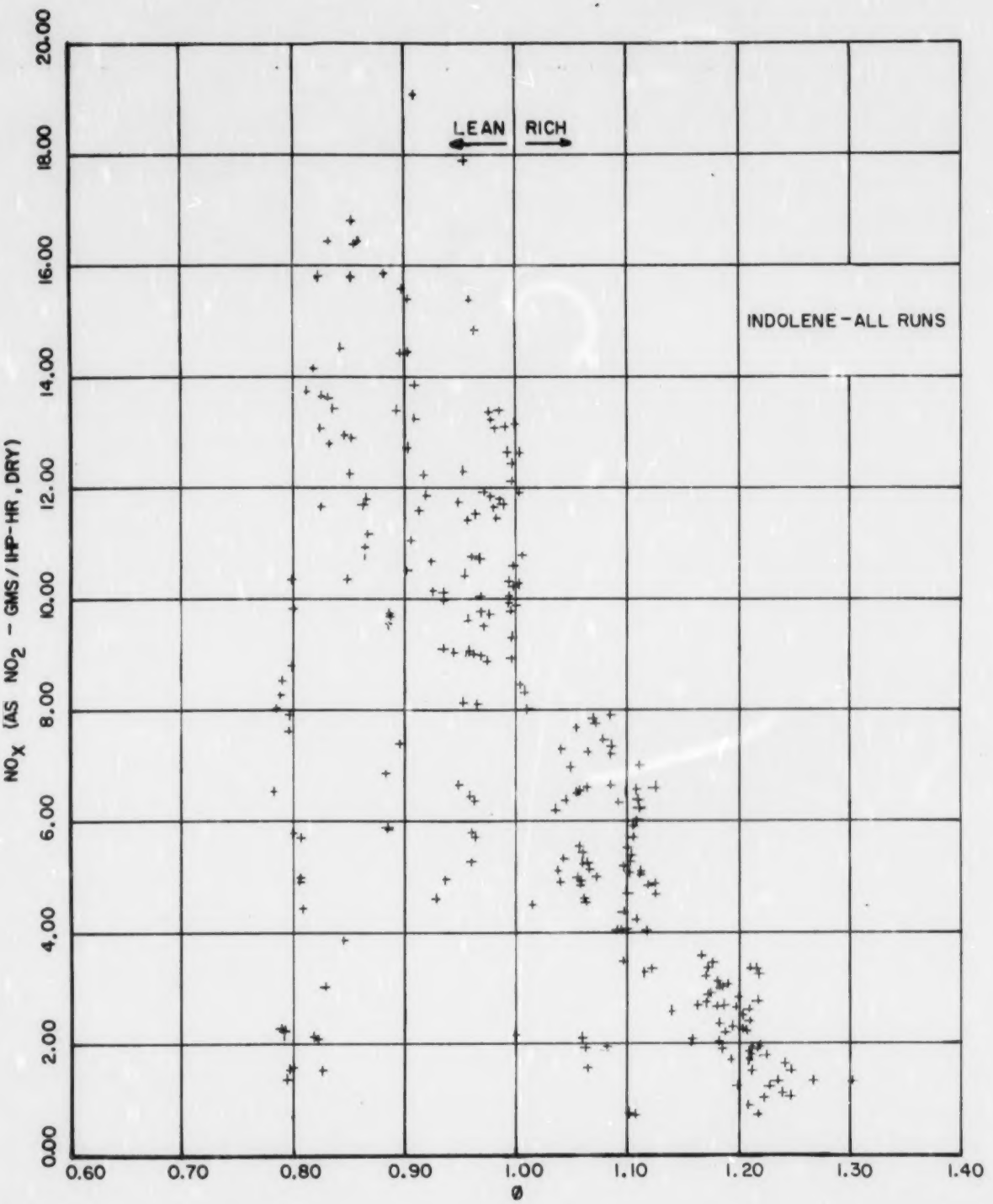

FIG. 19. OXIDES OF NITROGEN VS EQUIVALENCE RATIO-COMPOSITE CYLINDER DATA

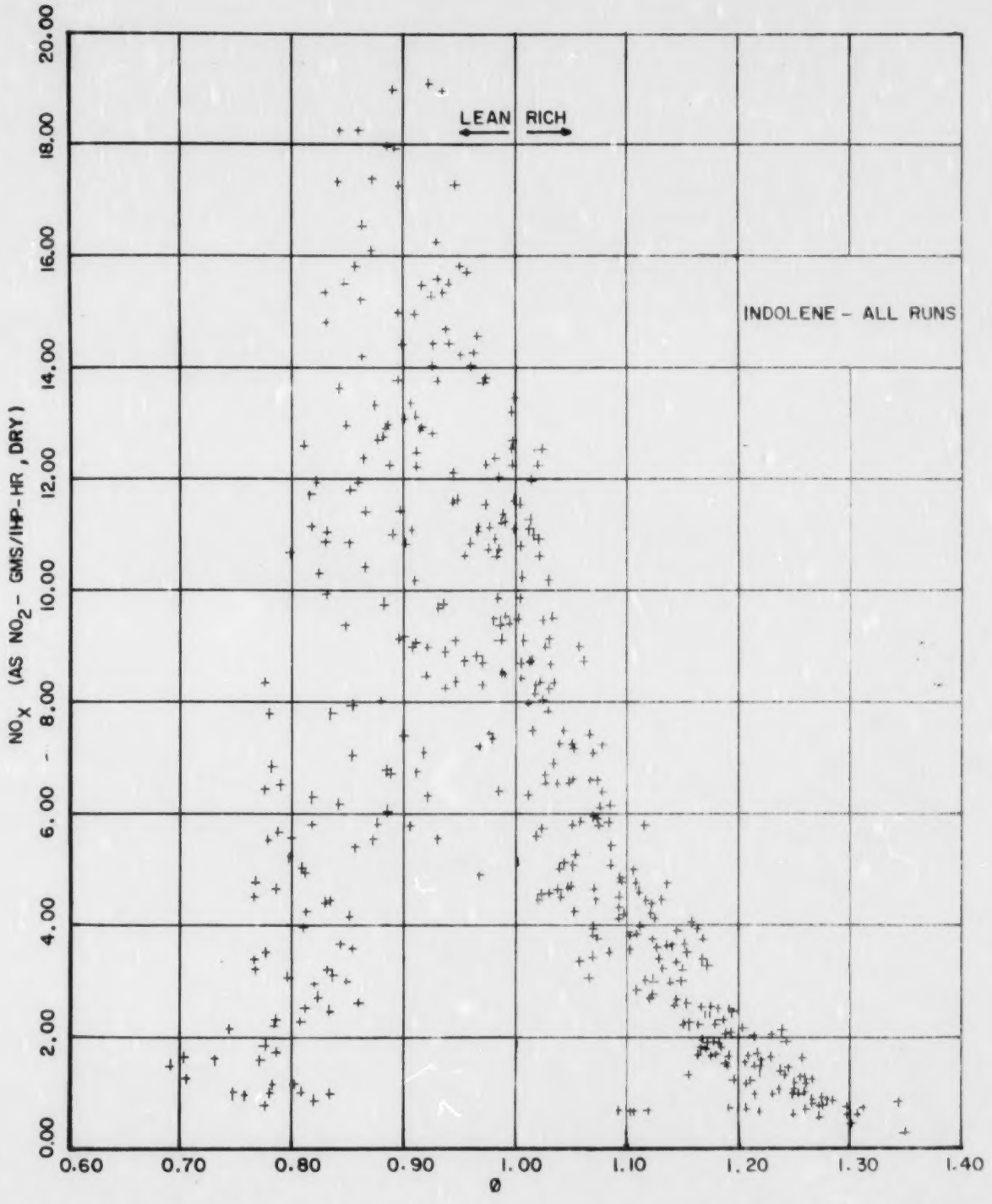

FIG. 20: OXIDES OF NITROGEN VS EQUIVALENCE RATIO - INDIVIDUAL CYLINDER DATA

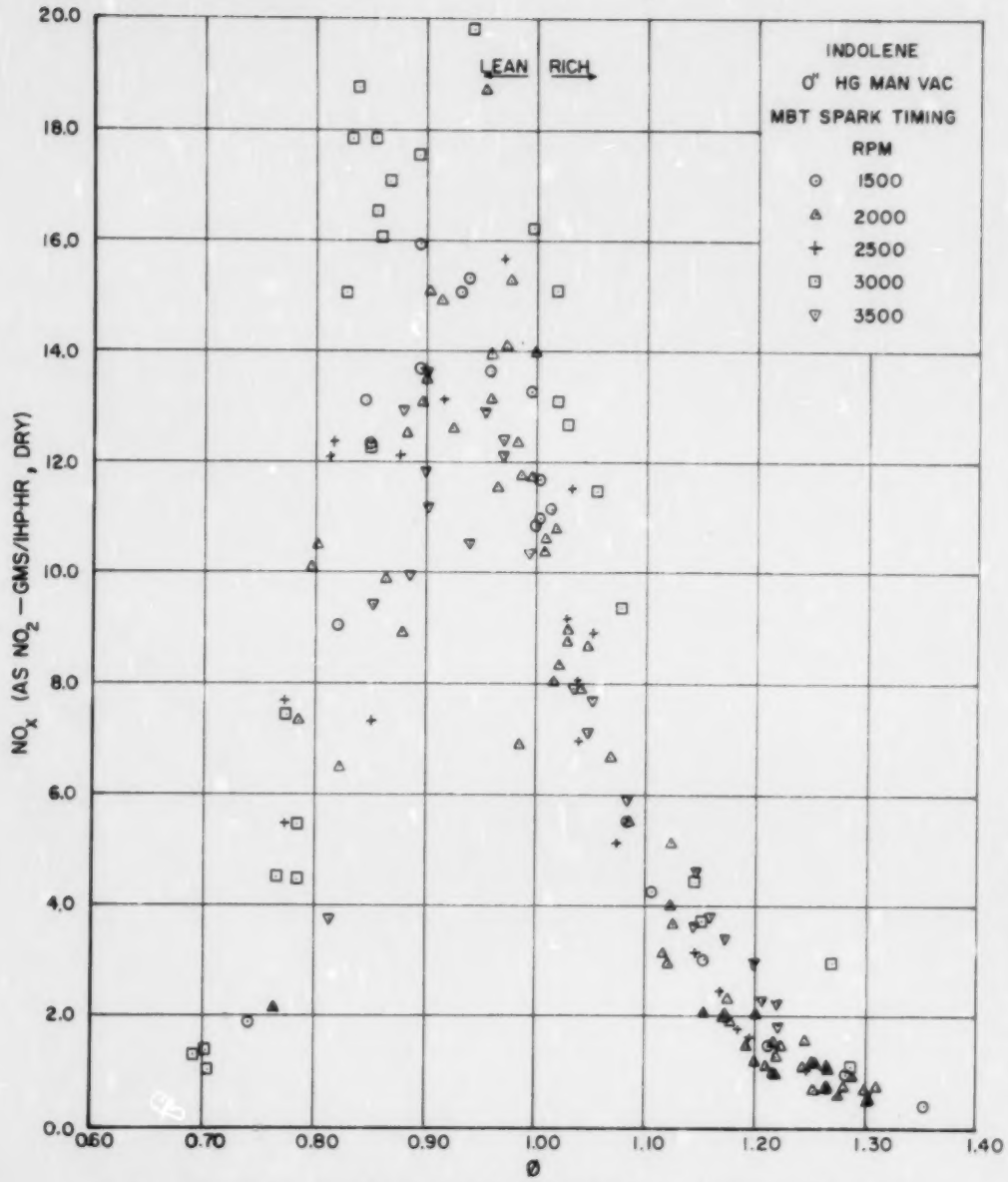

FIG. 21 OXIDES OF NITROGEN VS. EQUIVALENCE RATIO—SPEED DEPENDENCY
INDIVIDUAL CYLINDER DATA

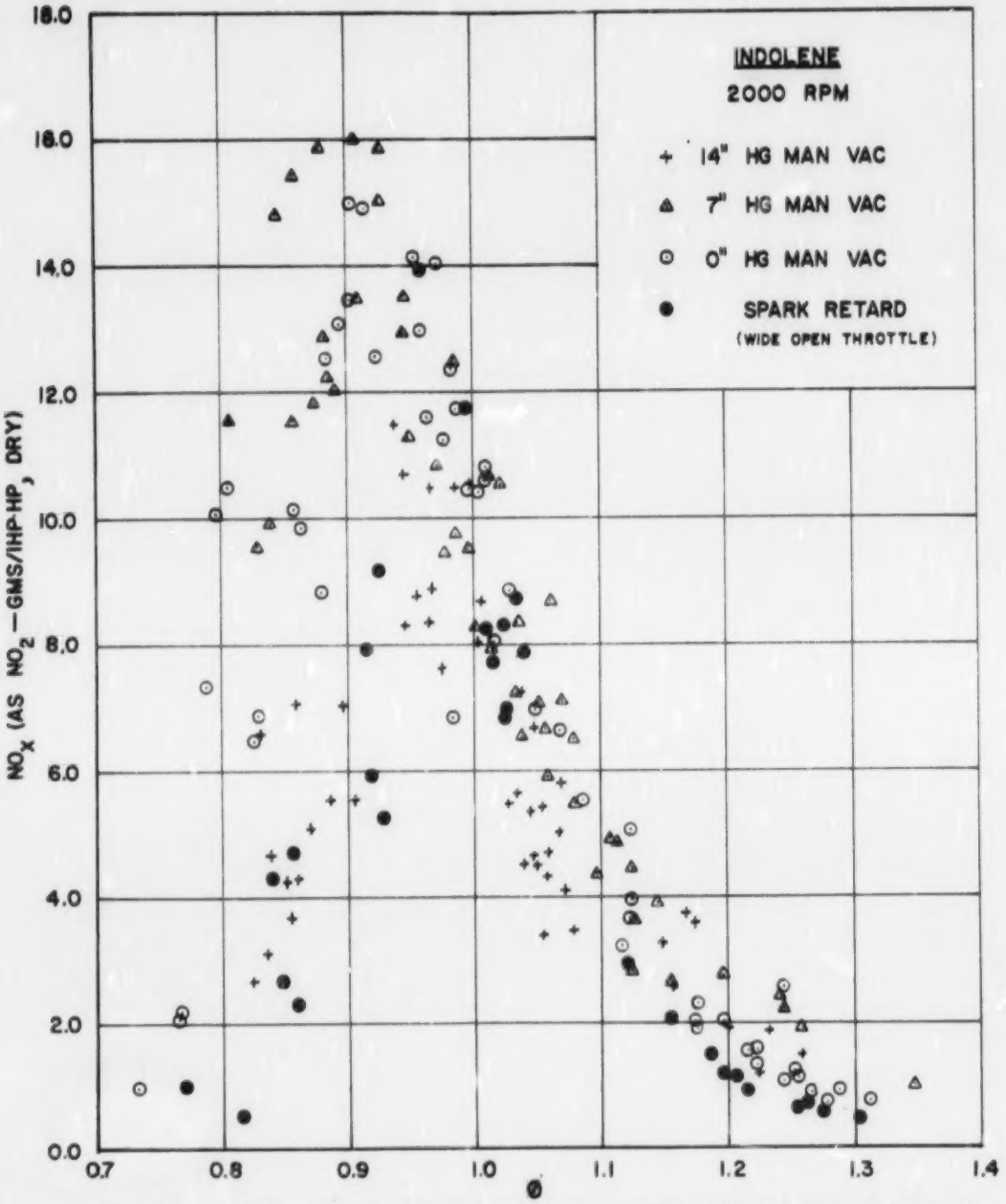

FIG. 22 OXIDES OF NITROGEN VS. EQUIVALENCE RATIO-LOAD DEPENDENCY
INDIVIDUAL CYLINDER DATA

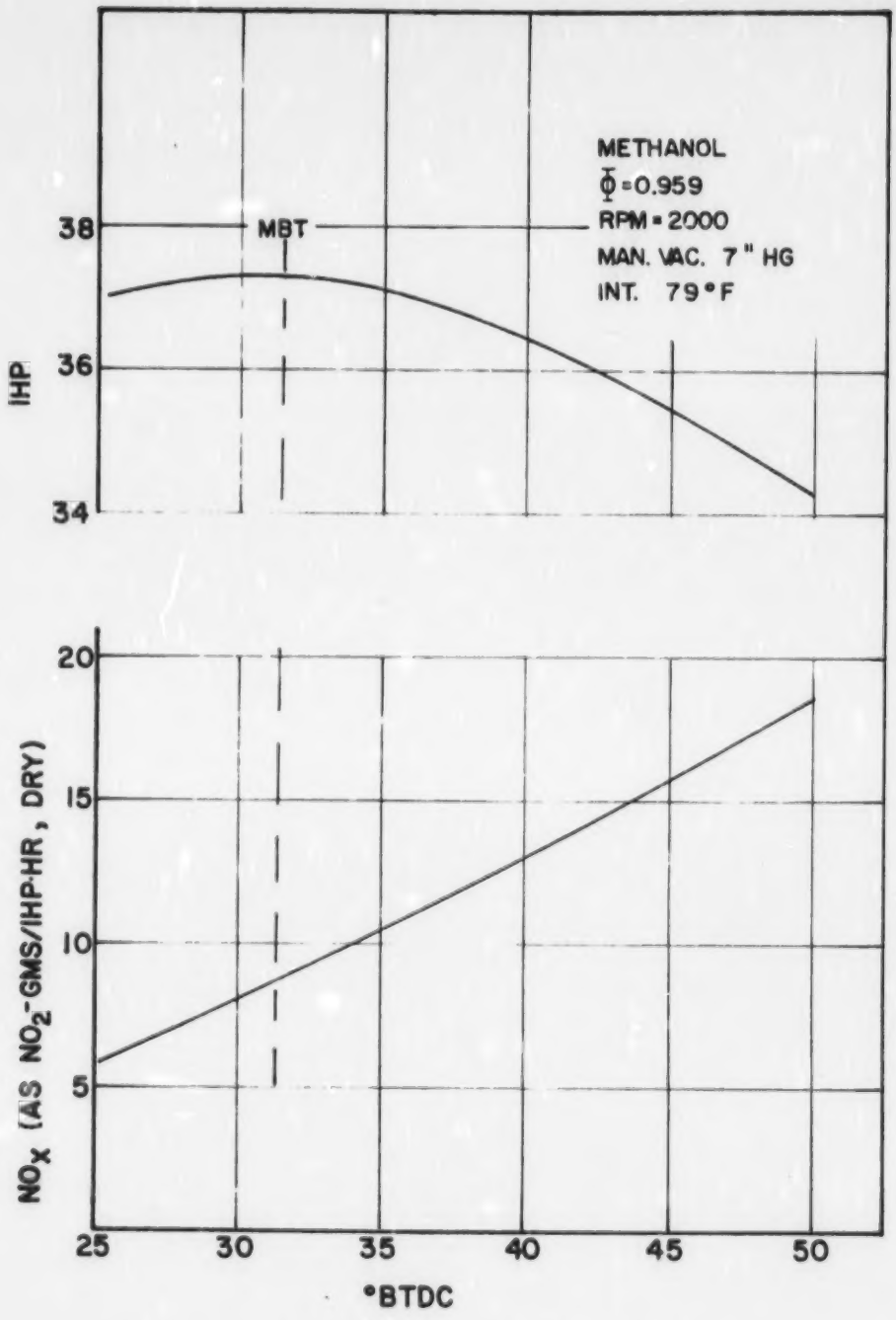

FIG. 23: EFFECTS OF SPARK TIMING ON NO_x & IHP

begin to decrease. (This is a standard technique used in the industry for control over NO_X.)

Figure 24 shows the spark advance effect on NO_X in more detail. Here, all engine variables are fixed and spark advance appears as a parameter. Note now the coherency of the data in comparison to the previous NO_X plots. Each set of our solid symbols (▲, ●, ◆, ▼) represents the individual cylinder contributions of NO_X for a particular engine steady state test point. In particular, note the four cylinder contributions indicated by ▲ at the far left of the graph. These represent one engine condition where ϕ_{cyl} varied from 0.73 to 0.86. The spark timing was 33°BTDC. The richest cylinder yields just over 14 gms NO_X/ihp-hr while the leanest yields about 1.5 gms NO_X/ihp-hr.

In summary, the indolene NO_X data indicates that spark advance and equivalence ratio are the two most important factors affecting the emissions of NO_X in multicylinder engines. The non-optimized spark setting for individual cylinders, together with ϕ variations among the cylinders, leads to large variations in NO_X on a cylinder-to-cylinder basis. The effects of speed and load on NO_X are obscured by the effects of spark advance and ϕ.

IV.1.4.5 Comparative NO_X, UBF, and Aldehydes: Due to the increased maldistribution when operating on methanol (see Figures A3 and A4, Appendix) the setting of MBT spark timing has an even more pronounced effect on the NO_X. This is shown in Figure 25, where the 2000 RPM results appear for the three engine load conditions. Again, the solid symbols represent the individual cylinder contributions for an engine test point at full load. This graph can be compared with its indolene counterpart, Figure 22. NO_X for MBT is lower with methanol by roughly a factor of two (note scale change in Figure 25). The possibilities of operating at very lean ϕ for reducing NO_X become evident; however, this depends on the degree to which the cylinder-to-cylinder variations in ϕ can be reduced.

Unburned fuel, as well as aldehydes, is a wall quench phenomenon and the description of their behavior in terms of the chosen engine variables is simplistic. At this time we do not present any explanations for either beyond the general trends that they exhibited as a function of ϕ. Figure 26 is a comparative plot of UBF for the two fuels at 2000 RPM. The data indicates no particular benefit for one fuel over the other when presented on this mass basis. However, on a ppm volume basis, methanol yields about half the UBF emissions that indolene does.

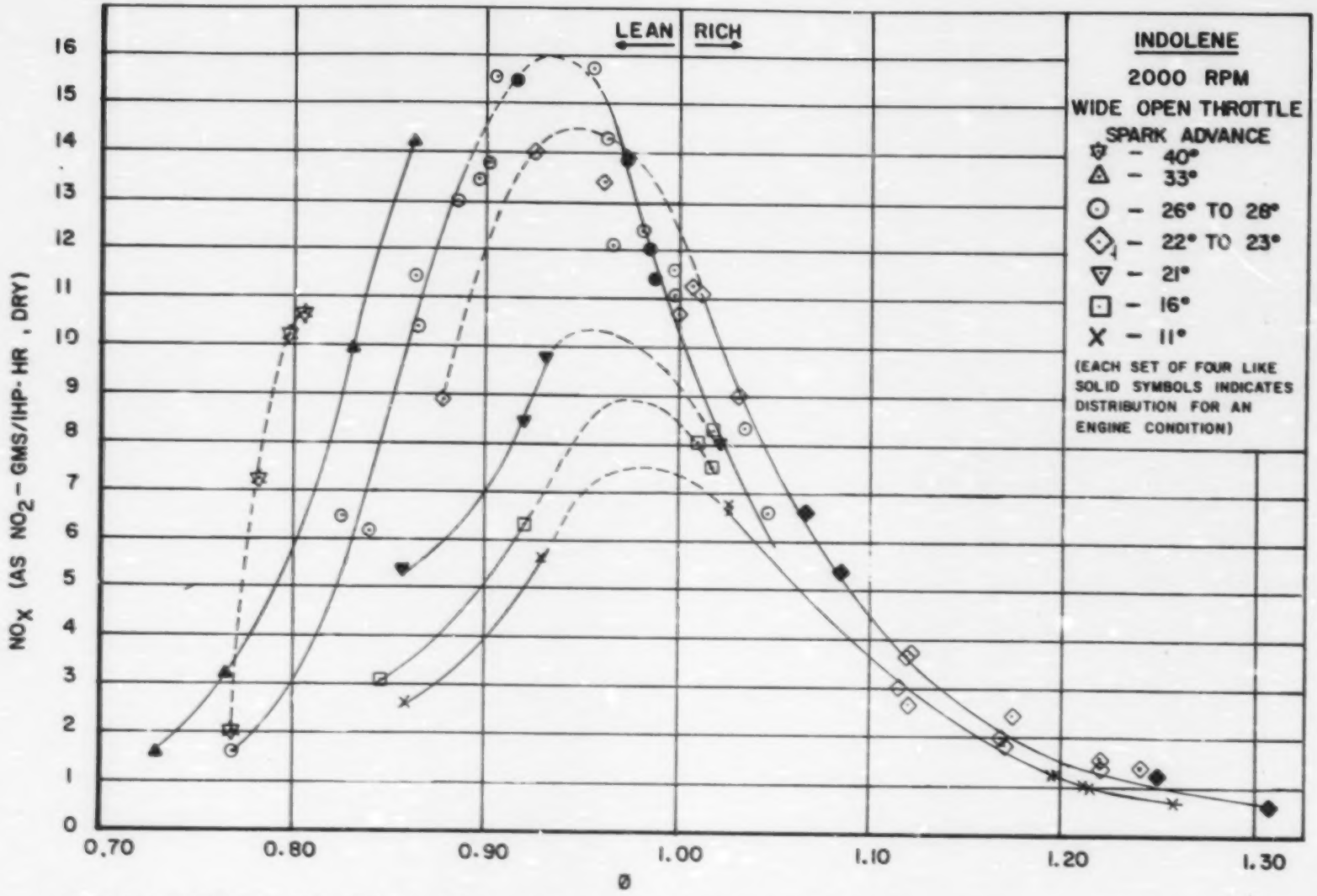

FIG. 24: EFFECTS OF SPARK ADVANCE ON THE OXIDES OF NITROGEN - INDIVIDUAL CYLINDER DATA

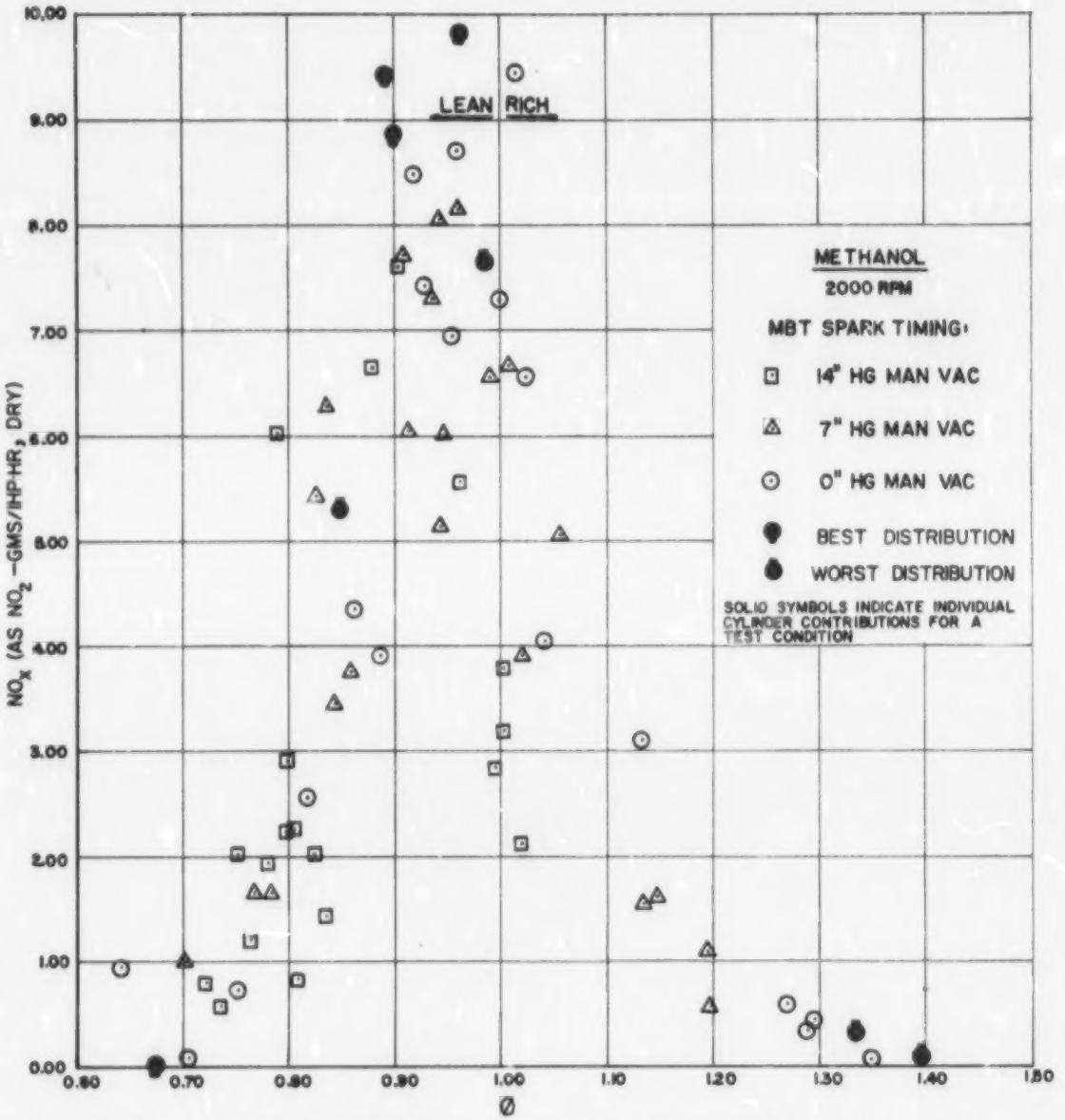

FIG 25 OXIDES OF NITROGEN VS. EQUIVALENCE RATIO
INDIVIDUAL CYLINDER DATA

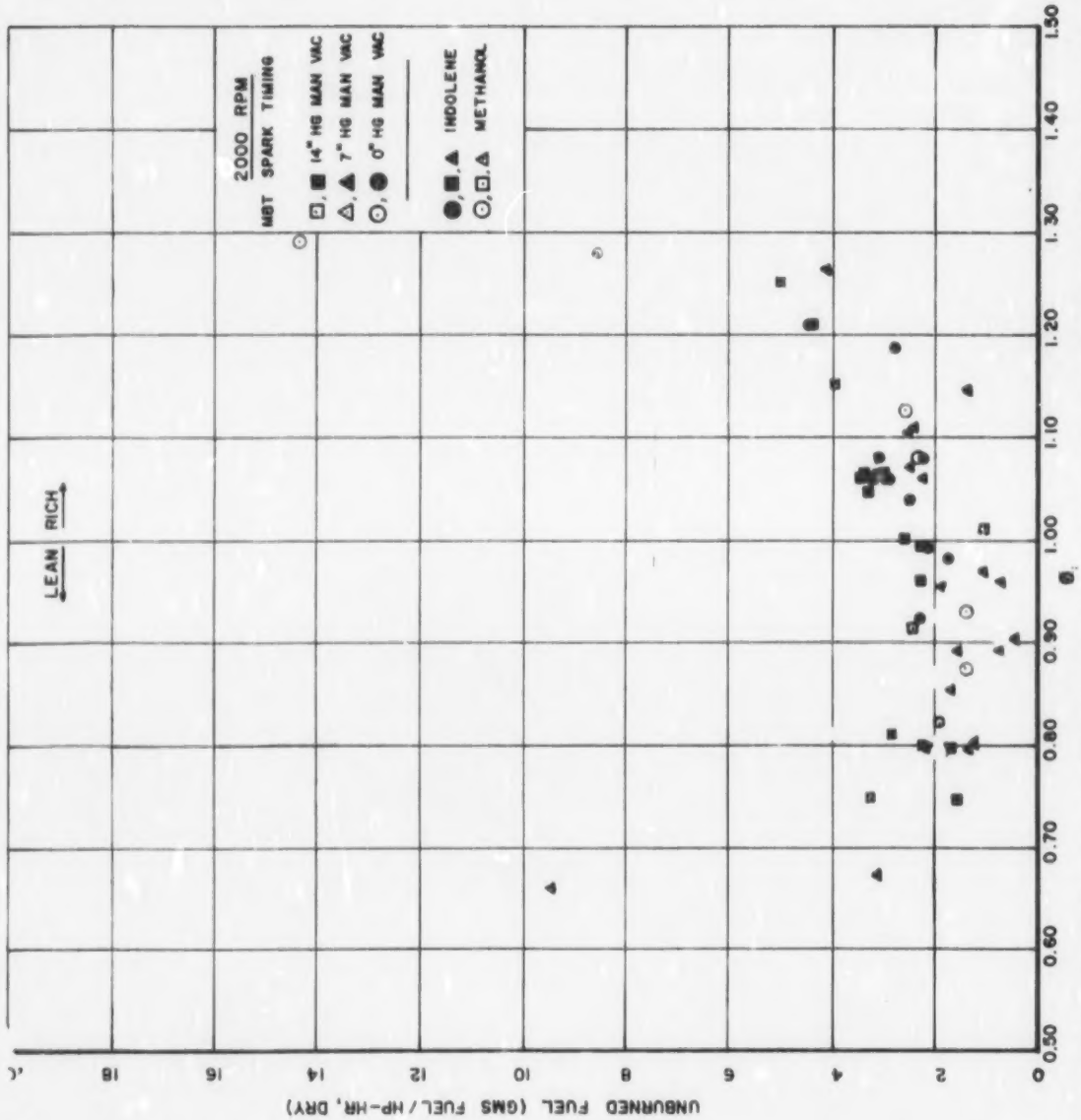

FIG.26: UNBURNED FUEL VS EQUIVALENCE RATIO - METHANOL VS INDOLENE - COMPOSITE CYLINDER DATA

The one aspect of emissions which appears inferior for methanol when compared to indolene is the aldehyde emissions. Figure 27 shows the comparative evidence. Methanol gives two to eight times the amount of aldehydes on a gms/ihp-hr basis. In the extended lean operating range methanol shows even higher values. However, it appears that an oxidation catalyst would most likely eliminate this particular species.

IV.1.5 Conclusions and Projected Activities: The initial results for methanol support earlier work of the authors and other investigators;[1] namely, that methanol reduces exhaust emissions with the exception of aldehydes and increases fuel economy relative to gasoline fueled spark ignition engines. This is made possible in part through the extended lean misfire limit of methanol and its more efficient combustion characteristics.

However, the combination of typical production carburetion and intake manifold appears to preclude best engine performance and control over exhaust emissions because of resulting variations in equivalence ratios among the cylinders. On the basis of the experimental evidence, this appears to hold true for both indolene and methanol; however, with methanol the maldistribution is worse.

In light of the steady state evidence, alternative air-fuel induction systems will be investigated in an attempt to alleviate cylinder-to-cylinder equivalence ratio variations. Three systems will be investigated as part of the second year activity schedule. Two of these systems are described in the following sections.

Additional tasks included in the second year activity schedule are listed below:

Task A - Completion of the Methanol Base Line:

A few iterations on the stock carburetor modification will also be included in the testing sequence.

Task B - Transient Engine Performance:

This will include cold starting, warm-up, and acceleration/deceleration modes for both indolene and methanol in the four-cylinder engine. This work will be carried out using the second engine and a fast time response emissions measurement system. The testing will utilize the stock and the modified stock carburetor (indolene and methanol, respectively) primarily. Initial assessment of the alternative fuel-air induction system in these transient modes will occur during the latter portion of the grant period.

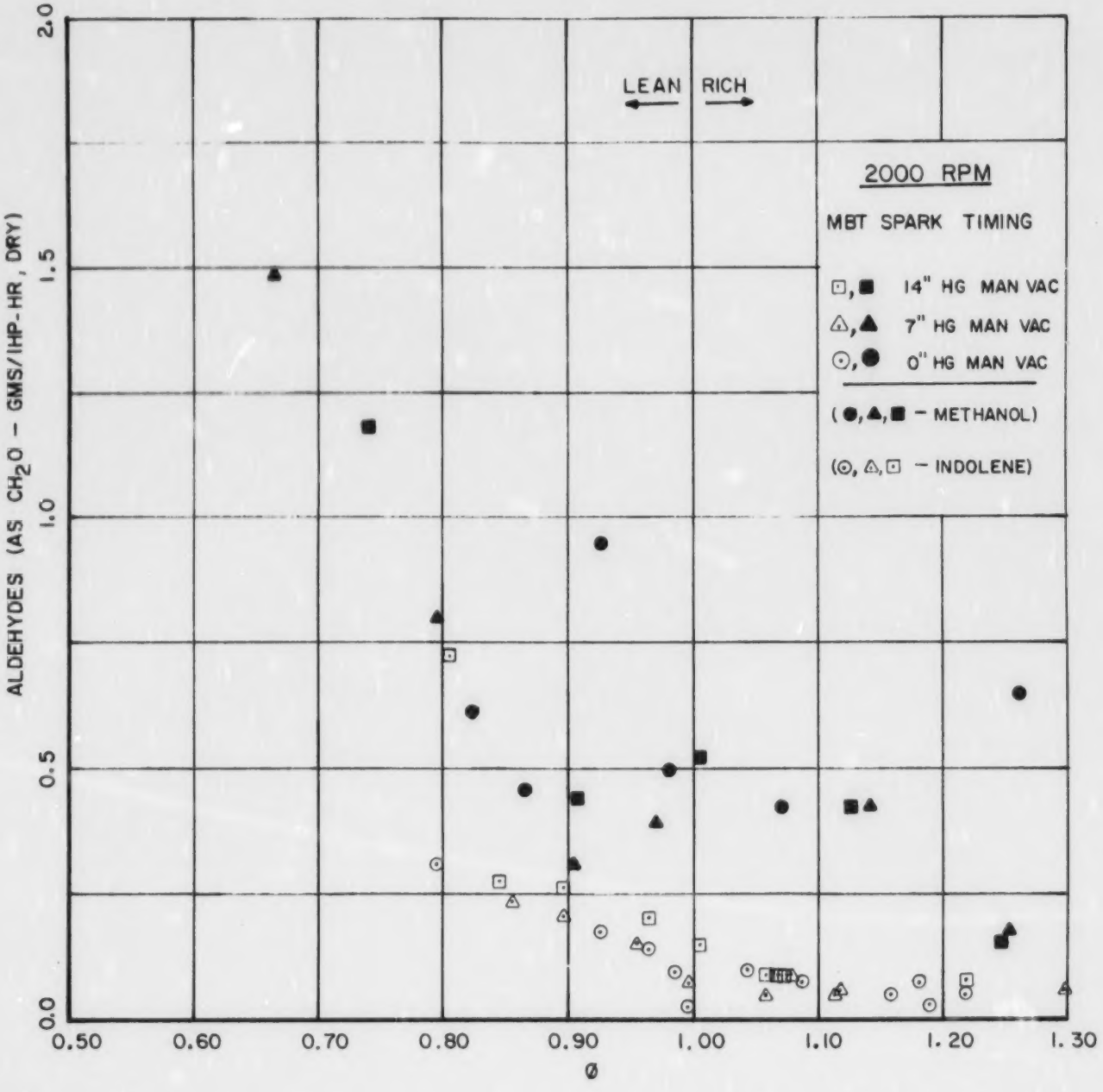

FIG. 27 ALDEHYDES AS A FUNCTION OF EQUIVALENCE RATIO-METHANOL vs INDOLENE

IV.2 ALTERNATIVE FUEL INDUCTION SYSTEMS

There are two major problems of fuel preparation frequently identified with venturi carburetor, intake manifold systems. They are poor nebulization of the fuel and poor mixing with the air. The consequences are loss of performance and excessive pollutant emissions because the spark advance and air-fuel ratio cannot be simultaneously optimized for all cylinders for given speed and load conditions. Evidence of such problems has been presented in Section IV.1. Two alternative fuel preparation systems have been identified for experimental study.

IV.2.1 The WHB Shock Wave Induction System: This system is the result of returning to the first principles in examining the instantaneous air-fuel requirements of an operating engine and satisfying these requirements with a minimum of hardware. The basic hardware consists of an intake duct coupled directly to each intake port through a mounting plate which carries a sliding throttle mechanism, a metering orifice in the wall of the intake duct, and a floatless fuel supply system which utilizes a fuel return line for maintenance of liquid level.

When the intake valve opens and the piston begins its downstroke, expansion waves propagate outward through the intake duct, initiating air flow into the duct and fuel flow through the metering orifice. The expansion waves are reflected from the open end of the duct as compression waves delayed by the round trip travel time in the duct, so that the resultant pressure difference at the metering orifice closely approximates the time derivative of the air mass flow rate in the duct. Since suitable fuels are 600-700 times as dense as air, the resultant fuel mass flow rate can be made proportional to the air mass flow rate on an instantaneous basis by proper selection of metering orifice dimensions. Subsequent wave reflections are prevented by a viscous acoustical resistance in the form of a narrow slot through the wall of the duct, providing critical damping for an otherwise resonant acoustical system.

Wave motion in the duct generates a substantial non-turbulent pressure gradient near the wall; the metering orifice outlet is positioned to maximize the effectiveness of this pressure gradient in atomizing the fuel issuing from the orifice. Mean fuel droplet diameters of less than 10 microns have been produced at 900 RPM engine speed (CFR engine) at wide open throttle in a 33 mm diameter duct.

Because an intake duct is coupled directly to each port, the mixture transit time from metering orifice to intake valve can be reduced by an order

of magnitude compared to a conventional system with a distributing manifold, so the fuel droplets have much less time to fall out of the air stream. They will not recombine into larger droplets or be deposited on the walls of the intake tract as in a conventional system because no significant changes in mixture direction occur along their path. Significant reductions in fuel consumption and/or emission of unburned hydrocarbons and carbon monoxide result from the improved mixture preparation. Using this system with gasoline as a fuel on a dynamometer mounted, General Motors Vega engine resulted in a 20% torque increase at full throttle conditions over the normal engine operating range. The brake specific fuel consumption curve was lower than the OEM curve for this comparative testing. Emissions measurements were not measured for a sufficient number of test points to allow contrasting statements to be made.

Earlier laboratory work using a CFR engine with the same type of fuel induction system showed it to perform successfully on either gasoline or methanol by changing the fuel orifice. This combined evidence served as the basis for selecting this product as an alternate fuel preparation system to the OEM venturi carburetor, manifold system. The comparative performance testing using methanol and gasoline fuels is expected to take place in the early months of the second year of this grant.

IV.2.2 Electronically Controlled Fuel Injection System: During the first three months of this year a performance and emissions test program was carried out to evaluate a slant-six Plymouth Valiant equipped with the prototype of the fuel injection system to be used subsequently in the Pinto engine test program. This testing was done for Lawrence Livermore Laboratory of ERDA in exchange for a Pinto engine fuel injection system. The familiarity and operational expertise of the controller gained by this test program will prove useful for the subsequent tests which are part of this grant plan.

To date, the electronically controlled fuel injection system mounted in the Plymouth Valiant has shown good results during steady state tests in controlling air-fuel ratio and cylinder distribution. The transient response of the system showed reduction in air-fuel variations by a factor of two in comparison to a conventional venturi carbureted engine, however, more development and testing is needed in this area. A prototype of this system is currently being tested on a laboratory CFR engine for further improvements before mounting the system on the Pinto test engine. A brief description of the electronically controlled fuel injection system follows.

Figure 28 reveals the major components of the system. The injectors and other fuel handling components are Bosch products, currently being used by an American automobile manufacturer. Note that the fuel pressure regulator is referenced to the intake manifold pressure and therefore a constant pressure difference will be maintained across the injectors. Consequently, the injectors are operated either fully on or off with the control of opening and closing times provided by the electronic controller.

The electronic control unit integrates signals from a manifold pressure transducer, air temperature sensor, tachometer circuit and water temperature sensor. The linear output of the manifold vacuum transducer and tachometer circuit can be modified by their respective function generators to obtain a linear curve or a curve consisting of three straight line segments with two break points. The slope and break points are adjustable over a wide range. The modified air pressure and RPM signals are essentially multiplied together. The resulting product is then further modified by the air temperature signals and engine temperature.

The final signal level is proportional to the injection pulse width. Injection timing is accomplished by a magnetic switch mounted on the distributor shaft and can be varied over 720 degrees of crankshaft revolution range.

The flexibility of control of this system in air-fuel ratio management and fuel injection timing should be apparent from the brief preceding description. It has been successfully operated with both methanol and gasoline in the Valiant vehicle. Hence, it is anticipated that the system being acquired for the Pinto engine should provide an excellent basis for comparison of the two fuels with a fuel injection system.

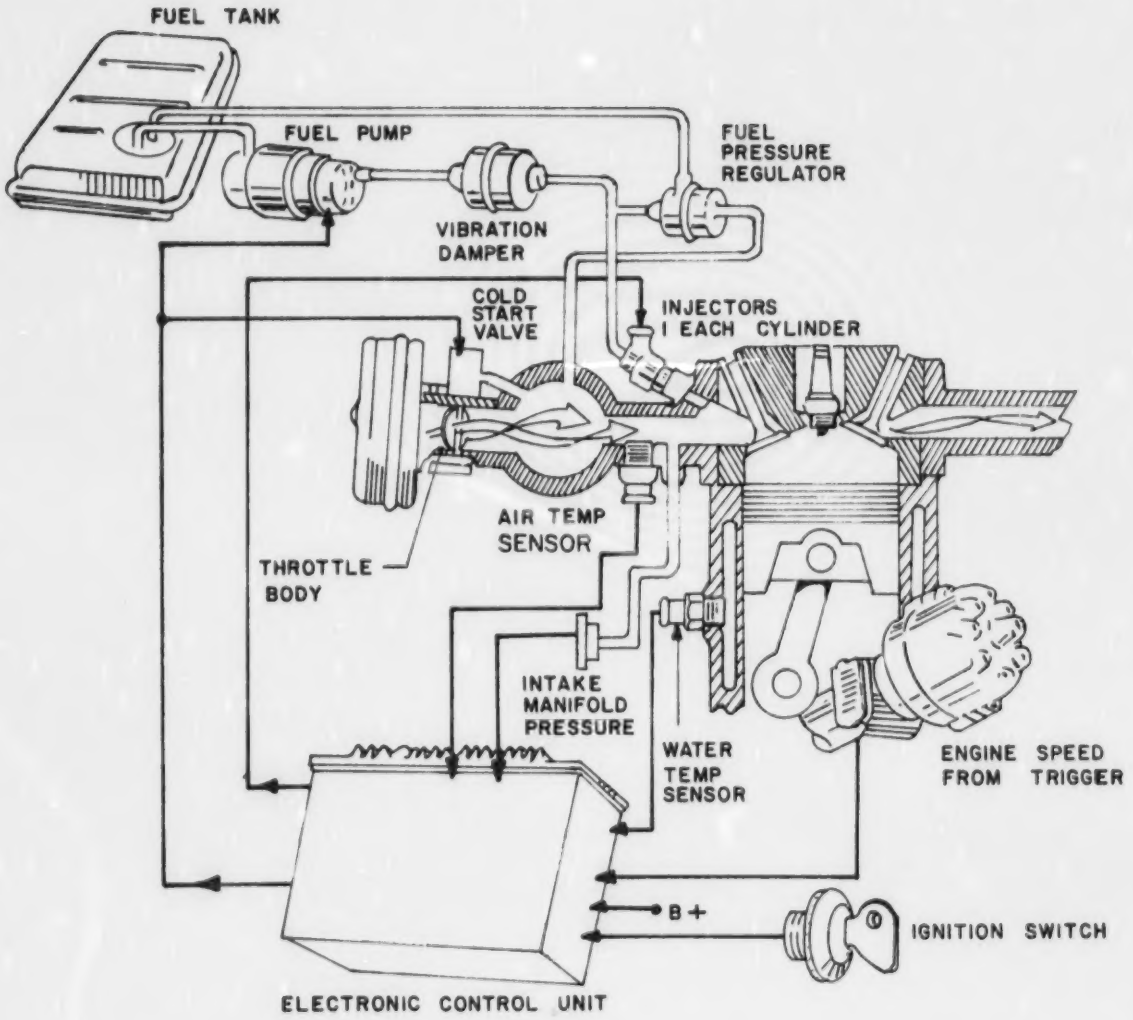

FIG. 28 ELECTRONIC FUEL INJECTION SYSTEM

IV.3 COLD STARTING

Cold starting of methanol fueled automotive engines has been accomplished most frequently by use of an auxiliary gaseous fuel. Both propane and butane are acceptable. The City vehicle that is now entering its fifth year of operation has always used propane for cold weather starts. These auxiliary fuels present no special problems to an experienced operator. However, they are seen as a nuisance and a source of consumer complaint if they were to be incorporated in vehicles operated by the public.

Blending of volatile constituents, such as butane, with pure methanol has also been shown to be successful.[8] In Section IV.4, the vapor pressure-temperature relationship for one such blend is displayed. Even though such a blend offers a cold start solution, it is still seen by the investigators as violating a significant methanol fuel safety factor. Methanol does not explosively ignite at atmospheric pressure and room temperature. When blended with butane, this quality would be sacrificed. Thus, a primary goal of the investigators is the catalytic generation of a combustible gaseous mixture for cold start in conjunction with high quality liquid fuel nebulization to sustain engine operation after the first few gas fueled cylinder firings.

Progress to date on the cold start aspect of the program has been very limited except for delineation of the possibility specified. None the less, this problem is seen as one of the few germane arguments against pure methanol as a fuel for automobiles. Hence, the investigators believe that it must receive a significant portion of the research effort in the coming year of activities.

IV.4 INFLUENCES RESULTING FROM VARIATIONS IN COMPOSITION OF METHANOL BASED FUELS

There are many possible additives which may be combined with methanol either inadvertently through low cost production or intentionally to seek improved performance. Methanol's excellence in pure form as an automotive fuel in terms of performance, thermal efficiency, anti-knock quality and emissions is such that no additives are needed except for cold starting. However, it is also frequently considered as a gasoline extender by using it in blend form with gasoline. Hence, evaluation of additives to methanol resulting in methanol based fuels must address the following questions:

(1) Is cold starting enhanced?

(2) Are emissions or performance degraded?

IV.4.1 Volatility of Fuels: In order to have comparative data, the measurement of the volatility of a fuel must be done under controlled conditions. The two procedures which are being used in this study were ASTM D 86, Distillation of Petroleum Products, and ASTM D 323, Vapor Pressure of Petroleum Products (Reid Method). Since petroleum products consist of mixtures of hydrocarbons with different boiling points, the temperatures at which different percentages of the fuel have evaporated give a measure of its volatility. This forms the basis for ASTM D 86. The other procedure depends on the vapor pressure of a fuel, such as gasoline, which is measured at 100°F in a pressure bomb having a 4 to 1 volume ratio of air to liquid. This procedure is designated as ASTM D 323, Reid Vapor Pressure (RVP).

The relationship between volatility as measured by the ASTM procedures and performance criteria have been defined[9] and are summarized in Table 2.

It should be noted that the characteristics in Table 2 are applicable to gasolines. Some of them can be seriously questioned for methanol based fuels. However, as a starting point for comparative evaluations, these measurement procedures will be used and then subsequently challenged where it seems appropriate.

IV.4.2 Types of Fuels Tested: The fuels that have been examined to date for volatility comparisons are given in Table 3. These include the gasoline used in the test program and some methyl alcohol blends which may be considered for cold start enhancement over straight methanol or for use as gasoline extenders.

The indolene-methanol blends were tested to determine the effect of small versus large ratios of gasoline to methanol in gasoline-methanol blends. The 5% butane-methanol blend was prepared as a result of the work of Tillman[10] on use of butane in methanol to improve cold starting.

TABLE 2: VOLATILITY CHARACTERISTICS AND PERFORMANCE

Low Temperature for 10% Evaporated and High RVP	Low Temperature for 50% Evaporated	High Temperature for 90% Evaporated
Improved cold starting	Better warm up	Improved fuel economy
Vapor lock under hot operating conditions	Better acceleration	Resistance to knock
Increased vapor formation in fuel tanks and carburetors	Increased tendency for carburetor icing and resultant stalling	Poorer mixture distribution in intake manifold
		Increased combustion chamber deposits
		Excessive varnish and sludge deposits in engine

TABLE 3: FUELS USED IN VOLTALITY COMPARISON STUDIES

Chevron unleaded	- winter grade
Chevron unleaded	- summer grade
5% indolene	- 95% methanol
95% indolene	- 5% methanol
4% isobutanol	- 16% methanol - 80% Chevron unleaded
5% butane	- 95% methanol

The isobutanol-methanol-gasoline blend is one that is being studied in Sweden, and purports to have a suitable distillation curve and no problems with phase separation or vapor lock.[11]

The results of the ASTM distillation are plotted in Fig. 29. The addition of 5% methanol to indolene causes a depression of the distillation curve as compared to indolene alone to about 20% evaporated. The curve then rises to meet the indolene curve. A similar initial depression is noted with the Swedish blend. For a better comparison, the ASTM distillation curve data points for 10%, 50% and 90% evaporated and the final boiling point are given in Table 4. The Reid vapor pressure data is given in Table 5. Note that the addition of 5% methanol to indolene caused an increase of a little over 1 psi in the Reid vapor pressure. The addition of 16% methanol (and 4% isobutanol) to Chevron unleaded gasoline increased the RVP by about 3.5 psi. Of the four methanol blends that were prepared, the 95% indolene - 5% methanol and the 4% isobutanol - 16% methanol - 80% Chevron unleaded seem to most closely approximate the desired performance characteristics as defined in Table 2.

The actual performance with 100% methanol has proven satisfactory in test engines, street vehicles and racing cars, even though it seriously violates the criteria of Table 2 by having a poor RVP and a constant boiling temperature rather than a distillation curve. One report[12] describes a malfunction involving methanol-gasoline blends which was labeled "acceleration vapor lock". It was attributed to departure from their suggested vapor lock index (VLI).

$$VLI = RVP + 0.13\% \text{ distilled @ } 70°C$$

An alternate explanation could be the leaning effect associated with adding methanol to the fuel without modification of the accelerator pump. Vapor lock is a dynamic phenomena involving heat transfer rate, fuel flow rate, vapor pressure-temperature relationship and heat of vaporization. For closely related fuels, such as gasoline blends, the VLI may be satisfactory. However, a more carefully developed index capable of handling a broad range of fuels should contain at least some of the factors just mentioned.

Cold start problems with pure methanol are known to exist. Blending is one way of avoiding this problem while at the same time extending gasoline supplies. From the results of these initial volatility tests, the two fuel blends that appear to be prime candidates for further evaluation are the 95% indolene-5% methanol, and the 4% isobutanol-16% methanol-80% Chevron unleaded.

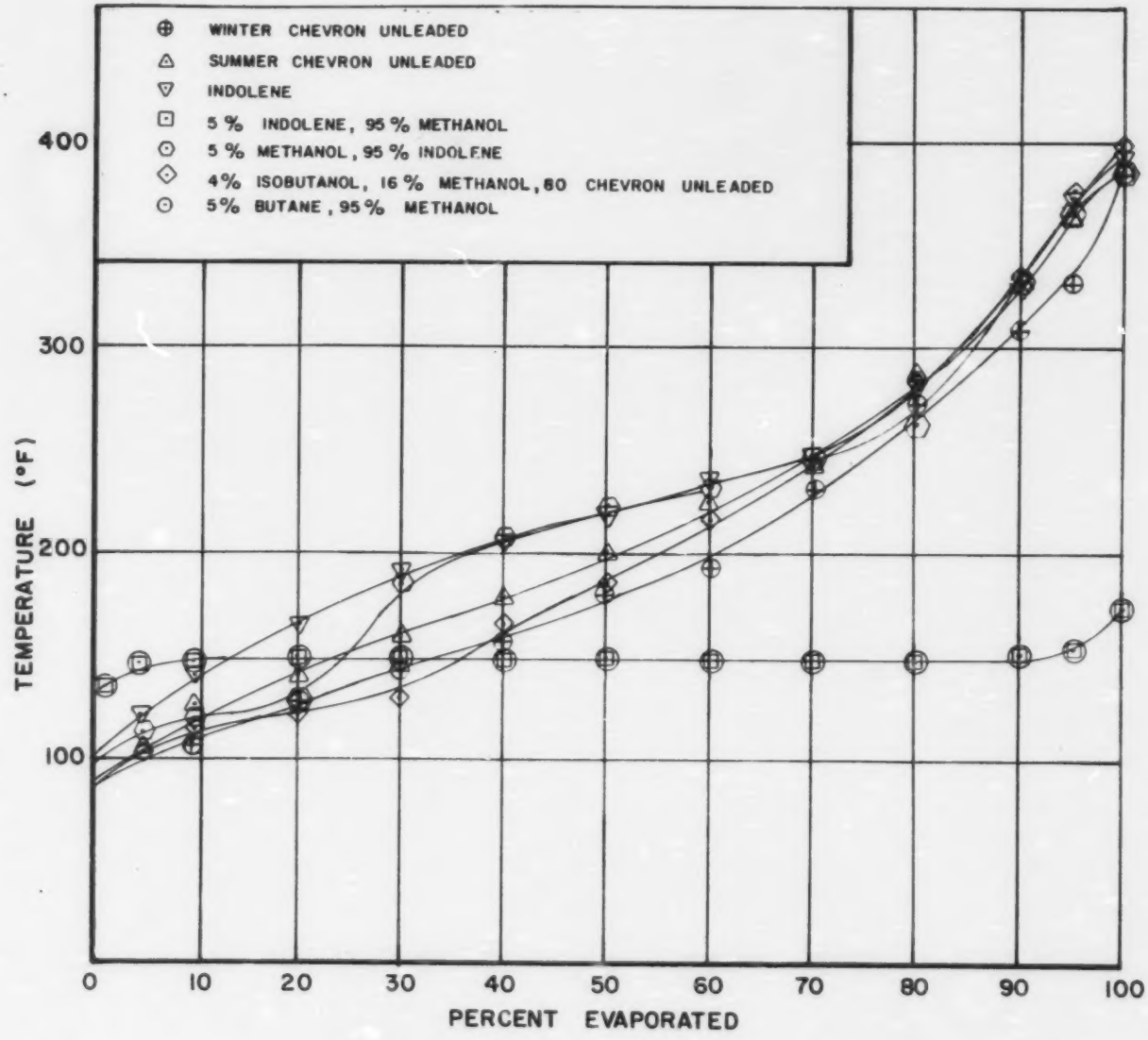

FIG. 29 ASTM DISTILLATION

TABLE 4: ASTM DISTILLATION, °F

% Evaporated	Chevron Unleaded Summer	Chevron Unleaded Winter	Indolene	5% Indolene 95% MEOH	95% Indolene 5% MEOH	4% Isobutanol 16% MEOH 80% Chevron	5% Butane 95% MEOH
10	124	108	139	148	120	114	148
50	202	179	221	150	223	184	150
90	334	308	331	152	331	334	152
FBP	400	380	392	170	384	400	170

TABLE 5: REID VAPOR PRESSURE

Fuel	Reid Vapor Pressure (psi)
Chevron Unleaded-Winter	7.65
Indolene	8.75
95% Indolene, 5% MEOH	9.90
5% Indolene, 95% MEOH	5.20
4% Isobutanol, 16% MEOH, 80% Chevron Unleaded-Winter	11.10
5% Butane, 95% MEOH	15.10
100% MEOH	3.85

It is evident that use of distillation equipment and RVP procedures provides some useful information. Hence, examinations of additional fuel candidates using these procedures will continue during the coming year with emphasis on combinations involving methanol based fuels resulting from low cost,high volume production of methanol. It is also evident that further study is required to present a vapor lock index that can correctly handle methanol-gasoline fuel blends. This, too, will be part of our continuing investigation. Engine experiments using the more desirable fuel candidates resulting from these studies will subsequently follow.

IV.5 ENGINE WEAR

The question of whether there is an increase in engine wear with the use of methanol has not been clearly answered. A recent survey[13] has summarized information indicating both viewpoints. In one case, excessive wear of piston rings and cylinders was reported.[14] Other information indicated that wear is no greater with alcohols than with gasoline.[15] With this conflicting background, it was considered important to incorporate in our comparative methanol/gasoline fuel study the relative effects of these fuels on wear. Wear data has been accumulated from the start of the current program including the break-in period of both engines with gasoline fuels. By following the wear history from the beginning of the tests a comparison could be made between wear rates occurring during successive gasoline, methanol and methyl fuel operations on the same engine.

The procedure selected for the determination of internal wear of the test engine is based on the analysis of the crankcase oil for specific wear metals by atomic absorption spectrophotometric techniques.[16] The procedure is based on the fact that the trace elements present in the crankcase oil are an indication of wear of the component parts of the engine made up of those particular metals. This is a well known procedure and has been used routinely to permit forecasting of impending failure of specific parts of an engine.[17]

The materials that would be expected to wear in the 2.3 litre Pinto test engines used in this study are shown in Table 6. The elements considered most likely to show up in the engine crankcase oil, as engine wear proceeded, were copper, iron, lead, chromium, aluminum and tin. Hence, they were selected for analysis.

IV.5.1: Pinto Engine Wear Results: Wear data has been accumulated for over 256 hours of gasoline fueled operation on the Pinto engine number 1 and after 69 hours (including 48 hours with gasoline and 21 hours with pure methanol) on the Pinto engine number 2. In most cases crankcase oil samples were taken every 10 hours and analyzed for the wear metals by atomic absorption spectrophotometry.

The procedure for the calculation of accumulated wear metals included adjustment of the chemical analysis data to compensate for the addition of fresh oil. The adjusted values were to be as if no oil were removed or had leaked out. Therefore, the values should show a continual accumulation of wear metals.

TABLE 6: MATERIALS IN PINTO ENGINE[18]

Journal and Main Bearings	-	Cu-Pb Alloy Plate
Cam	-	Cast Iron, Phosphate Coat
Block	-	Cast Iron, Phosphate Coat
Piston	-	Ni and Al
Piston Rings	-	#1 - Cast Iron - Molycoat #2 - Cast Iron - Phosphate #3 - Cast Iron Oil - Steel with Cr and Black Oxide
Crankshaft	-	Nodular Iron
Cam Bearings	-	Al, Sn, Si, or Al, Pb, Cu
Valves	-	Exhaust - Austenitic, Cr Plate Stem Al Diffused Face Inlet - Austenitic, Mn, Phos. Stem. Al Diffused Face
Rocker Arms	-	Cast Iron with Mn
Oil Pump	-	Al, Cu, Zn, Mg
Distributor and Pump Bearings	-	Steel Backed Babbit
Distributor and Pump Shaft	-	Cast Iron Phosphate Coat

The data for the Pinto engine number 1 is summarized in Table 7 and the data for the Pinto engine number 2 is shown in Table 8. The significant wear metals in all cases were copper, iron and lead. The accumulated wear of these three metals during the break-in period of the Pinto engine number 1 is shown in Fig. 30. A plot of the entire 256 hours of operation is shown in Fig. 31, which shows correlations of the adjusted amount of wear metals in the oil samples with events occurring during operation of the engine. Specifically, the increase in lead content shows interesting correlations with heavy load operations at 60 to 80 hours and a sharp increase at 180 hours when a loss of oil pressure occurred. There was a steady increase in iron and copper wear prior to the detection of scuffing of the cylinder walls at about 50 hours of operation.

Except for lead, there was a decided drop in the major wear metals after the change of the oil filter at 182 hours. It is possible that the new oil filter picked up some of the wear metals left in the crankcase oil which had not been picked up by the old oil filter. Why the lead continued to increase while the copper and iron decreased might be attributed to either continued wear of a component containing lead or a preferential pick up of the copper and iron by the filter. The wear study on the Pinto engine number 1 included only gasoline fueled operations up to the time of this report.

The wear data for copper, iron and lead for the Pinto engine number 2 are plotted in Fig. 32. For this engine, the gasoline-fueled operations ceased after 47 hours. There was no change in the trend after the change over to methanol. However, there is insufficient operating time with methanol to expect any significant change. Future operation of both engines with methanol should reveal whether methanol causes an increase in wear above that experienced with gasoline.

TABLE 7: ACCUMULATED WEAR METALS IN ENGINE OIL OF PINTO ENGINE NO. 1
(MG/1000 GMS)

Events	Sample No.	Operation Hours	Copper Cu	Iron Fe	Lead Pb	Chromium Cr	Aluminum Al	Tin Sn
	1	10	32	16	4.1	0.2	< 2.0	< 2.0
	2	20	34	20	5.3	0.2	< 2.0	< 2.0
Oil Leaks	3	30	33	22	6.3	0.2	< 2.0	< 2.0
	4	40	--	--	--	0.2	< 2.0	< 2.0
Cyl.Scuffing	5	50	38	31	8.3	0.2	< 2.0	< 2.0
	6	60	29	27	6.8	0.2	< 2.0	< 2.0
	7	82	24	23	19	0.5	< 2.0	< 2.0
	8	90	21	20	20	0.4	< 2.0	< 2.0
	9	101	25	24	22	0.7	< 2.0	< 2.0
	10	110	23	23	20	0.8	< 2.0	< 2.0
	11	120	21	22	21	0.8	< 2.0	< 2.0
	12	130	23	25	26	1.5	< 2.0	< 2.0
	13	140	23	27	31	1.9	< 2.0	< 2.0
	14	150	21	25	32	2.4	< 2.0	< 2.0
	15	160	21	25	32	2.1	< 2.0	< 2.0
	16	172.75	23	28	33	2.2	< 2.0	< 2.0
	17	180.25	21	25	32	2.3	< 2.0	< 2.0
Oil Press.Drop	17A	180.65	18	21	30	1.5	< 2.0	< 2.0
Oil Fltr.Changed	18	182.25	17	27	40	0.9	< 2.0	< 2.0
Oil Change	19	185.25	10	17	29	0.2	< 2.0	< 2.0
	20	198.05	15	27	42	0.2	< 2.0	< 2.0
Oil Leak	21	215.9	11	22	37	1.6	< 2.0	< 2.0
Extensive Leak	22	225.3	11	25	40	2.0	< 2.0	< 2.0
	23	235.85	12	25	45	2.4	< 2.0	< 2.0
Oil Leakage	24	245.6	12	27	48	2.8	< 2.0	< 2.0
	25	256.5	11	27	45	2.8	< 2.0	< 2.0

TABLE 8: ACCUMULATED WEAR METALS IN ENGINE OIL OF PINTO ENGINE NO. 2
(MG/1000 GMS)

Events	Sample No.	Operation Hours	Copper Cu	Iron Fe	Lead Pb	Chromium Cr	Aluminum Al	Tin Sn
	1	3.42	30	15	13	0.17	< 2.0	< 2.0
	2	6.07	34	16	15	0.24	< 2.0	< 2.0
	3	8.05	32	17	15	0.36	< 2.0	< 2.0
	4	10.02	34	18	16	0.48	< 2.0	< 2.0
	5	19.35	40	26	19	0.74	< 2.0	< 2.0
Oil Changed	6	30.05	43	30	21	0.76	< 2.0	< 2.0
	7	47.77	49	43	25	0.93	< 2.0	< 2.0
Methanol Fuel	8	59.22	51	50	27	1.01	< 2.0	< 2.0
	9	69.38	56	54	29	1.12	< 2.0	< 2.0

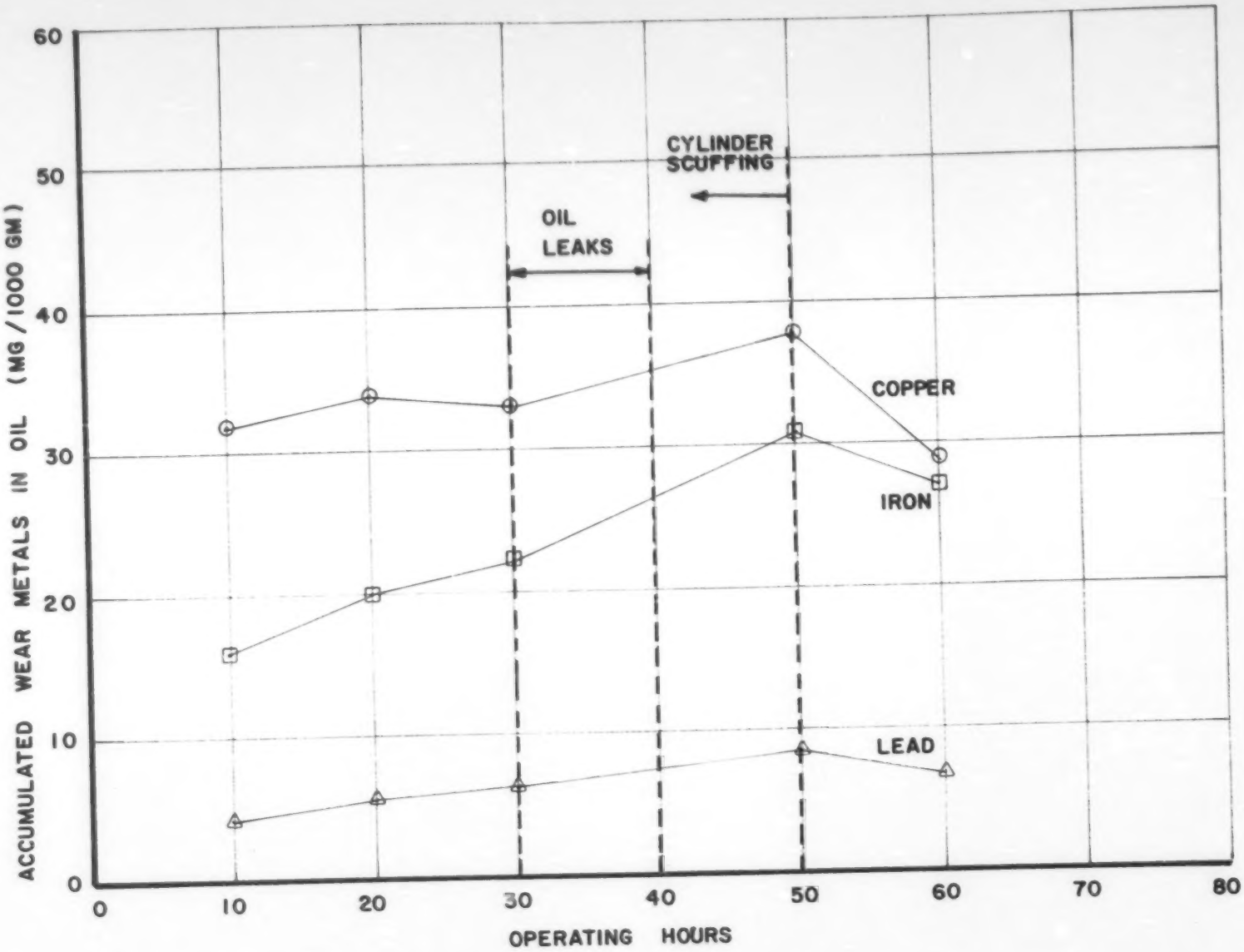

FIG. 30 WEAR OF PINTO ENGINE NO. 1 DURING BREAK-IN

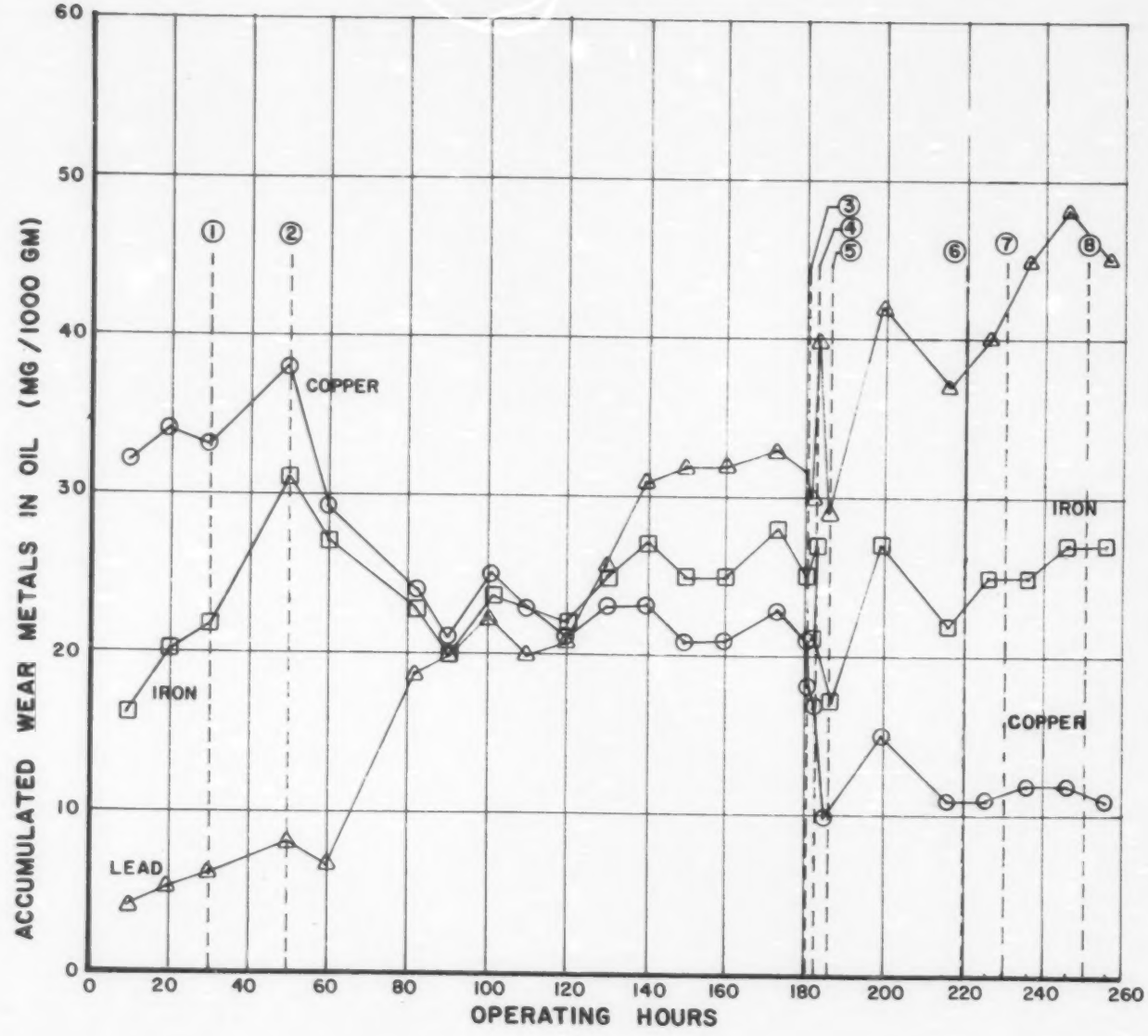

EVENTS

1. EXTENSIVE OIL LEAKAGE
2. CYLINDER SCUFFING DETECTED
3. OIL PRESSURE DROP
4. OIL FILTER CHANGED
5. OIL CHANGED
6. OIL LEAKAGE
7. EXTENSIVE OIL LEAKAGE
8. OIL LEAKAGE

FIG. 31 WEAR OF PINTO ENGINE NO. 1

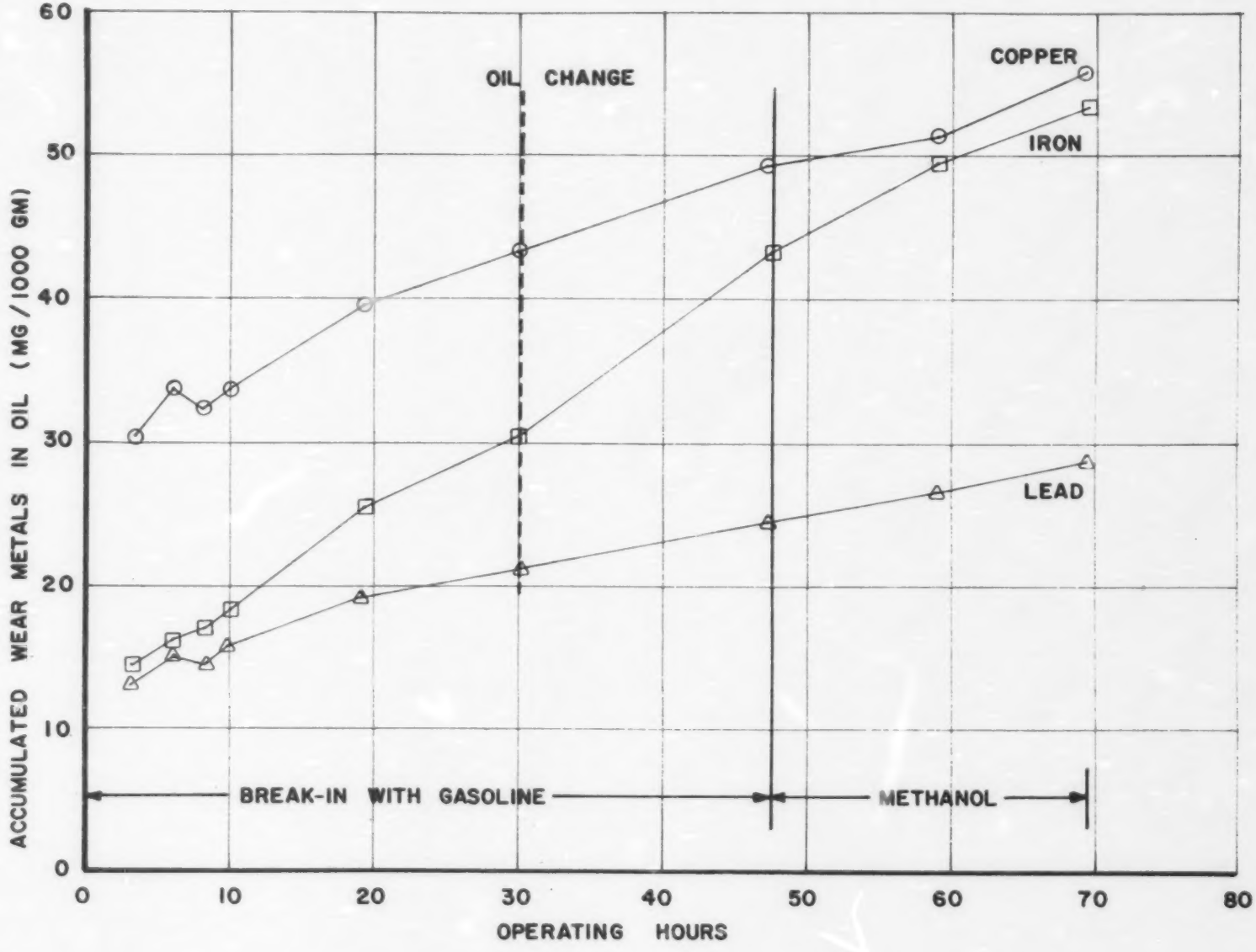

FIG. 32 WEAR OF PINTO ENGINE NO 2

IV.6 THERMOCHEMICAL ENGINE PROCESS MODELING

Effective research relative to a complex phenomenon, such as the thermochemical events in an internal combustion engine, requires an intelligent mix of experimentation and analytical modeling. Modeling of these processes can provide an explanation for the trends in pollutant emissions and engine performance produced by the experimental Pinto test engine and found in the literature. This analytical process has been accomplished by creating a thermodynamic and chemical kinetic computer model of the actual processes occurring in an S.I. engine.

The combustion process in an internal combustion engine is a complex phenomenon which directly relates to such operating variables as power output, thermal efficiency, exhaust composition, and cold starting. In particular, exhaust emissions are affected by engine speed, load, air-fuel ratio, spark timing, but these effects cannot easily be predicted. It is therefore necessary to accurately model the thermochemical events occurring during an actual engine cycle.

Recent investigations have developed fairly good S.I. engine simulations[19,20,21] but they do not include vaporization of liquid fuel (methanol's low pollution characteristics are somewhat linked to its high heat of vaporization) or complete chemical kinetic combustion reactions which are essential in accurately studying pollutant formation (especially in the quench zone). We have included these important considerations in modeling of a jet turbine combustor.[2]

Researchers at the University of Santa Clara have been developing an Otto cycle computer model with complete chemical kinetics to predict the kinetic combustion and pollutant formation processes in an S.I. engine. This model consists of two programs which work hand-in-hand to model the S.I. engine's thermochemical processes. The first program is a chemical equilibrium model of the Otto cycle to predict the thermodynamic properties of the gases during the cycle. This program was developed from a NASA combustion and rocket program.[22] It has been modified to contain the following simulations which are diagramed in Fig. 33. During the intake stroke, liquid fuel and air are mixed and heated in the intake manifold, allowing an equilibrium amount of vaporization of the fuel. This heated charge is then induced into the cylinder where it is mixed completely with the exhaust residual. Further vaporization of the liquid fuel occurs at this point. As the intake valve closes, the mixture is compressed isentropically and adiabatically to the point of ignition. By this time, the fuel is completely vaporized. The unburned charge is considered to be

FACTORS BEING CONSIDERED IN COMBUSTION MODELING

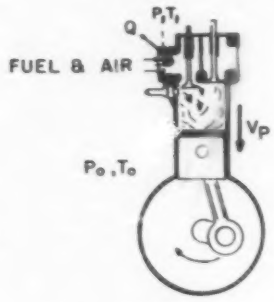

(A) INTAKE STROKE

ASSUMPTIONS

1. LIQUID FUEL AND AIR MIXED AND HEATED IN INTAKE MANIFOLD
2. LIQUID FUEL ALLOWED TO VAPORIZE
3. CHARGE MIXED WITH EXHAUST RESIDUAL
4. FURTHER VAPORIZATION OF LIQUID FUEL

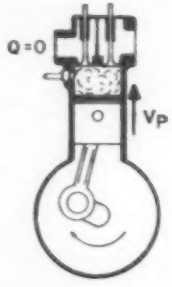

(B) COMPRESSION STROKE

1. INTAKE VALVE CLOSES
2. ISENTROPIC COMPRESSION OF CHARGE TO POINT OF IGNITION
3. NO HEAT TRANSFER
4. NO REACTION OF FUEL AND AIR
5. LIQUID FUEL COMPLETELY VAPORIZED

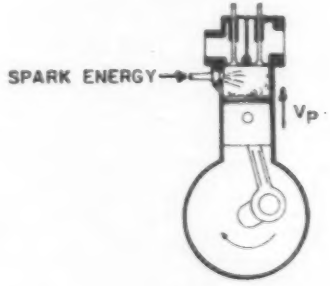

(C) IGNITION

1. SPARK ENERGY ADDED TO CHARGE ENERGY OF FIRST INCREMENT
2. FIRST INCREMENT OF FUEL AIR MIXTURE COMBUSTED

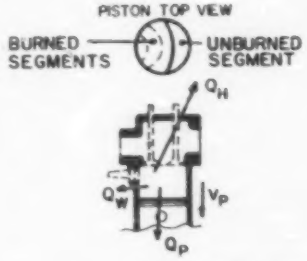

(D) COMBUSUTION

1. FLAME FRONT TRAVELS IN MODIFIED CYLINDRICAL BURNING PATTERN
2. CONSTANT PRESSURE COMBUSTION OF EACH ELEMENT, HEAT TRANSFERRED TO CYLINDER FROM BURNED SEGMENTS, ISENTROPIC COMPRESSION TO NEW VOLUME
3. UNBURNED SEGMENT CONSIDERED NON-REACTING
4. CHEMICAL KINETICS OF BURNED SEGMENTS CHEMICALLY DETERMINE SPECIES CONCENTRATIONS

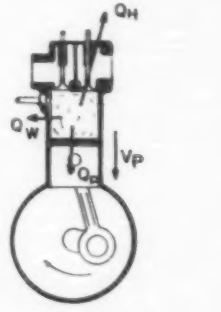

(E) EXPANSION STROKE

1. HEAT TRANSFER TO CYLINDER
2. EXPANSION OF GASES TO NEW VOLUME
3. CHEMICAL KINETICS DETERMINE SPECIES CONCENTRATION

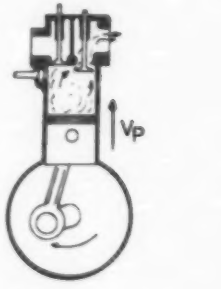

(F) BLOW DOWN

1. EXHAUST VALVE OPENS
2. ADIABATIC ISENTROPIC BLOW DOWN OF GASES TO ATMOSPHERIC PRESSURE
3. CHEMICAL KINETICS DETERMINE SPECIES CONCENTRATION

FIGURE 33

Reproduced from best available copy.

frozen chemically during this portion of the cycle. The combustion of the fuel and air is initiated by the spark firing. Ignition energy is added to the chemical reaction which starts combustion. The combustion process modeling in this program allows for finite-rate combustion, heat transfer to cylinder walls, turbulence, and piston motion. The finite rate combustion is considered to be of the stratified zone type[23] where each burned segment of gas is assumed to be separate with homogeneity only within the segments. The flame front, which expands in a modified cylindrical pattern, has its motion defined by a modified Semenov flame speed equation[24] coupled with a turbulent factor based on inlet velocity.[25] In the combustion processes each new segment of unburned gas goes through a constant pressure combustion, followed by a constant pressure heat transfer from all burned segments to the head, piston crown, and cylinder walls. This in turn is followed by compression of all segments to the new volume determined by the piston motion. By the time the flame front has completely swept the cylinder, consuming all the unburned charge, the expansion stroke has begun. During the remainder of this stroke heat is transferred to the cylinder and then the gases are expanded to the new volume defined by the piston motion. This is continued until the point where the exhaust valve opens, where an isentropic, adiabatic blow down of exhaust products to atmospheric pressure occurs.

The other complementary computer program is a complete chemical kinetics program similar to the one used in Reference 2. It follows the equilibrium program from the point of ignition through the blow down process with a complete set of kinetic reactions and rates. Thus, the thermodynamic properties of the gases are determined by the equilibrium program, while the exhaust composition is determined by the kinetics program.

The reaction set for the combustion of methanol has previously been developed in Reference 2. This reaction set has provided good results in our gas turbine simulation and therefore it can be used directly in predicting combustion reactions in the S.I. engine model. Since methanol is a relatively simple molecule chemically, the combustion reaction set is complete. The complexity of gasoline combustion, however, requires some simplification. First, gasoline will be simulated by isooctane, C_8H_{18}, since its thermodynamic properties are similar to actual gasolines. Second, the reaction set for isooctane combustion will be developed using a global combustion model similar to that developed for octene in Reference 2. In a global model the fuel and air react to form simple hydrocarbons, carbon monoxide, and simple free

radicals, thereby ignoring intermediate pyrolysis reactions in fuel combustion. Experimental ignition delay data obtained from Reference 26 will be used to determine the initiation reaction rates for the octane global combustion model reaction set.

As a first test of the S.I. engine model, methanol was combusted with air in stoichiometric proportions at the conditions described in Table 9. As can be seen from that table the agreement between the predicted and actual results is good, especially for the NO_x exhaust emissions. Therefore, it is expected that with further fine tuning of the computer model this can be used to predict the effects of varying the parameters currently being used in the methanol test matrix. This fine tuning might include such additions as valve timing, quench zone modeling, a better turbulent flame speed model and more accurate tuning to the Pinto test engine.

Once predictive confidence has been established, the S.I. engine simulation becomes extremely useful in studying the effects of changing engine variables on the exhaust composition, especially NO_x and CO. It is possible to study combinations of liquid and gaseous fuels to determine the degree of liquid fuel vaporization and the heats required to maintain a given inlet mixture temperature. This is a very important feature since methanol's high heat of vaporization radically affects the engine's performance and emissions characteristics. The effects of changing air-fuel ratio, ignition timing and compression ratio can also be examined. The net result is a low cost means of studying a complex interactive thermochemical cycle of events. It should greatly reduce the expensive experimental hardware modifications required to find the best mix of engine performance and emissions suppression for a methanol fueled engine.

TABLE 9

INPUT PARAMETERS:

ϕ	=	1.00
Fuel	=	Methanol
Intake Manifold Temp.	=	283.11°K
Intake Manifold Pressure	=	1 atm
Exhaust Residual Fraction	=	0.0404
Engine Speed	=	2000 RPM
Ignition Timing	=	30°BTDC

ENGINE DATA:

	Predicted	Actual*
ihp	12.0	12.4
isfc (lb/ihp-hr)	0.905	0.887
η_{vol} %	78	80.5
η_{th} %	32.8	33.6

EXHAUST DATA (molar %, dry basis):

	Predicted	Actual**
CO	0.12	0.49
CO_2	14.90	14.31
H_2	0.12	0.28
O_2	0.03	0.41
NO_X	1882 ppm	1899 ppm

*Taken from Pinto test engine runs 517 and 518.

**Taken from Pinto test engine run 518, cylinder 3, ϕ = 0.999.

V. REFERENCES

1. H. G. Adelman and R. K. Pefley, "Methanol as an Automotive Fuel", presented at the AIChE 80th National Meeting, Boston, Massachusetts, September 7-10, 1975.

2. H. G. Adelman, L. H. Browning and R. K. Pefley, "Predicted Exhaust Emissions from a Methanol and Jet Fueled Gas Turbine Combustor", AIAA Paper No. 75-1266, presented at AIAA/SAE 11th Propulsion Conference, Anaheim, California, September 29 to October 1, 1975.

3. G. Blair Martin, "Evaluation of NO_x Emission Characteristics of Alcohol Fuels in Stationary Combustion Systems", presented at the AIChE 80th National Meeting, Boston, Massachusetts, September 7-10, 1975.

4. L. W. Huellmantel, S. G. Liddle and D. C. Hammond, "Combustion of Methanol in an Automotive Gas Turbine", 1975 GMR Symposium: Future Automotive Fuels, Warren, Michigan, October 6-7, 1975.

5. E. Faltermayer, "The Clean Synthetic Fuel That's Already Here", Fortune Magazine, Vol. XCII, No. 3, September 1975, pp. 146-154.

6. G. D. Ebersole and F. S. Manning, "Engine Performance and Exhaust Emissions - Methanol Versus Indolene", SAE Transactions, Vol. 81, Paper No. 720692 (1972).

7. B. A. D'Alleva and W. G. Lovell, "Relation of Exhaust Gas Composition to Air-Fuel Ratio", SAE Journal, Vol. 38, No. 3, March 1936, pp. 90-96.

8. R. M. Tillman and R. G. Jackson, "Automotive Uses of Methanol Fuel", presented at the Engineering Foundation Conference: Methanol as an Alternate Fuel, Henniker, New Hampshire, July 1974.

9. SAE Information Report, "Automotive Gasoline - SAE J312b", 1975 SAE Handbook, Society of Automotive Engineers, Inc., Warrendale, Pennsylvania, p. 439.

10. R. M. Tillman, O. L. Spilman and J. M. Beach, "Potential for Methanol as an Automotive Fuel", SAE Paper No. 750118, Society of Automotive Engineers, Detroit, Michigan, February 24-28, 1975.

11. "The Swedish Methanol Project with Operating Plan", The Swedish Methanol Development Company, Stockholm, October 1, 1975.

12. "Methanol-Gasoline Blends: How Promising Are They?", Automotive Engineering, Vol. 82, No. 12, December 1974.

13. R. R. Adt, Jr., R. D. Doepker, and L. E. Poteat, "Methanol-Gasoline Fuels for Automotive Transportation - A Review", U.S. Environmental Protection Agency, Alternative Automotive Power Systems Division, Ann Arbor, Michigan, November 1974.

14. R. M. Tillman, data presented at Bureau of Mines sponsored technical meeting, Denver, Colorado, September 5, 1974.

15. J. D. Rogers, "Ethanol and Methanol as Automotive Fuel", Report No. P813-3, E. I. DuPont De Nemours and Co., Inc., 1973.

16. E. A. Means and D. Ratcliff, "Determination of Wear Metals in Lubricating Oils by Atomic Absorption Spectroscopy", Atomic Absorption Newsletter, Vol. 4, No. 1, January 1965, pp. 174-179.

17. R. L. Klug, "Scheduled Oil Sampling as a Maintenance Tool",Paper No. 720372, presented at Earthmoving Industry Conference, Society of Automotive Engineers, April 1972.

18. M. Stroben, Personal Communication, Ford Motor Company, Detroit, Michigan, November 18, 1975.

19. F. J. Zeleznik, "Combustion Modeling in Internal Combustion Engines", prepared for Combustion Science and Technology, December 20, 1974.

20. H. Hiroyasu and T. Kadota, "Computer Simulation for Combustion and Exhaust Emissions in Spark Ignition Engine", 15th Symposium on Combustion, Combustion Institute, 1974, pp. 1213-1223.

21. G. G. Lucas and E. H. James, "A Computer Simulation of a Spark Ignition Engine", SAE Paper No. 730053, January 8-12, 1973.

22. S. Gordon and B. J. McBride, "Computer Program for Calculation of Complex Chemical Equilibrium Compositions, Rocket Performance, Incident and Reflected Shocks, and Chapman-Jouguet Detonations", NASA Report No. SP-273, 1971.

23. G. G. Lucas and K. Varde, "Analysis of Nitric Oxide Formation in Spark Ignition Engine with Heat Transfer and Effect of Ignition Point", SAE Paper No. 740189, February 25-March 1, 1974.

24. NASA Report 1300, "Basic Considerations in the Combustion of Hydrocarbon Fuels with Air", prepared by Propulsion Chemistry Division, Lewis Flight Center, 1957.

25. B. S. Samaga and B. S. Murthy, "On the Problem of Predicting Burning Rates in a Spark Ignition Engine", SAE Paper No. 750688, June 3-5, 1975.

26. B. P. Mullins, "Studies on the Spontaneous Ignition of Fuels Injected into a Hot Air Stream", National Gas Turbine Establishment, England, Report Nos. 89, 90, 97 and 107, 1952, Fuel, 32, 343 (1953).

APPENDIX

Equivalence Ratio Determination:

Calculation of the equivalence ratio (ϕ) was based on measurements of the molar concentration of the exhaust constitutents. Known fuel composition combined with these molar exhaust concentrations provides the basis for the solution of the combustion reaction equation. Redundant exhaust emissions instrumentation permits cross-checking (two solutions) of the equation. The difference in calculated A/F (or ϕ) from these two chemical balances gives an indication of the error introduced by the emissions analyzers.

The combustion of a fuel with air may be expressed in the following general form (assuming the fuel to be composed only of carbon, hydrogen and oxygen)

$$a\ C_xH_yO_z + b\ (O_2+3.76N_2) \rightarrow c\ CO_2 + d\ CO + e\ H_2O + f\ O_2 + g\ H_2 + h\ (3.76)N_2 + i\ C_xH_yO_z + j\ NO_2 + k\ HCHO \quad (1)$$

where the coefficients a through k are molar concentrations or molar percents. The last three terms on the right side of the equation are unburned fuel, oxides of nitrogen (as NO_2), and aldehydes (as formaldehyde), respectively. As a general rule, HCHO is so small that it is within the measurement uncertainty of the principal combustion species of CO_2, CO, and O_2. Therefore, it can be neglected in balancing the equation.

CO_2, CO, O_2, $C_xH_yO_Z$ and NO_2 (c, d, f, i, j known) were measured directly. H_2 was calculated by use of the water-gas reaction and an equilibrium constant of 3.5:

$$d\ CO + e\ H_2O \rightleftarrows c\ CO_2 + g\ H_2$$

where

$$K_{eq} = \frac{[CO] \times [H_2O]}{[CO_2] \times [H_2]} = \frac{d \cdot e}{c \cdot g} \quad (2)$$

The constituent species in the equation are expressed as moles or mole fraction. Equations (1) and (2), together with the measured species, provide a like number of equations and unknowns. The unknown coefficients (a, b, g, h) may now be calculated by conservation of the constituent atoms:

Fuel (carbon):

$$a = \frac{c+d}{x} + i \tag{3}$$

Water (hydrogen):

$$e = \frac{(a \cdot y - 2 \cdot g - y \cdot i)}{2} \tag{4}$$

Substituting (2) into (4) to eliminate g yields,

$$e = \frac{y(a-i)}{2(1+0.285) \cdot \frac{d}{c})} \tag{5}$$

Air (oxygen and Nitrogen):

$$b = \frac{(2 \cdot c + d + e + 2 \cdot f + i \cdot z + 2 \cdot j)}{2} \tag{6}$$

$$h = b - \frac{j}{7.52} \tag{7}$$

The air to fuel ratio can now be calculated. In terms of the measured species and known fuel composition, this carbon balance procedure yields,

$$A/F = \frac{\text{lbm air}}{\text{lbm fuel}} = 2.38 \cdot \frac{[2 \cdot c + d + \frac{y(a-i)}{2(1.0+0.2857 \cdot \frac{d}{c})} + 2 \cdot f + i \cdot z + 2 \cdot j]}{[\frac{(c+d)}{x} + i]} \cdot \frac{MW_{air}}{MW_{fuel}} \tag{8}$$

In the experimental emissions measurements the combustion water was condensed from the exhaust sample stream before measurement of CO_2, CO, and O_2. This was at 33°F, which yields 0.006 mole fraction of water in the sample stream leaving the condenser. A new balance of the chemical equation can be derived which will yield a check on Equation (8).

This A/F we term a nitrogen balance and it requires an iterative scheme for determining the unknown coefficients of Equation (1). Conservation of constituent atoms begins with a guess of the combustion water mole percent (TH2O):

Air (nitrogen and oxygen) (dry balance):

$$h = \frac{(100\% - [c + d + 0.6 + f + g + i + j])}{3.76} \tag{9}$$

Substituting (2) into (9) to eliminate g yields,

$$h = \frac{f + \frac{d \cdot TH20}{(c \cdot 3.5)(1-TH20/100)} + i + j}{3.76} \tag{10}$$

and

$$b = h + \frac{j}{7.52} \tag{11}$$

Conserving hydrogen atoms yields a new estimate of the water,

$$e = \frac{(a \cdot y - [2 \cdot \frac{d \cdot TH20}{(c \cdot 3.5)(1-TH20/100)} + i \cdot y])}{2} \tag{12}$$

e is then compared with TH20. If the two are within a chosen tolerance, then the calculations are complete. Otherwise, the value calculated in (12) is substituted into (10) and the calculations are repeated. After the sufficient number of iterations, the air to fuel ratio can be calculated using (11) and (3) and the respective molecular weights.

$$A/F = \frac{\text{lbm air}}{\text{lbm fuel}} = 4.76 \cdot \frac{(100\% - [c+d+e+f+\frac{d \cdot e}{(c \cdot 3.5)(1-TH20/100)} + i + 1.5j])}{3.76} \Big/ [\frac{(c+d)}{x} + i] \cdot \frac{MW_{air}}{MW_{fuel}} \tag{13}$$

Equation (13) can be compared with Equation (8). The difference in the two A/F's is indicative of the combined measurement error in CO_2, CO, and O_2.

ENGINE SETTINGS: 2000 RPM
14" HG MAN VAC
SPARK – 35° BTDC
$\phi \sim 1.06$

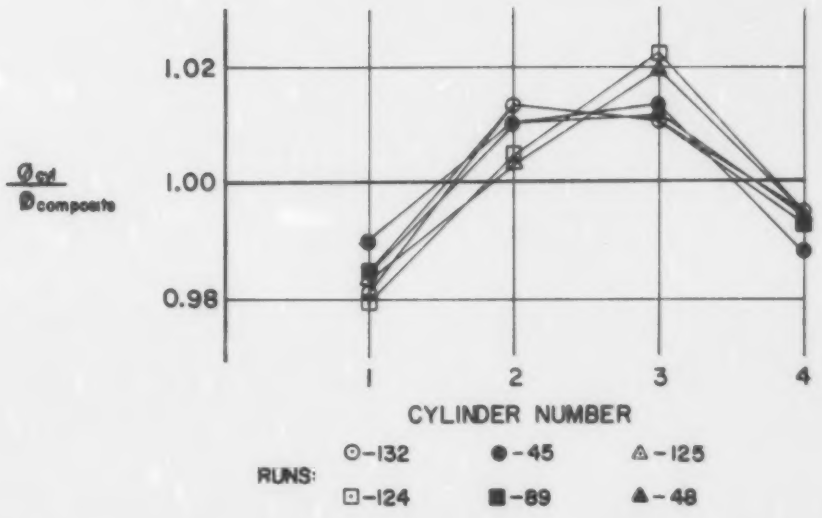

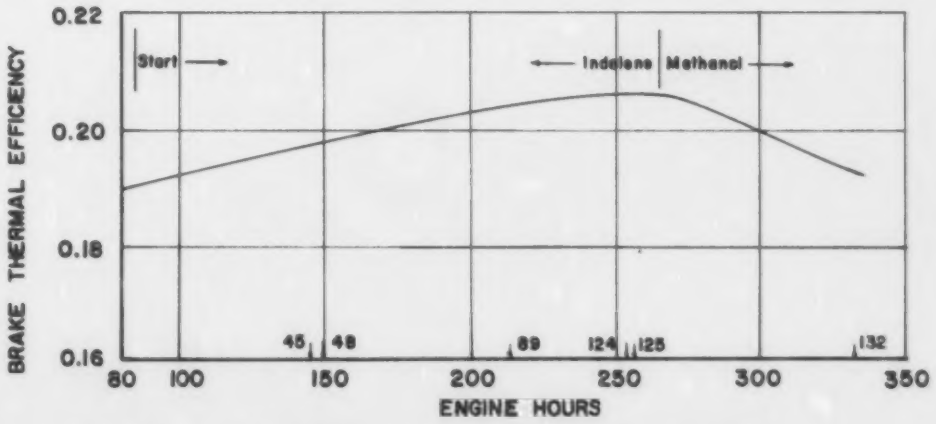

FIG. A-1 MALDISTRIBUTION & PERFORMANCE TRENDS
FOR INDOLENE
REPETITIVE TEST POINTS

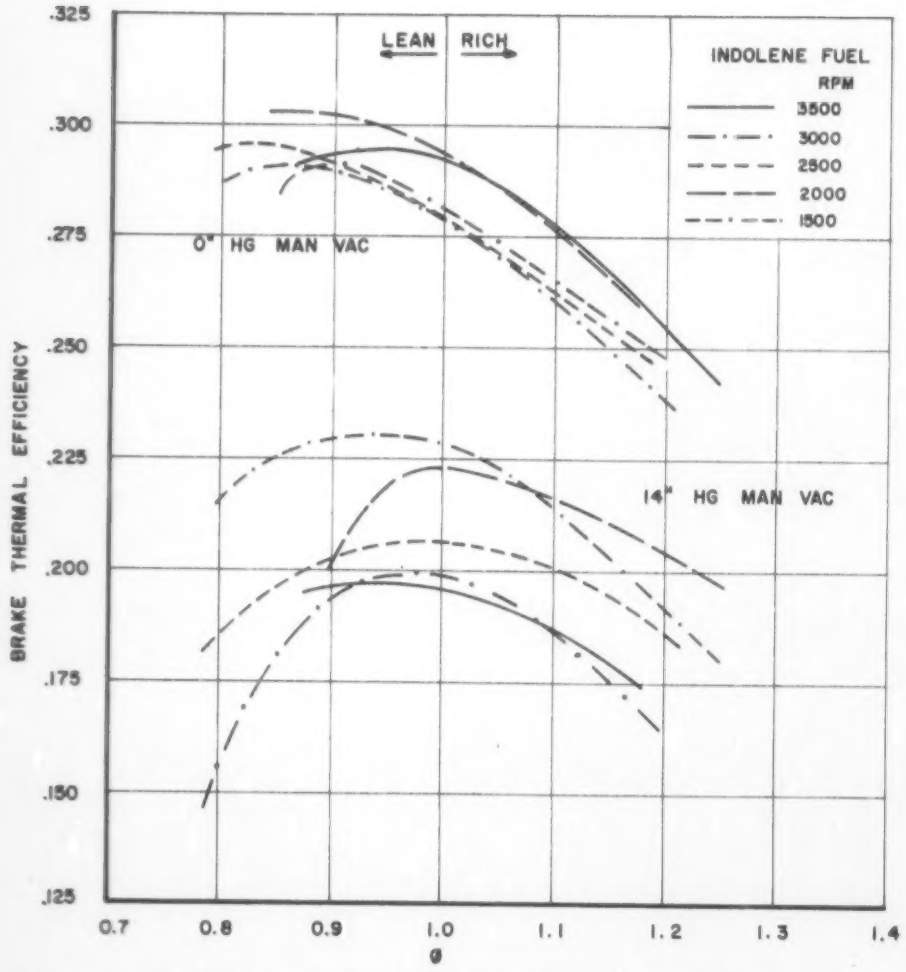

FIG. A2: TRENDS IN BRAKE THERMAL EFFICIENCY – PART AND FULL LOAD COMPARISONS AT VARIOUS SPEEDS

INDOLENE
2000 RPM
0" HG MAN VAC

INDOLENE
2000 RPM
7" HG MAN VAC

INDOLENE
2000 RPM
14" HG MAN VAC

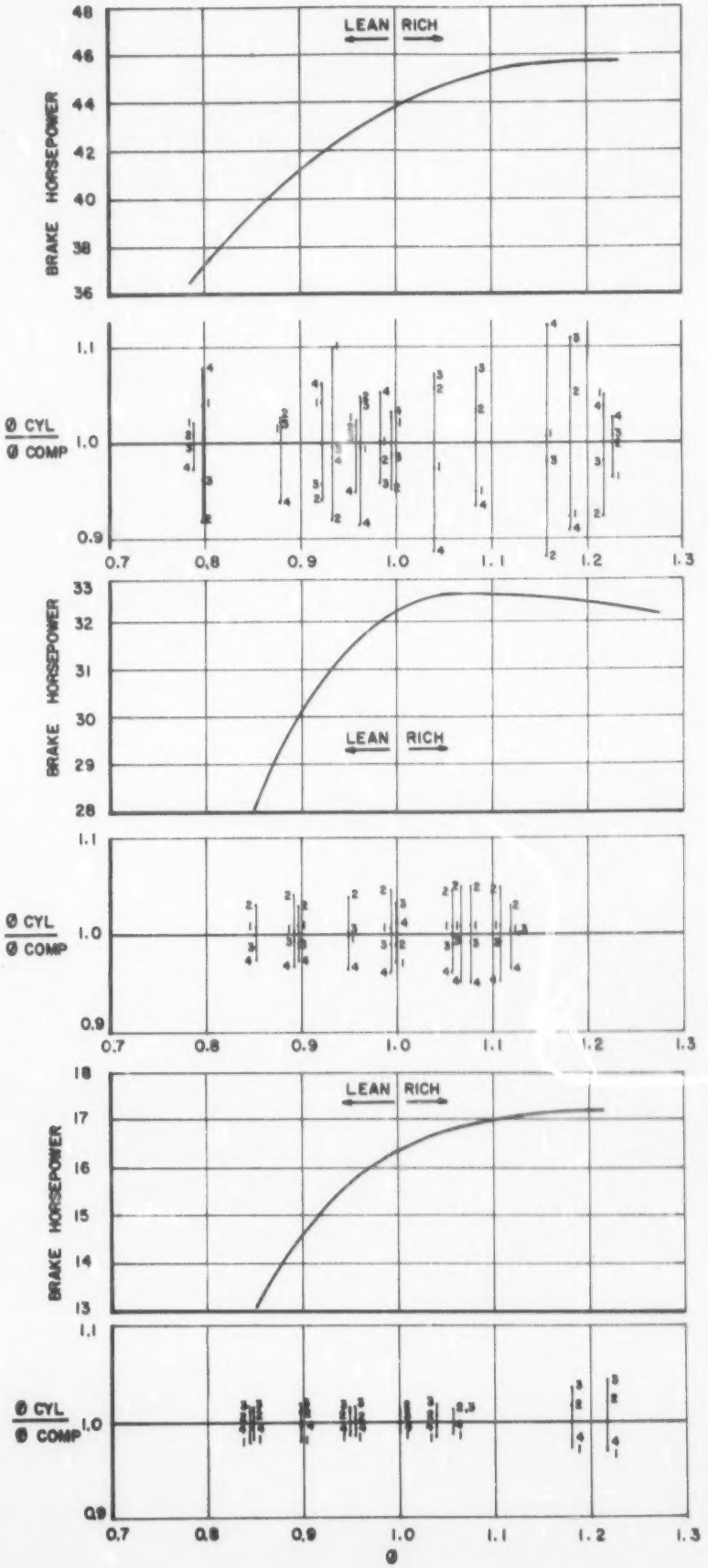

FIG. A3: BRAKE HORSEPOWER AND MALDISTRIBUTION – INDOLENE

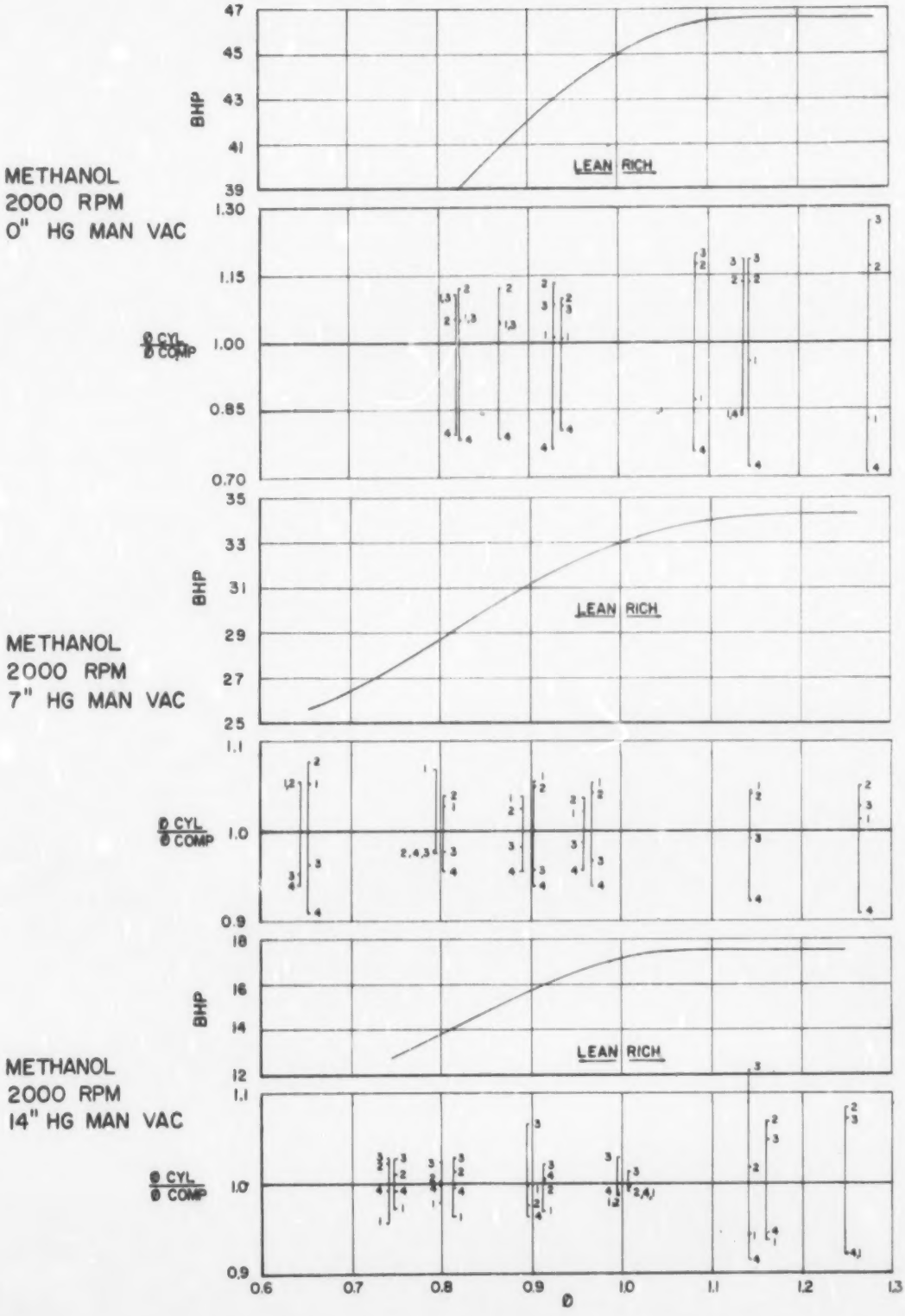

FIG A4: BRAKE HORSEPOWER AND MALDISTRIBUTION-METHANOL

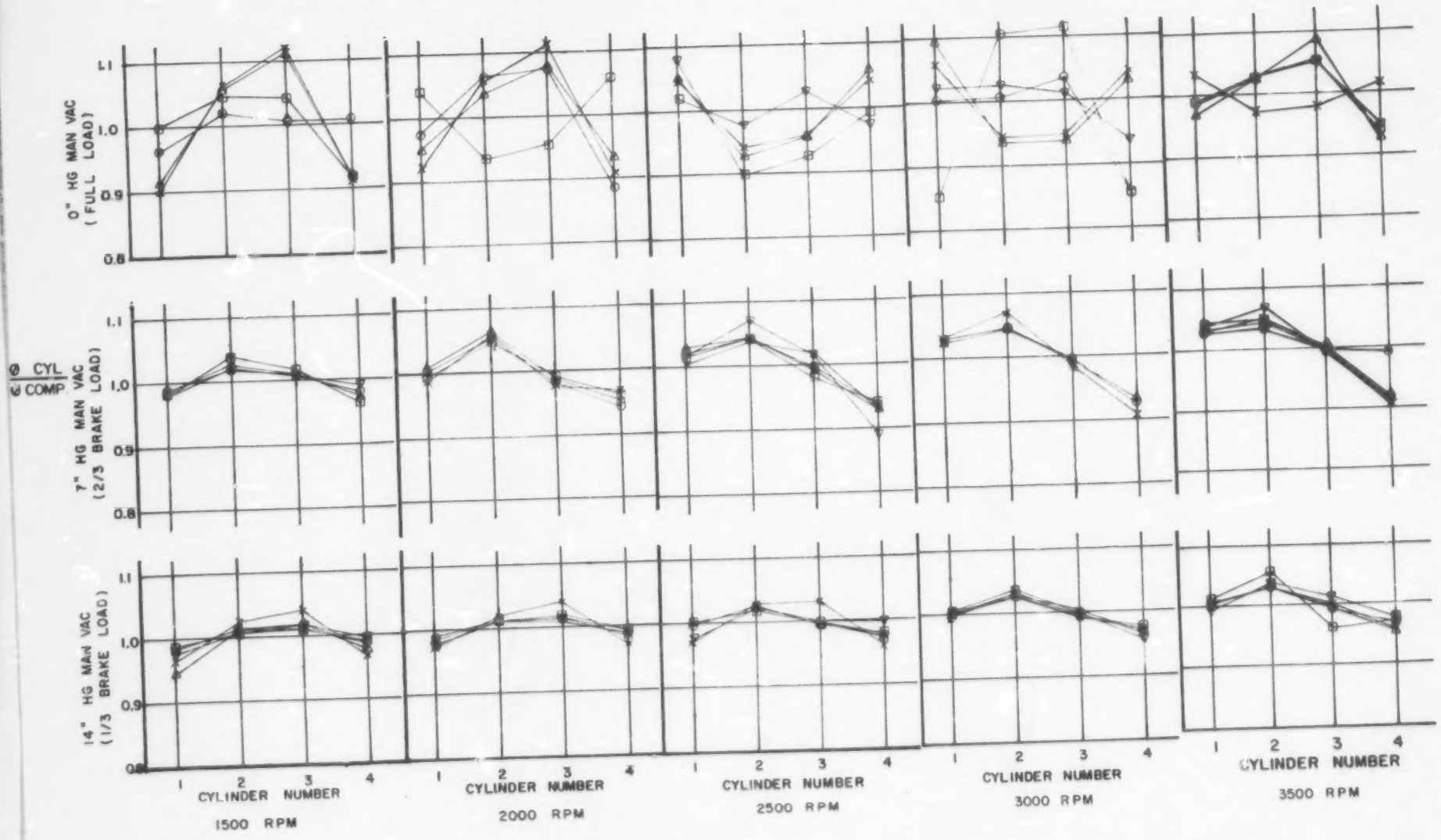

Ø COMP

▽ — 0.8
□ — 0.9
○ — 1.0
△ — 1.1
X — 1.2

FIG. A5: CYLINDER TO CYLINDER EQUIVALENCE RATIO VARIATIONS – INDOLENE

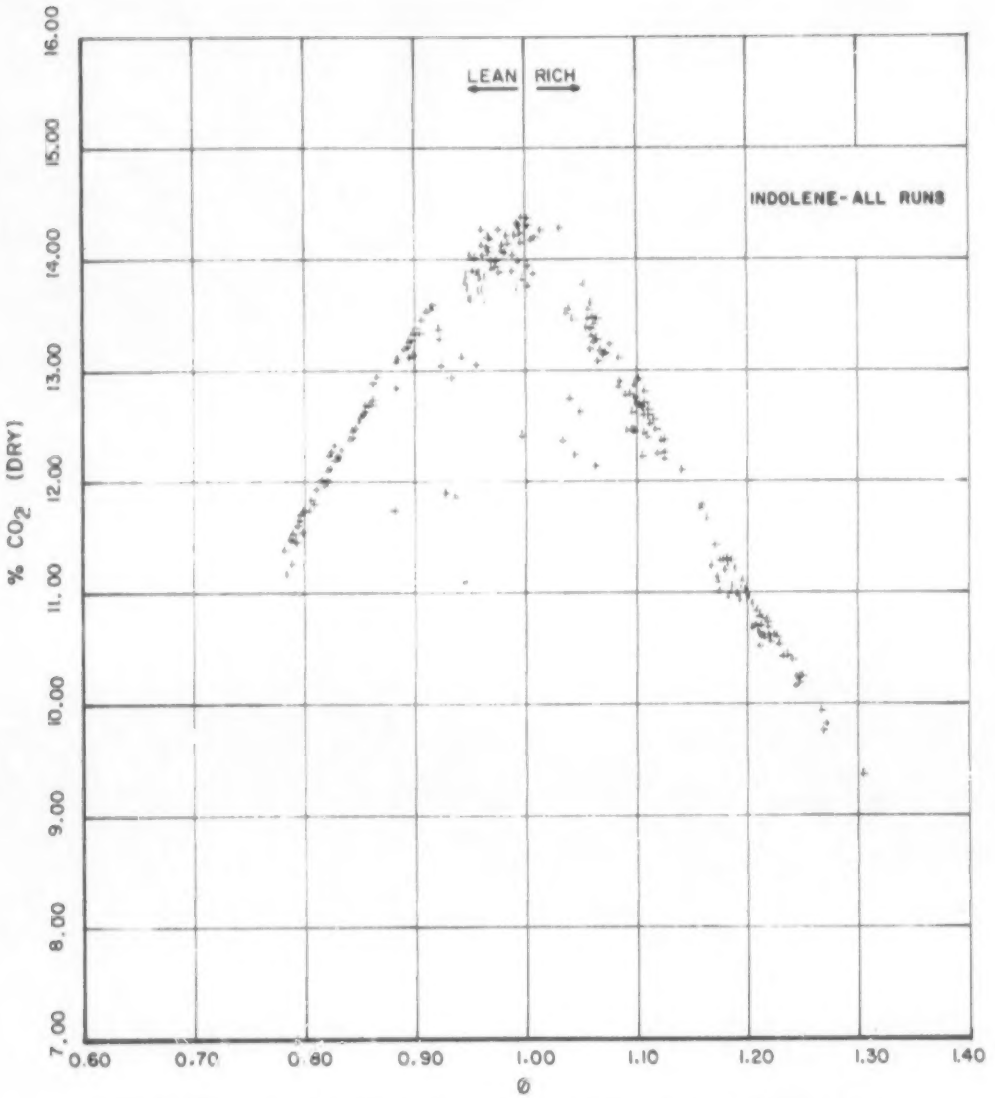

FIG. A6: CO_2 VS EQUIVALENCE RATIO – COMPOSITE CYLINDER DATA

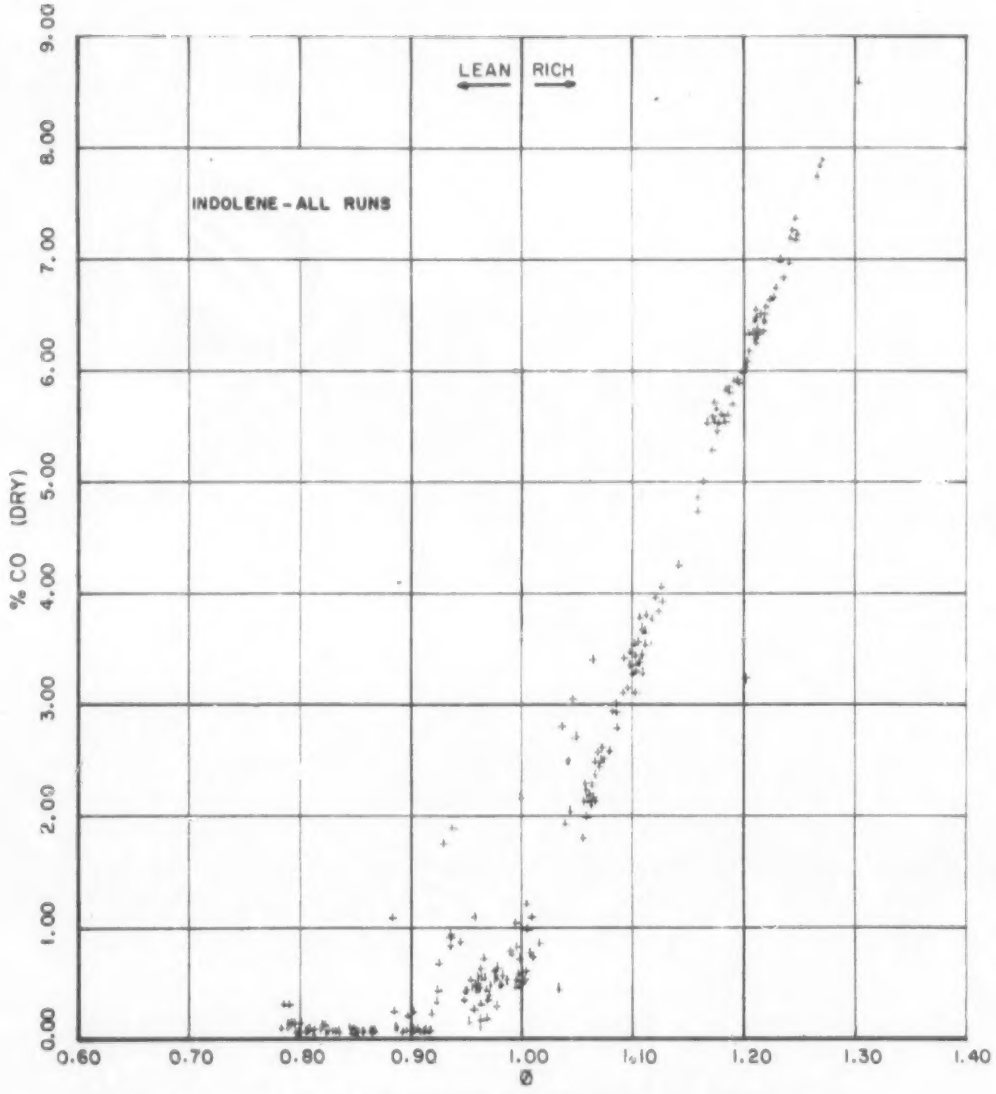

FIG. A7: CO vs EQUVALENCE RATIO - COMPOSITE CYLINDER DATA

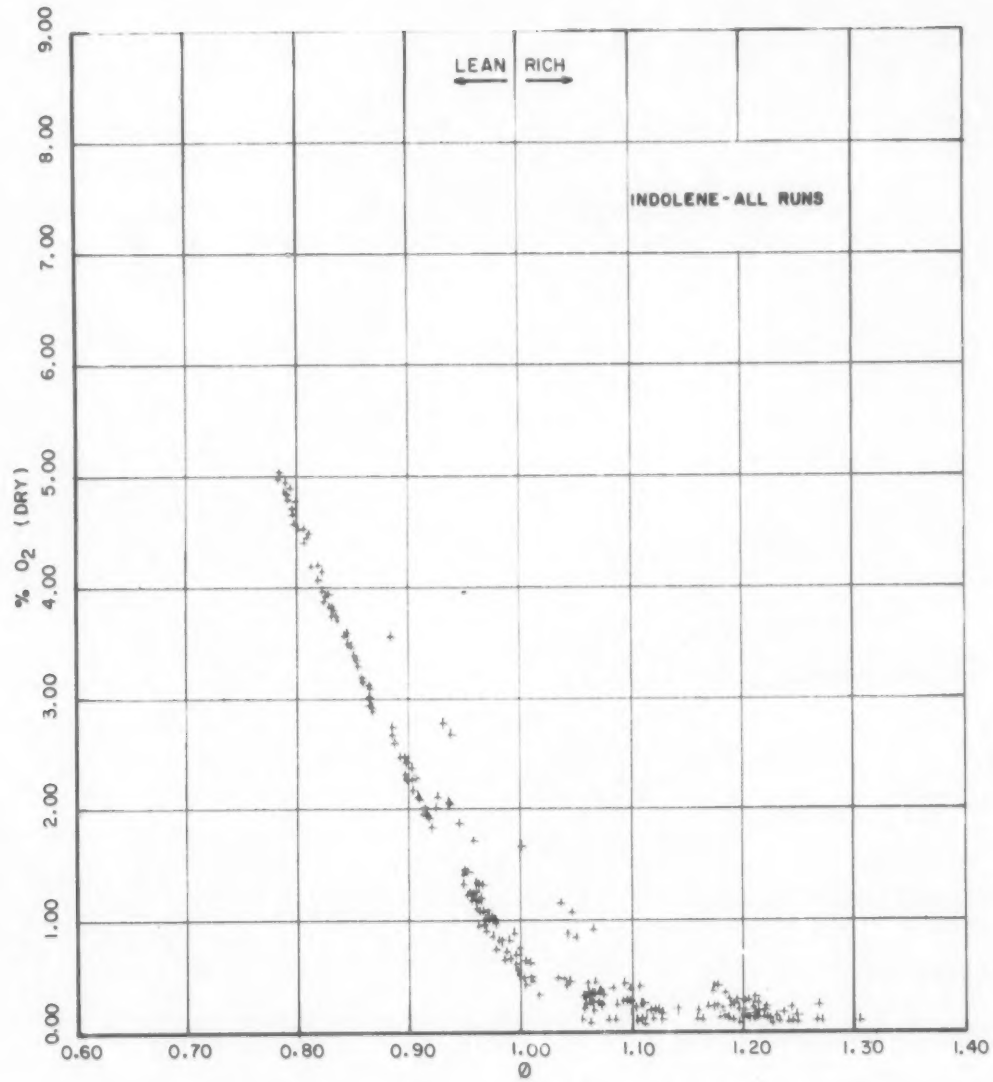

FIG. A8: O_2 VS EQUIVALENCE RATIO – COMPOSITE CYLINDER DATA